ROMA TRE
UNIVERSITÀ DEGLI STUDI

DOCTORAL SCHOOL IN BIOLOGY

Section: "Biology Applied to Human Health"

XXIV cycle

INVOLVEMENT OF PEROXISOMES AT THE ONSET AND DURING THE PROGRESSION OF ALZHEIMER'S DISEASE IN A TRANSGENIC MOUSE MODEL.

COINVOLGIMENTO DEI PEROSSISOMI ALL'ESORDIO E DURANTE LA PROGRESSIONE DELLA MALATTIA DI ALZHEIMER IN UN MODELLO MURINO TRANSGENICO.

Candidate: Francesca FANELLI

Tutor: Dr. Sandra MORENO

Coordinator: Prof. Paolo VISCA

A.Y. 2010 - 2011

CONTENTS

ABSTRACT

Alzheimer's Disease (AD) is the most common form of dementia, characterized by progressive neurodegeneration. Histopathological changes, including formation of beta-amyloid (Aβ) plaques, neurofibrillary tangles, followed by inflammation and neuronal loss, are especially prominent in the hippocampus and the neocortex.
The classical hypothesis to explain the pathogenic events occurring in AD, the so-called amyloid cascade, involves a critical and early role of Aβ peptide, involving production of reactive oxygen species (ROS) and consequent oxidative stress (Sayre *et al*., 2008). Even though Aβ toxicity is still widely accepted, this hypothesis has been recently challenged by Nunomura (2010) who proposed oxidative stress as the primary culprit in AD pathogenesis.
In this scenario, peroxisomes may play an important role, as they are involved in a wide variety of metabolic processes, including ROS and lipid metabolism (Schrader and Fahimi, 2008). It known that loss of peroxisomes makes neuronal cells vulnerable to oxidative stress and leads to degeneration (Stamer *et al*., 2002). On the other hand, peroxisomal proliferation attenuates Aβ-dependent toxicity in hippocampal neurons (Santos *et al*., 2005).
This PhD project aims to investigating the possible involvement of peroxisomes in AD onset and progression, with special reference to their role in oxidative stress. To this purpose we examined the transgenic mouse strain Tg2576, which recapitulates human pathological phenotype and is especially suited to the study of early stages, for it is characterized by slow progression (Jacobsen *et al*., 2006, D'Amelio *et al*., 2011). Our study was performed on early, advanced, and late stages of the disease (3, 6, 9, 12, 18 months of age), focusing on the hippocampus and neocortex, i.e., the areas where primary neuronal injury is known to occur.
First, we analyzed the distribution of neuronal and glial markers, in WT and Tg2576 ageing/diseased mice, in order to detect possible alterations in brain organization. Our data show that the overall cytoarchitecture is conserved during normal aging, while in the pathological genotype, neuronal layering gradually changes starting from 9 months and appears dramatically altered at 18 months, when hyperproliferated and hypertrophic astrocytes and microglia cells are detected in both the neocortex and hippocampus. Consistently with the observed cytoarchitectural alterations, Congo Red staining demonstrates that small amyloid plaques are already present in the neocortex at 9 months, while their first appearance in the hippocampal formation occurs at 18 months.
Main objective of this PhD project was to investigate age-dependent variations of several peroxisome-related proteins in Tg2576 and WT hippocampus and neocortex in the course of the disease. Specifically, we characterized the peroxisomal population from a molecular and morphological point of view, examining the expression of biogenesis markers, membrane proteins, and matrix enzymes.

Our biochemical, morphological and ultrastructural data concur to demonstrate a significant peroxisomal induction in 3-month-old diseased hippocampus, as assessed by the peroxin Pex5p, the peroxisomal membrane protein PMP70, and acyl-CoA-oxidase (AOX, the first enzyme of the fatty acid peroxisomal β-oxidation pathway), all of which show higher levels in Tg2576, compared to controls. This increase, paralleled by detectable oxidative modifications to biomolecules and by PPARα activation in Tg2576 hippocampus, suggests an early response to redox imbalance, mediated by PPARα, which is known to be induced by oxidized lipids.

Strikingly, the other crucial enzyme for the peroxisomal β-oxidation pathway, i.e., thiolase (THL), is unchanged at 3 months, indicating possible inefficiency of the β-oxidation pathway in the Tg2576 than in the WT. This would imply accumulation of VLCFA-derived intermediates in the brain, in line with the recent findings on the brain of AD patients (Kou *et al*., 2011). Even more remarkably, at this early stage, catalase (CAT) levels show no genotype-based differences, suggesting that increased H_2O_2 production by AOX is not accompanied by its efficient removal. These data, together with the low expression levels shown by another major H_2O_2-scavenging enzyme, glutathione peroxidase (GPX1), strongly favour the idea that oxidative stress occurs early in AD. To this respect, it is also worth noting that mitochondrial superoxide dismutase (SOD2) is increased in the hippocampus of 3-month-old Tg2576 mice. Despite its commonly referred role as a ROS scavenger, this enzyme could even act as a pro-oxidant in this context. Indeed, the augmentation of SOD2, converting superoxide ion to H_2O_2, in the absence of parallel increase in any of the H_2O_2 scavengers, likely contributes itself to redox imbalance. Therefore, our data prefigures an early oxidative stress condition occurring in the hippocampus, strongly supporting the idea that this is the primary culprit in AD pathogenesis (Nunomura *et al*., 2010). Indeed, our data on the oxidative damage markers 8-OHG/OHdG and acrolein confirm this view.

During the progression of AD pathology, peroxisomal population undergoes dramatic changes, in that several proteins, including PMP70, Pex14p, and AOX, are decreased in 6-month-old Tg2576 hippocampus. This may reflect an impaired peroxisomal biogenesis or autophagic removal of excess organelles. Interestingly, in the hippocampus relatively high levels of CAT are detected at this age in the pathological genotype, suggesting a late response to peroxisomal induction, in agreement with what described in the liver following peroxisomal agonists administration (Reddy *et al*., 1986).

At 9 and 12 months, hippocampal levels of PMP70, AOX, and THL are relatively stable in both conditions. Other antioxidant enzymes show interesting changes at more advanced stages of the disease. Indeed, GPX1 and SOD1 increase from 6 to 9 months of age in the Tg2576 hippocampus, suggesting a late response, not involving the peroxisomes. However, at 12 months, when amyloid plaques start to form, GPX1, SOD1 and SOD2 show significantly lower levels in the Tg2576 mice, with respect to WT. Accordingly, decreased activities of SOD1 and GPX have

been reported in patients with symptomatic AD by Casado *et al*. (2008). The situation observed in 12-month-old Tg2576 hippocampus, closely resembling that of SOD1 and of GPX1, may reflect a decreased ability of neurons of this region to respond to Aβ-mediated insult, possibly involving ROS generation.

A striking result regarding peroxisomes was obtained on 18-month-old mouse hippocampus. In fact, a peak of PMP70 expression is observed irrespective of the genotype, allowing to hypothesize a change in peroxisomal population related to the ageing process. Consistently, its main regulator, PPARα, shows intense immunoreactivity in the aged hippocampus, in both WT and Tg2576 animals. This late increase of peroxisomal number, not accompanied by induction of any of the peroxisomal matrix enzymes, may indicate the occurrence in the hippocampus of an attempt to counteract cellular damage, which however fails to result in improved efficiency of the organelles, either as ROS scavengers, or as lipid metabolizing sites. Indeed, AOX levels remain stably low at 18 months, while THL is dramatically decreased at the same age, allowing to hypothesize that inefficient β-oxidation is associated with normal and pathological aging. Antioxidant enzymes show protein-specific variations in the aged hippocampus. Overall, it is conceivable that a pro-oxidant environment is still present in the cytosol, rather than in peroxisomes, since decreased levels of GPX1 and SOD1 are observed in Tg2576 mice, while CAT is unchanged.

Concerning the characterization of the peroxisomal population in the neocortex, our data show a delayed response in this brain area, with respect to the hippocampus, as well as substantial region-based differences in the susceptibility to Aβ-mediated damage. The reason for this behaviour may relate to the relatively high anti-oxidant enzyme levels, which likely make the neocortex less susceptible to oxidative stress than the hippocampal formation (Cimini *et al*., 2009). In fact, at 3 months of age we failed to detect any variations in the expression levels of peroxisomal proteins. Nevertheless, catalase showed a delocalization, as assessed by immunoelectron microscopy, being found at extraperoxisomal sites, including the nucleus, cytosol, and post-synaptic densities. This evidence leads us to hypothesize that the presence of catalase to sensitive sites may contribute to enhancing protection against oxidative damage. The most relevant quantitative change in the neocortex are observed in 6-month-old Tg2576 mice, where significantly lower levels of peroxisomal proteins (PMP70, CAT) are detected, with respect to WT. Molecular data concerning peroxisomal β-oxidation enzymes show no statistically significant variations during aging or disease progression, indicating that no perturbation of this pathway occur in the neocortex.

In conclusion, while 3 months of age is an especially promising time point for Tg2576 mice for devising therapies aimed at delaying or even preventing AD onset (Cimini *et al*., 2009; D'Amelio *et al*., 2011), the 6-month-old time point seems a more critical period, in which different approaches could be designed to counteract AD-like neurodegeneration. Based on our results, we suggest that potential therapies using PPARα agonists may be beneficial around 6 months of age.

RIASSUNTO

La malattia di Alzheimer (AD) è la più comune forma di demenza dell'età adulta, caratterizzata da un progressivo e devastante disturbo neurodegenerativo che comporta un globale declino cognitivo, disturbi della memoria e del comportamento. Dal punto di vista istopatologico, fenomeni di gliosi e atrofia tissutale interessano inizialmente la corteccia temporale per poi estendersi anche a quella frontale. A livello microscopico le lesioni caratteristiche sono rappresentate da depositi proteici presenti sia nei compartimenti extracellulari, noti come placche amiloidi dovute all'aggregazione del peptide beta-amiloide (Aβ), sia in quelli intracellulari, noti come grovigli neurofibrillari, contenenti la proteina tau fosforilata.

È stato ampiamente dimostrato che il peptide Aβ, prodotto dalla proteolisi della proteina precursore dell'amiloide (APP), gioca un ruolo chiave nell'eziologia e nella patogenesi dell'AD. Una delle teorie più accreditate, nota come ipotesi della cascata amiloidea, pone l'accumulo di Aβ come principale causa della malattia. Secondo questa ipotesi, uno sbilanciamento tra la produzione di Aβ e il suo smaltimento porterebbe ad una progressiva degenerazione neuronale e a demenza. E' noto come il peptide Aβ eserciti un'azione neurotossica portando alla produzione di specie reattive dell'ossigeno (ROS) con conseguente stress ossidativo (Sayre *et al*., 2008).

Sebbene la tossicità indotta dall'Aβ sia ancora ampiamente riconosciuta, l'ipotesi della cascata amiloidea è stata recentemente messa in discussione da Nunomura (2010) il quale propone lo stress ossidativo come evento precoce nella patogenesi dell'AD.

L'importanza dei perossisomi nel funzionamento del sistema nervoso è nota sin dalla loro scoperta ed è rappresentata dal fatto che questi organelli sono coinvolti in un'ampia varietà di processi anabolici e catabolici, tra i quali il metabolismo delle ROS e dei lipidi (Schrader e Fahimi, 2008). E' stato dimostrato che la perdita dei perossisomi rende le cellule neuronali vulnerabili allo stresso ossidativo portando a degenerazione (Stamer *et al*., 2002); inoltre, la proliferazione perossisomiale attenua la tossicità Aβ-dipendente in neuroni ippocampali (Santos *et al*., 2005).

Queste evidenze ci hanno dunque spinto a pensare che i perossisomi giocassero un ruolo importante nella malattia di Alzheimer. Pertanto, lo scopo di questo progetto di Dottorato è stato quello di indagare il possibile coinvolgimento dei perossisomi all'esordio e durante la progressione della malattia, con particolare riferimento al loro ruolo nello stress ossidativo.

A questo proposito abbiamo scelto di analizzare una linea murina transgenica, Tg2576, che sovra-esprime un'isoforma Alzheimer-associata del precursore umano della proteina amiloide (APP). Questo modello ricapitola il fenotipo patologico tipico della malattia umana, pertanto rappresenta uno straordinario strumento per lo studio dei diversi meccanismi cellulari, biochimici, comportamentali ed

elettrofisiologici che caratterizzano in modo specifico le fasi precoci della malattia umana (Jacobsen *et al*., 2006, D'Amelio *et al*., 2011).
Lo studio è stato condotto su animali WT e Tg2576 di diverse età (3, 6, 9, 12, 18 mesi) al fine di analizzare le fasi precoci, avanzate e tardive della malattia. In particolare abbiamo focalizzato l'attenzione sulle due aree primariamente colpite dal danno neuronale, l'ippocampo e la corteccia cerebrale.
In una prima fase del progetto di ricerca abbiamo condotto un'analisi morfologica analizzando la distribuzione tissutale di *marker* neuronali e gliali in animali WT e Tg2576 di tutte le età considerate, al fine di individuare possibili alterazioni nell'organizzazione cerebrale. I nostri dati mostrano che la citoarchitettura è conservata durante l'invecchiamento fisiologico mentre, nel genotipo patologico, la stratificazione neuronale gradualmente cambia a partire dai 9 mesi risultando poi drammaticamente alterata a 18 mesi, età in cui sia l'ippocampo che la neocorteccia appaiono ricchi di astrociti iperproliferati ed ipertrofici e di cellule microgliali attivate.
L'analisi immunoistochimica condotta su sezioni incluse in paraffina di cervelli WT e Tg2576 a 18 mesi di età, con anticorpi diretti contro NeuN, GFAP e IbaI, rispettivamentente utilizzati come *marker* neuronali, astrocitari e microgliali, ha messo in luce le caratteristiche tipiche delle placche senili. In particolare, queste si estendono a tutti gli strati della corteccia da quelli più superficiali a quelli più profondi, causando imponenti alterazioni nell'organizzazione degli strati cellulari. Infatti i neuroni appaiono disorganizzati e orientati in maniera anomala a causa della presenza di estese placche amiloidi. Differentemente, nella formazione ippocampale, le placche sono preferenzialmente localizzate nello strato radiato del CA1 e del CA3, in siti distanti dai corpi cellulari delle cellule piramidali, così che il *layering* rimane conservato, anche se sono comunque evidenti alterazioni distrofiche dei prolungamenti neuritici. L'analisi morfologica ha inoltre evidenziato la presenza di numerosi astrociti fortemente positivi per la GFAP, i cui corpi cellulari sono disposti intorno alle placche, come a formare una barriera di contenimento, mentre i loro prolungamenti si inseriscono all'interno arricchendo il *core* della placca. Cellule microgliali attivate e immunopositive per Iba1 sono state inoltre trovate intorno e all'interno delle placche amiloidi.
I dati relativi al *pattern* di espressione di NeuN, non dimostrano alcuna variazione età- e genotipo-dipendente nel numero di cellule positive nonché nei livelli di immunocolorazione. Questa evidenza, in accordo con dati riportati da altri Autori (Jacobsen *et al*., 2006), suggerisce che non si verifica una massiva morte neuronale né durante il fisiologico invecchiamento né durante il progredire della malattia. Coerentemente con queste osservazioni riguardo alle alterazioni della citoarchitettura cerebrale, la colorazione con Rosso Congo ha dimostrato la presenza di piccole placche nella neocorteccia già a 9 mesi di età, mentre la prima comparsa a livello della formazione ippocampale si verifica a 18 mesi.

Il principale obiettivo di questo progetto di Dottorato è stato quello di analizzare possibili variazioni genotipo-dipendenti di varie proteine perossisomiali nell'ippocampo e nella neocorteccia di animali WT e Tg2576 all'esordio e durante la progressione della malattia. In particolare, è stata caratterizzata la popolazione perossisomiale da un punto di vista morfologico e molecolare, esaminando l'espressione di marcatori di biogenesi, proteine di membrana ed enzimi di matrice. Le analisi di *western blot* condotte su estratti proteici ippocampali di animali WT e Tg2576 alle diverse età considerate, hanno dimostrato una precoce e significativa induzione perossisomiale nell'ippocampo di animali Tg2576 di 3 mesi di età. Infatti, alti livelli della proteina perossisomiale di membrana PMP70 sono stati osservati nel genotipo patologico rispetto a quello normale. Per confermare questa induzione dei perossisomi in una fase così precoce della malattia, abbiamo condotto un'indagine di immunolocalizzazione ultrastrutturale "pre-embedding" per la PMP70. L'osservazione al microscopio elettronico ha confermato tale induzione poichè è stato osservato un più alto numero di perossisomi nei neuroni ippocampali di animali Tg2576 rispetto a quelli WT.

Dal momento che questi organuli svolgono un ruolo importante nel metabolismo lipidico, è stata esaminata l'espressione di due enzimi di matrice coinvolti nel *pathway* di β-ossidazione perossisomiale, l'acil-CoA ossidasi (AOX) e la tiolasi (THL), che catalizzano rispettivamente la prima e l'ultima reazione del ciclo. I nostri dati biochimici e morfologici dimostrano che il pattern di espressione dell'AOX è conforme a quello della PMP70, in quanto più alti livelli di AOX sono presenti nell'ippocampo di animali Tg2576 rispetto alla controparte WT.

Sorprendentemente, la tiolasi non mostra variazioni genotipo-dipendenti a 3 mesi, indicando una possibile inefficienza della via di β-ossidazione negli animali Tg2576. Questo potrebbe implicare un accumulo cerebrale di intermedi lipidici derivati dai VLCFA, cosa che è stata recentemente dimostrata verificarsi nel cervello di pazienti affetti da AD (Kou *et al*., 2011).

L'induzione di AOX osservata nella fase di esordio della malattia, potrebbe causare un accumulo di perossido di idrogeno, dal momento che l'AOX è un'ossidasi che produce H_2O_2. Pertanto abbiamo analizzato l'espressione di alcuni enzimi ROS-*scavenger*, focalizzando in primo luogo l'attenzione sulla catalasi (CAT), l'enzima perossisomiale di matrice per eccellenza. Tale proteina non mostra alcuna differenza genotipo-dipendente nell'ippocampo di 3 mesi, suggerendo quindi che l'eccessiva produzione di H_2O_2 da parte dell'AOX non sia accompagnata da una sua efficiente rimozione.

Abbiamo poi esteso l'analisi ad altri enzimi coinvolti nella difesa antiossidante, quali la glutatione perossidasi (GPX1), e le superossido dismutasi (SOD1 e SOD2). E' da notare che i suddetti enzimi, pur essendo principalmente localizzati in altri distretti cellulari (la GPX1 e la SOD1 nel citosol, la SOD2 nei mitocondri), sono stati recentemente trovati anche all'interno dei perossisomi (Schrader e Fahimi, 2006).

I nostri risultati riguardanti l'espressione di catalasi, GPX1 e SOD1, che mostrano livelli relativamente bassi nell'ippocampo di animali Tg2576, supportano fortemente l'idea che condizioni di stress ossidativo si instaurino precocemente, rappresentando forse il *primum movens* nella cascata di eventi patogenetici che caratterizzano l'AD (Nunomura *et al*., 2010). A tal proposito, vale la pena sottolineare come la SOD2 sia incrementata nell'ippocampo di animali Tg2576 di 3 mesi di età. In contrasto con il suo comune ruolo di *scavenger*, l'enzima potrebbe, in questo contesto, agire come molecola pro-ossidante, dal momento che questo enzima converte lo ione superossido in H_2O_2. In assenza di un concomitante incremento degli enzimi che smaltiscono l'H_2O_2, la SOD2 potrebbe essa stessa contribuire ad uno sbilanciamento redox.
Per verificare l'esistenza di uno stress ossidativo precoce, abbiamo condotto analisi immunoistochimiche utilizzando due *marker* di danno ossidativo, l'acroleina e l'8-idrossiguanosina, per individuare rispettivamente modificazioni ossidative a carico dei lipidi e degli acidi nucleici. Abbiamo così potuto dimostrare la presenza di alti livelli di immunoreattività negli animali Tg2576 rispetto a quelli WT già a 3 mesi di età.
La presenza di lipidi ossidati nel tessuto ippocampale transgenico porta ad ipotizzare che questi comprendano ligandi del PPARα, in accordo con quanto riportato in letteratura (Yeldandi *et al*., 2000). Pertanto, si può ragionevolmente supporre che la proliferazione perossisomiale sia indotta dall'attivazione del PPARα da parte di specie lipidiche ossidate, generate in seguito ad uno squilibrio redox che presumibilmente coinvolge primariamente il mitocondrio. L'intervento del PPARα è supportato dai dati di immunoistochimica che mostrano elevati livelli del recettore nell'ippocampo di topo Tg2576 di 3 mesi. Inoltre, la microscopia elettronica dimostra la presenza del recettore nel compartimento nucleare di neuroni ippocampali transgenici, dove svolge la sua funzione di fattore di trascrizione. In questo contesto, i perossisomi proliferati, più ricchi di ossidasi che di catalasi, non sarebbero però in grado di sopperire alla richiesta di degradazione di ROS, ma piuttosto, contribuirebbero alla loro formazione, determinando così un danno ossidativo auto-sostenuto.
Durante la progressione della malattia, la popolazione perossisomiale subisce drammatici cambiamenti, infatti i livelli di espressione della PMP70, Pex14p e AOX sono fortemente diminuiti nell'ippocampo di animali Tg2576 di 6 mesi di età. Questa diminuzione potrebbe essere dovuta sia ad una danneggiata biogenesi perossisomiale, sia ad una rimozione mediante processi autofagici degli organelli in eccesso.
E' interessante notare come, nell'ippocampo, alti livelli di CAT sono osservati a questa età nel genotipo patologico, suggerendo una risposta tardiva di questa specifica proteina all'induzione perossisomiale. Questa evidenza è in accordo con dati presenti in letteratura su quanto si verifica nel fegato in seguito a somministrazione di agonisti dei proliferatori perossisomiali (Reddy *et al*., 1986).

A 9 e 12 mesi, i livelli ippocampali di PMP70, AOX e THL sono relativamente stabili in entrambi le condizioni genetiche mentre gli enzimi antiossidanti mostrano interessanti cambiamenti a stadi avanzati della malattia. Infatti, a 12 mesi, età in cui le prime placche iniziano a formarsi a livello della formazione ippocampale, GPX1, SOD1 and SOD2 mostrano livelli significativamente più bassi di espressione negli animali Tg2576, rispetto a quelli WT. I nostri dati sono in accordo con quanto dimostrato da Casado e coll. (2008) riguardo al fatto che pazienti con una patologia AD conclamata mostrano una diminuita attività di SOD1 e GPX1 rispetto a soggetti di controllo. Pertanto, la situazione riscontrata a 12 mesi nell'ippocampo di animali Tg2576 può riflettere una diminuita capacità dei neuroni ippocampali di rispondere all'insulto mediato dal peptide Aβ, portando alla produzione di ROS.

Un sorprendente risultato riguardante i perossisomi riguarda l'analisi degli estratti proteici ippocampali di animali a 18 mesi, età in cui un picco di espressione di PMP70 è stato osservato in entrambi i genotipi, suggerendo un cambiamento nella popolazione perossisomiale correlato al processo di invecchiamento. Coerentemente, anche il PPARα mostra un'intensa immunoreattività nell'ippocampo di 18 mesi, sia negli animali WT che in quelli Tg2576. Questo tardivo incremento del numero dei perossisomi non accompagnato da alcuna induzione degli enzimi di matrice, potrebbe indicare un tentativo di contrastare il danno cellulare, cui però non corrisponde una migliorata funzionalità degli organelli. Infatti a 18 mesi i livelli di AOX rimangono stabilmente bassi mentre la THL è drammaticamente diminuita, dimostrando che un inefficiente metabolismo lipidico era associato sia al fisiologico che al patologico invecchiamento.

A questa età le difese antiossidanti mostrano delle variazioni proteina-specifiche facendoci supporre che un ambiente pro-ossidante sia ancora presente nel citosol piuttosto che nei perossisomi, da momento che i livelli di GPX1 e di SOD1 sono diminuiti negli animali Tg2576 mentre la CAT rimane invariata.

La suscettibilità al danno Aβ-mediato appare fortemente correlata all'area cerebrale considerata. Infatti i nostri risultati sulla corteccia cerebrale, mostrano una risposta ritardata di quest'area rispetto a quanto si verifica nell'ippocampo. La ragione di questo diverso comportamento potrebbe risiedere nel fatto che la neocorteccia ha relativamente più alti livelli di enzimi anti-ossidanti che la rendono meno suscettibile al danno ossidativo rispetto all'ippocampo (Cimini *et al*., 2009).

A 3 mesi non osserviamo nessuna variazione nei livelli di espressione delle proteine perossisomiali. In maniera rilevante, l'analisi immunoistochimica per la CAT su sezioni di corteccia cerebrale ha evidenziato una delocalizzazione della proteina nei neuroni degli animali Tg2576. Questa è stata verificata con esperimenti di microscopia elettronica che hanno dimostrato la presenza di immunoprecipitati anche in siti extraperossisomiali come il nucleo, il citosol e le densità post-sinaptiche. Questa evidenza ci ha spinto a ipotizzare che la presenza di catalasi in siti sensibili possa contribuire ad incrementare la protezione contro il danno ossidativo.

I cambiamenti più rilevanti da un punto di vista quantitativo che coinvolgono la neocorteccia, si osservano a 6 mesi, quando livelli significativamente bassi di proteine perossisomiali (PMP70, CAT) sono presenti negli animali Tg2576 rispetto ai controlli WT.

Dati molecolari riguardanti gli enzimi coinvolti nel *pathway* di β-ossidazione perossisomiale non mostrano differenze statisticamente significative durante il normale invecchiamento o durante la progressione della malattia, dimostrando che nessuna perturbazione di questo ciclo interessa la neocorteccia.

Riguardo l'espressione degli enzimi antiossidanti, la GPX1 mostra un picco di espressione nella corteccia di animali transgenici di 9 mesi. Questa evidenza, insieme all'incremento dei livelli di SOD1 e SOD2 a 12 mesi, fa supporre una risposta antiossidante compensatoria nella neocorteccia, concomitante con la deposizione delle placche senili, in accordo con dati di altri Autori (Papolla *et al*., 1998; Smith *et al*., 1998; Apelt *et al*., 2004). In particolare, si suppone un ruolo specifico dello ione superossido nel mediare l'azione neurotossica dell'Aβ (Keller *et al*., 1998; Celsi *et al*., 2004).

In conclusione, i risultati ottenuti nel corso del mio progetto di Dottorato dimostrano che cambiamenti molecolari che coinvolgono i perossisomi, avvengono precocemente a livello della formazione ippocampale negli animali Tg2576.

I 3 mesi di età rappresentano un *time-point* particolarmente promettente per disegnare terapie farmacologiche volte a prevenire o ritardare l'esordio della malattia (Cimini *et al*., 2009; D'Amelio *et al*., 2011). Noi crediamo che a questa età sarebbero opportuni trattamenti con molecole antiossidanti che avessero come *target* primario lo stress ossidativo. Molteplici sono i lavori presenti in letteratura che prendono in esame gli effetti di agonisti dei PPAR in diversi modelli murini di AD (Mandrekar-Colucci e Landreth, 2011). Queste molecole sono in grado di agire contrastando i processi infiammatori e il danno ossidativo attraverso differenti vie di segnalazione. Tuttavia, l'uso di ligandi del PPARα, a nostro avviso, dovrebbe essere considerato con qualche *caveat* riguardo il periodo di trattamento. Infatti, l'induzione perossisomiale potrebbe risultare dannosa a 3 mesi di età negli animali Tg2576 dal momento che potrebbe esacerbare il danno neuronale mediato dall'H_2O_2. Sulla base dei nostri risultati noi suggeriamo che la somministrazione di agonisti del PPARα debba avvenire intorno ai 6 mesi di età, al fine di revertire i sintomi iniziali tra cui le disfunzioni del metabolismo lipidico.

Section I

Introduction and Objectives

Chapter 1
Alzheimer's Disease

Alzheimer's disease (AD) is the most common form of dementia, accounting for 60-80% of all cases. The prevalence of dementia is below 1% in individuals aged 60-64 years, but shows an almost exponential increase with age, so that in people aged 85 years or older the prevalence is between 25% and 50% in the Western world (Finder, 2010).
This neurodegenerative disorder is characterized by a progressive decline in cognitive function, which typically begins with deterioration in memory and behavioural deficits. The gradual loss of independence of the patient leads to a heavy personal and financial toll on the family, resulting as major public-health problem that afflicts an estimated 24 million people in the world, with an expected increase to over 81 million people by the year 2040, mainly due to increased life expectancy (Ferri *et al*., 2005).
Besides ageing, which is a major risk factor for the disease, epidemiological studies have suggested several tentative associations. Reduced brain size, low educational and occupational attainment, low mental ability in early life, and reduced mental and physical activity during late life can be linked to AD (Mayeux, 2003; Ballard *et al*., 2011). Other risk factors are associated with vascular disease, including hypercholesterolaemia, hypertension, atherosclerosis, smoking, obesity, and diabetes. Nevertheless, while vascular risk factors and cerebrovascular disease clearly underlie vascular dementia, an etiological role for vascular changes in amyloid β (Aβ) deposition and, hence, AD remains unclear (Reitz *et al*., 2011).

1.1 Forms of AD

Alzheimer's disease is a heterogeneous disorder that is usually classified according to its age of manifestation in: early-onset AD (EOAD) and late-onset AD (LOAD), called also sporadic form. These two forms are clinically indistinguishable; however, the former is generally more severe than the latter and it is associated with a more rapid progression. Moreover, the two forms of AD are associated with different patterns of genetic epidemiology (Bekris *et al*., 2010).

1.1.1 EOAD

EOAD is an autosomal dominant disorder which accounts for 1 to 6% of all cases, ranging roughly from 30 to 65 years. The only identified deterministic factors causing EOAD are the presence of mutations in the amyloid precursor protein gene (*APP*), located on chromosome 21, or in the presenilin genes (*PSEN1* and *PSEN2*), located respectively on chromosome 14 and 1 (Harvey *et al*., 2003).
AD-linked missense mutations in *APP* affect the processing of the encoded protein, since the mutations are positioned in or near the Aβ-coding exons 16 and 17. At present, 182 different AD-related mutations have been identified in *PSEN1*, while only 14 AD-linked mutations have been detected in *PSEN2* (Alzheimer Disease

Mutation Database, 2010). To summarize, all three AD genes lend support to a common pathogenic AD pathway, with a pivotal role for Aβ.

1.1.2 LOAD

LOAD, or sporadic form, is the most common form of AD and the majority (>95%) of the patients who develop this disease are aged more than 65 years. Although environmental factors can increase the risk of developing sporadic form of AD, behind it there is a significant genetic background. An association between the apolipoprotein E (*APOE*) ε4 allele and AD has been reported by Poirier *et al.* (1993). *APOE* ε4 allele advances the clinical onset of the disease by almost 10 years (Blennow *et al*., 2006) and its presence is associated with memory impairment, Mild Cognitive Impairment (MCI), and progression from MCI to dementia (Farlow *et al*., 2004).

The molecular mechanism by which ApoE would act is not completely clear. It is known that this lipoprotein acts as a cholesterol transporter in the brain with ε4 isoform being less efficient than the other variations (*APOE* ε2, and *APOE* ε3), resulting in a low recovery of membrane lipids and neuronal repair (Poirier *et al*., 1993). On the other hand, ApoE is essential for Aβ deposition, promoting plaques formation possibly by acting as a pathological chaperone (Holtzman *et al*., 2000).

Therefore, the APOE ε4 allele has been calculated to account for most of the genetic risk in LOAD (Raber *et al*., 2004).

1.2 Mild Cognitive Impairment (MCI)

In most cases, AD begins insidiously with cognitive and memory deficits that can be confused with the reduction of the ability to learn new information, that is physiological during brain aging (Forlenza *et al*., 2010).

Therefore, it is a difficult task to clinically differentiate incipient AD from normal cognitive aging and from the subtle cognitive changes that arise in other forms of dementia. Individuals in predementia stage of AD have been most commonly categorized according to the definition of Mild Cognitive Impaimernt (MCI) (Petersen *et al*., 1999) (Fig. 1.1).

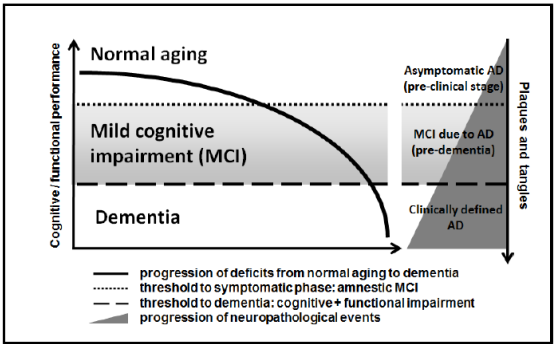

Fig. 1.1 Progression of cognitive and functional impairment and of neuropathological events in the transition from asymptomatic AD to MCI and clinically defined dementia of the AD type *(Forlenza et al., 2010).*

This idea was introduced to define an intermediate stage between normal

aging and clinical dementia and it is widely accepted today that the diagnosis of MCI selects a clinically and biologically heterogeneous group of patients. It is reasonable to assume that most patients who are prone to become demented will present at early stages symptoms compatible with the definition of MCI.

1.3 AD Histopathology

The major pathological hallmarks in the brain of AD patients are neurofibrillary tangles (NFTs), formed by hyperphosphorylated tau protein, and amyloid plaques, consisting of the Aβ peptide (Fig. 1.2). These lesions occur in brain regions involved in learning and memory, i.e. the hippocampus, the amigdala, and the cortical areas of the frontal, temporal and parietal lobes (Finder, 2010).

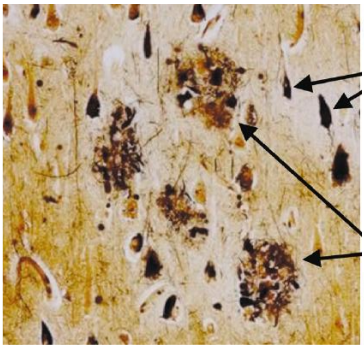

Fig. 1.2 Amyloid plaques and neurofibrillary tangles in the cerebral cortex in Alzheimer's disease. Plaques are extracellular deposits of Aβ surrounded by dystrophic neurites, reactive astrocytes, and microglia, whereas tangles are intracellular aggregates composed of a hyperphosphorylated form of the tau protein *(Blennow et al., 2006)*.

1.3.1 Neurofibrillary tangles and tau protein

Neurofibrillary tangles, which are intracellular filamentous inclusions, occur in AD and in other neurodegenerative disorders called tauopathies (Lee *et al*., 2001). The major component of the tangles is an abnormally hyperphosphorylated and aggregated form of tau.

Tau phosphorylation is regulated by the balance between multiple kinases, including glycogen synthase kinase 3β (GSK3β) and cyclin-dependent kinase 5 (CDK5), and serine/threonine phosphatases (PP-1 and PP-2A) (Iqbal *et al*., 2005). Tau hyperphosphorylation in AD starts intracellularly and leads to sequestration of normal tau, causing disassembly of microtubules and compromised axonal transport and synaptic function (Fig. 1.3).

There has been controversy over whether and how neurofibrillary tangles and amyloid plaques are pathogenically related to each other and to the neuronal and synaptic losses that characterise the disease. However, experimental evidence indicates that Aβ accumulation enhances tau aggregation (Lewis *et al*., 2001) and that Aβ-induced neurodegeneration and cognitive deficits requires the presence of endogenous tau (Rapoport *et al*., 2002; Roberson *et al*., 2007), thus suggesting a strong relationship between the two pathological events.

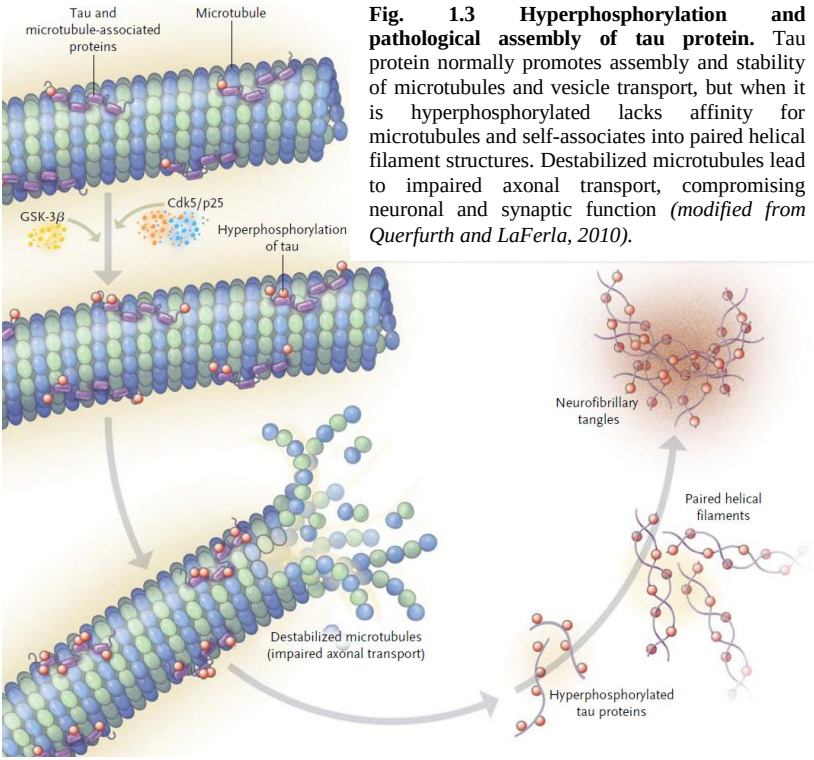

Fig. 1.3 Hyperphosphorylation and pathological assembly of tau protein. Tau protein normally promotes assembly and stability of microtubules and vesicle transport, but when it is hyperphosphorylated lacks affinity for microtubules and self-associates into paired helical filament structures. Destabilized microtubules lead to impaired axonal transport, compromising neuronal and synaptic function *(modified from Querfurth and LaFerla, 2010).*

1.3.2 Amyloid plaques and APP processing

The amyloid cascade hypothesis, which was formulated in the early 1990s, proposes that Aβ aggregation is upstream of all other pathological events (Hardy and Higgins, 1992; Hardy and Selkoe, 2002).

Aβ peptides originate from proteolysis of the APP by the sequential enzymatic action of two aspartyl proteases referred to as β-secretase (β-site amyloid precursor protein–cleaving enzyme 1, BACE-1), and γ-secretase, a protein complex with presenilin 1 at its catalytic core (Querfurth and LaFerla, 2010). This processing of APP is called amyloidogenic pathway, as opposed to the nonamyloidogenic pathway (Fig. 1.4).

Levels of different Aβ species can be elevated by enhanced production and/or reduced clearance; in particular, the Aβ42/Aβ40 ratio can be augmented, leading to a relative increase of soluble Aβ42 species that enhance oligomer formation, which causes subtle but permanent changes of synaptic function. In parallel, local inflammatory responses (microgliosis and astrocytosis) are observed, and synaptic spine loss and neuritic dystrophy also occur.

Over time, these events result in oxidative stress and altered neuronal ionic homeostasis, followed by hyperphosphorylation of tau protein. The cascade

culminates in widespread synaptic/neuronal dysfunction and cell death, leading to progressive dementia associated with extensive Aβ and tau pathology (Haass and Selkoe, 2007). This idea is also based on studies of genetic forms of AD, including Down's syndrome (Glenner and Wong, 1984; Busciglio *et al*., 2002), and by evidence that soluble Aβ42 oligomers and intermediate amyloid fibrils are neurotoxic *in vitro* and *in vivo* (Walsh and Selkoe, 2007).

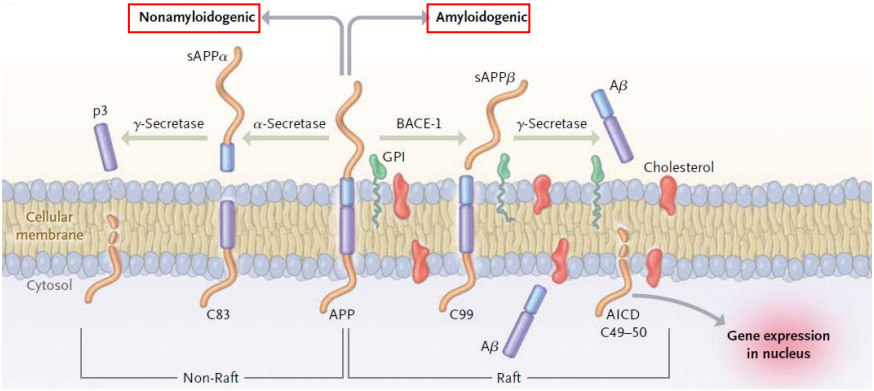

Fig. 1.4 Processing of APP: nonamyloidogenic and amyloidogenic pathways. APP is a transmembrane protein with a large N-terminal extracellular tail. In the first pathway, cleavage by α-secretase releases the soluble APP fragment (sAPPα). An 83-residue carboxy-terminal fragment (C83) is then digested by γ-secretase, liberating extracellular p3 and the amyloid intracellular domain (AICD) that is metabolised in the cytoplasm. Amyloidogenic processing is initiated by BACE-1, releasing a shortened sAPPβ. The retained C99 is also cleaved by γ-secretase complex, resulting in the production of several major Aβ species (Aβ38, Aβ40, Aβ42). A small tail of 50 amino acids (AICD fragment) is also released into the cytoplasm and targeted to the nucleus *(modified from Querfurth and LaFerla, 2010).*

It is worth mentioning that prior to the appearance of extracellular deposits, intraneuronal accumulation of amyloid oligomers and fibrils occurs in the hippocampus (Shie *et al*., 2003; Wirths *et al*., 2004). Takahashi *et al*. (2004) using immunoelectron microscopy showed intraneuronal Aβ42 in APP-transgenic mice in multivesicular bodies within dystrophic neurites. Recently, a 3D reconstruction study revealed fibrillar Aβ within individual synaptic compartments, in association with abnormal morphology (Capetillo-Zarate *et al*., 2011).

1.4 Role of oxidative stress in Aβ-mediated neurotoxicity

The mechanisms involved in Aβ toxicity are unknown, but there is evidence suggesting that oxidative stress plays a key role in AD pathogenesis, being considered as the common effecter of the cascade of degenerative events in this disorder (Sayre *et al*., 2008; Gella and Durany, 2009; Sultana and Butterfield, 2010). Oxidative stress occurs due to an imbalance in radical production of reactive oxygen species (ROS) and antioxidant defences. Evidence of oxidative

stress in AD is manifested through high levels of oxidised proteins, advanced glycation end products, lipid peroxides, and oxidative modifications to nuclear and mitochondrial DNA, as well as to cytoplasmic RNA (Lovell *et al*., 1995; Praticò *et al*., 1998; Nunomura *et al*., 2001). Consistently, impairment of cognitive and memory functions in preclinical AD correlate with decreased antioxidant defence mechanisms (Smith *et al*., 2010; Jomova *et al*., 2010).

It was demonstrated that intraneuronal Aβ has a causal role in neuronal oxidative damage because higher concentrations of Aβ lead to oxidative stress in various biological systems (Behl *et al*., 1994;Tabner *et al*., 2005). In fact, Aβ peptide itself is a source of hydrogen peroxide (H_2O_2) through metal ion reduction, with concomitant release of thiobarbituric acid-reactive substances (TBARS), a process probably mediated by formation of hydroxyl radicals (Miranda et al., 2000).

However, another line of experiments suggests a primary role for oxidative stress in the production and accumulation of Aβ *in vitro* and *in vivo* (Shen *et al*., 2008; Dumont *et al*., 2009). Indeed, a long period of gradual oxidative stress precedes and leads to the pathological AD symptoms, including Aβ deposition, neurofibrillary tangle formation, metabolic dysfunction, and cognitive decline (Bonda *et al*., 2010). In this view, it is worth noting that Aβ peptide can act as an antioxidant, suggesting a scenario in which intraneuronal Aβ accumulation represents a compensatory response to neuronal oxidative stress (Nunomura *et al*., 2010).

1.5 Transgenic mouse models of AD

Several animal models of AD offer the possibility to study at the molecular level some of the typical aspects of human disease (Fig. 1.5) (Elder *et al*., 2010).

Since mutations in the presenilin genes (*PS1* and *PS2*) are the most commonly recognized causes of early-onset AD, the respective mutant transgenic lines have been generated. These strains show impaired γ-secretase-mediated proteolytic cleavage of APP, resulting in increased Aβ42/Aβ40 ratio. While singly transgenic PS1 or PS2 mice do not develop plaques, when crossed with plaque-forming APP lines, earlier and more extensive plaque formation is found.

Different transgenic mouse lines were generated relying on strong promoters to drive expression of APP transgenes containing single or multiple familial AD mutations. Among these, APP23 transgenic mice, carry the double mutation Lys670 → Asn, Met671→ Leu (K670N,M67IL), which was found in a large Swedish family with early-onset AD, under the control of the mouse Thy-1 promoter. This strain develops cerebral amyloid angiopathy in addition to amyloid plaques, that appear at 6 months of age (Calhoun *et al*., 1999). TgCRND8 mice, in which a prion protein (PrP) promoter is used to drive expression of multiple APP mutations (Swedish and Indiana), are characterized by earlier and more dramatic amyloid deposition (Chishti *et al*., 2001). Another interesting model is represented by Tg2576 mouse strain, produced by Hsiao *et al*. (1996), the distinctive features of which are described below (1.5.1).

Line	Promoter	FAD Mutation	Amyloid Pathology
PDAPP	PDGF	APP-Indiana	Parenchymal plaques at 6–9 months of age
Tg2576	PrP	APP-Swedish	Parenchymal plaques by 11–13 months of age with some vascular amyloid
APP23	Thy-1	APP-Swedish	Parenchymal plaques by 6 months of age and prominent vascular deposition of amyloid
TgCRND8	PrP	APP-Swedish + Indiana	More aggressive parenchymal plaque pathology present by 3 months of age
APP-Dutch	Thy-1	APPE693Q associated with hereditary cerebral hemorrhage with Dutch-type amyloidosis	Vascular deposition of amyloid with few parenchymal plaques
PS1M146V	PDGF	PS1M146V	Elevated Aβ42 without plaque pathology
PSAPP	PS1M146V × Tg2576	PS1M146V + APP-Swedish	Earlier and more extensive plaque pathology in comparison with Tg2576 alone
3xTg	Thy-1.2 and native mouse	Transgenes containing Thy-1.2–driven APP-Swedish and tau P301L were coinjected onto a homozygous PS1M146V knock-in background.	Parenchymal plaques by 6 months of age combined with tau pathology by 12 months of age

Fig. 1.5 Select AD mouse model *(modified from Elder et al., 2010).*

1.5.1 Tg2576 model

In the Tg2576 mouse line, human APP695 cDNA containing the Swedish double mutation was inserted into a hamster prion protein (PrP) cosmid vector (Hsiao *et al*., 1996). This was then introduced into individual cells by microinjection of embryos C57BL/6 X SJL/N F2, which have given rise to the founders. The resulting transgenic mice express the mutant amyloid precursor protein (APPSwe) leading to high Aβ levels in the neocortex and hippocampus (Kawarabayashi *et al*., 2001).

Differently from other mouse models, the Tg2576 strain is a slowly progressive AD model, offering the opportunity to study even subtle age-dependent alterations. Tg2576 mice are characterized by: i) behavioural deficits (Ashe, 2001; Westerman *et al*., 2002); ii) neuritic dystrophy and altered synaptic function, in the absence of massive neuronal loss (Irizarry *et al*., 1997); iii) astrogliosis, microgliosis and activation of inflammatory processes in relation to amyloidosis (Tehranian *et al*., 2001).

A detailed analysis of Tg2576 mice, including morphological, electrophysiological and behavioural characterization has been accomplished by Jacobsen *et al.* (2006), who demonstrated that neuronal deficits in Tg2576 mice are established in a time-dependent manner. The earliest changes include a decrease in spine density, deficits in hippocampal neurotransmission and *in vivo* memory impairments as measured by contextual fear conditioning (CFC). Slower onset deficits include an increase in amyloid load, reactive astrocytes, and microglia (Fig. 1.6).

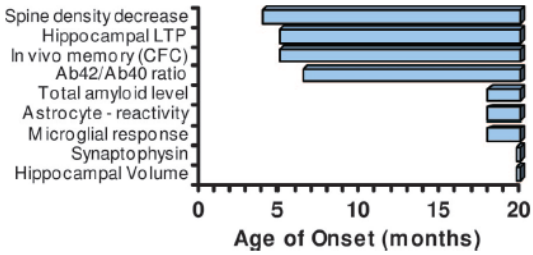

Fig. 1.6 Temporal progression of morphological and functional deficits in Tg2576 mice *(Jacobsen et al., 2006).*

Recently, the group I collaborate with has shown that the earliest signs of synaptic dysfunction in Tg2576 mice are detectable as early as 3 months of age (D'Amelio *et al.*, 2011). In particular, 3-month-old Tg2576 mice display enhanced caspase-3 activity in hippocampal CA1 synapses (Fig. 1.7), resulting in a downregulation of the surface expression of GluR1-containing AMPA receptor through proteolytic activation of calcineurin. GluR1 removal from the postsynaptic sites causes functional and structural synaptic alterations, resulting in glutamatergic transmission deficits, enhanced long-term depression (LTD), and reduced spine size and density.

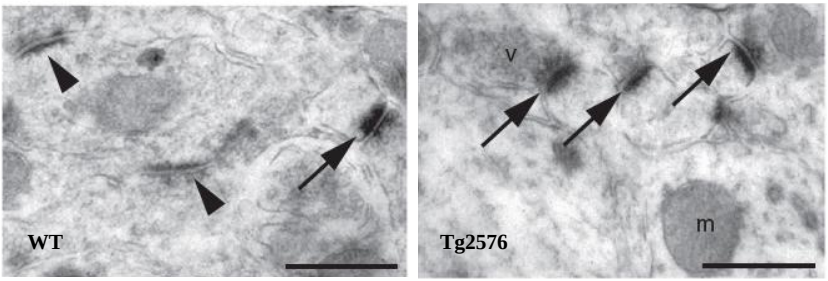

Fig. 1.7 Immunoelectron microscopy for cleaved caspase-3. Immunoreactive dendritic spines (arrows) are more numerous in Tg2576 hippocampus, compared to its WT counterpart. Arrowheads indicate caspase-3 negative post-synaptic densities *(D'Amelio et al., 2011)*.

In conclusion, D'Amelio's work provides strong evidence that caspase-3 plays a crucial non-apoptotic role for the early synaptic dysfunction, leading to impairment of memory performance, associated with Alzheimer-like pathology (D'Amelio *et al*., 2011).

Chapter 2
Peroxisomes

Peroxisomes were discovered in 1954 in mouse kidney by an electron microscopist (Rhodin, 1954). In 1966, De Duve and Baudhuin were the first to isolate peroxisomes from rat liver, and their biochemical studies led to the discovery of the colocalization of several H_2O_2-producing oxidases with the H_2O_2-degrading enzyme catalase in the matrix of peroxisomes. De Duve then proposed the functional term "peroxisome", which gradually replaced the former morphological designation, "microbody", coined by Rhodin.

Subsequent morphological studies revealed that peroxisomes are ubiquitous cytoplasmic organelles present in a wide variety of eukaryotic cells, from yeast to humans (Hruban *et al*., 1972). They display roughly spherical shape (0.1 - 1 μm in diameter), and a single-limiting membrane surrounding a finely granular matrix, which may contain crystalline inclusions (Fig. 2.1).

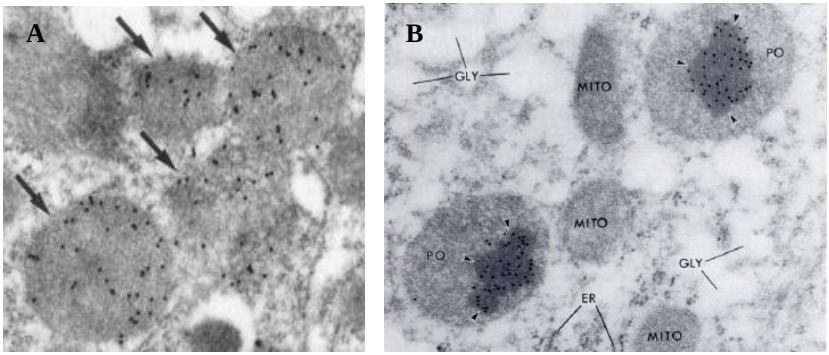

Fig. 2.1 Morphology and enzymatic content of mammalian peroxisomes. A) Immunoelectron microscopy of catalase in rat kidney, showing colloidal gold-labelled peroxisomes (arrows), with a finely granular matrix in the absence of a crystalline core. (*Moreno et al., 1995*). B) Immunoelectron microscopy of urate oxidase in rat liver, showing peroxisomes (PO), with a colloidal gold-labelled crystalline core. (*Volkl et al., 1988*).

Peroxisomes show a high heterogeneity with respect to morphology, protein content, and abundance in diverse tissues and during developmental processes, including aging (Stefanini *et al*., 1995; Terlecky *et al*., 2006). In the nervous tissue, they are especially small (0,1-0,2 μm in diameter), and their presence in neuronal and glial cells strongly relates to the brain region and cell population (McKenna *et al*., 1976; Arnold *et al.*, 1979; Cimini *et al*., 1993; Moreno *et al*., 1995, 1999; Farioli-Vecchioli *et al*., 2001; Schad *et al*., 2003).

Peroxisomes are also able to respond to environmental changes and extracellular stimuli by altering their enzyme content, morphology and abundance. Pharmacological studies have allowed identification of a class of chemically unrelated substances, collectively known as peroxisome proliferators, capable of

inducing remarkable increase in number and size of the organelles, especially in the liver (Reddy and Rao, 1987). Peroxisome proliferation is also accompanied by selective induction of peroxisomal proteins, mediated by peroxisome proliferator activated receptors (PPARs). These nuclear transcription factors (Issemann and Green, 1990) act as heterodimeric partners of other members of the same nuclear hormone receptor family, namely retinoid X receptors, and bind to the peroxisome proliferator response elements (PPREs) present on target genes.

The central role of peroxisomes in cell metabolism has emerged since their discovery (De Duve and Baudhuin, 1966), since they are involved in a wide range of anabolic and catabolic functions. This implies the presence of a large number of enzymes in the peroxisomal matrix. Indeed, about 50 metabolic enzymes have been identified in mammalian peroxisomes over the years. Moreover, some 32 proteins/genes, so-called peroxins (Pex), have been discovered, which are required for the biogenesis, assembly, and maintenance of functional peroxisomes (Platta and Erdmann 2007). Dysfunction of peroxins causes fatal human peroxisome biogenesis disorders (PBDs), which include the Zellweger syndrome spectrum (ZSS) disorders, neonatal adrenoleukodystrophy, infantile Refsum's disease and rhizomelic chondrodysplasia puntata (RCDP) type I (Fujiki, 2000; Steinberg *et al*., 2006). Interestingly, all the above human pathologies, as well as the knockout mouse models produced to mimic them, have severe neurological implications, thus emphasising the importance of peroxisomes in the differentiation and homeostasis of the nervous system (Baes, 2000; Depreter *et al*., 2003; Baes and Van Veldhoven, 2006).

2.1 Biogenesis of peroxisomes

Peroxisome formation, proliferation and maintenance have been debated for a long time, and the debate is not over.

The classic view considers peroxisomes as autonomous organelles, which form out of pre-existing peroxisomes, like mitochondria and chloroplasts (Lazarow and Fujiki, 1985). The "growth and division" model was supported by the discovery of the synthesis of peroxisomal proteins on free ribosomes, their post-translational transport into peroxisomes, and the observations of interconnections between peroxisomes. Notably, according to this model endoplasmic reticulum (ER) was deemed only to be a source of membrane lipids for the enlargement of pre-existing peroxisomes. Recent discoveries have challenged what has been considered for most of the past two decades the paradigm for peroxisome biogenesis.

According to the novel concept, ER contributes to peroxisome formation (Titorenko and Mullen, 2006). This model received strong support by the observation that loss of the peroxins Pex3p, Pex16p, or Pex19p, which are required for peroxisomal membrane protein (PMP) targeting/insertion, resulted in the absence of detectable peroxisomes/peroxisomal membranes, whereas reintroduction of the missing genes led to a *de novo* formation of peroxisomes from the ER. The Pex3p and Pex19p have been observed to initially localize to the

ER before maturing into import-competent peroxisomes, indicating that the ER is indeed the source of the newly synthesized membrane and organelle (Hoepfner *et al*., 2005). However, the physiological significance of the mechanism of *de novo* formation in comparison to the classical pathway of growth and division is still controversially discussed.

2.1.1 Peroxisomal matrix protein import

The protein import into peroxisomes is a complex process, which differs substantially from the import mechanisms into the ER, mitochondria or chloroplasts. The peroxisomes import fully folded, co-factor bound and even oligomeric proteins by shuttling receptors (Leon *et al*., 2006).

The import of most peroxisomal matrix proteins is mediated by two types of *cis*-acting peroxisomal targeting signals (PTSs): the C-terminal uncleavable tripeptide PTS1, and the nonapeptide presequence PTS2, located at the N-terminus. The PTS1- or PTS2-containing matrix proteins are recognized in the cytosol by soluble receptors (PTS1 by Pex5p, a tetra-tricopeptide repeat (TPR) domain protein, PTS2 by Pex7p, a WD40 domain protein), which guide them to a docking site at the peroxisomal membrane. After translocation of the receptor–cargo complex to the luminal side of the peroxisomal membrane, the cargo is released and the receptors shuttle back to the cytosol (Fujiki, 2000; Ma *et al*., 2011).

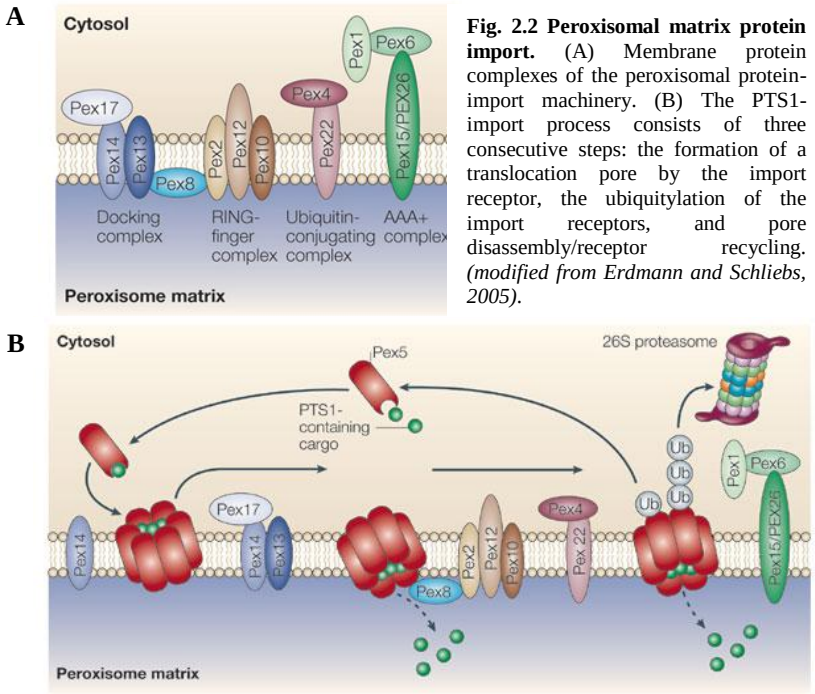

Fig. 2.2 Peroxisomal matrix protein import. (A) Membrane protein complexes of the peroxisomal protein-import machinery. (B) The PTS1-import process consists of three consecutive steps: the formation of a translocation pore by the import receptor, the ubiquitylation of the import receptors, and pore disassembly/receptor recycling. *(modified from Erdmann and Schliebs, 2005).*

In particular, upon the binding of PTS1 proteins, Pex5p (a tetrameric complex) disaggregates into dimers and is transported, in a currently unknown manner, to the peroxisome where it interacts with Pex14p and Pex13p. At the peroxisomal membrane, Pex14p is associated with Pex17p and at least temporarily with Pex13p. The putative peroxisomal import complex (importomer) is formed by the RING-finger subcomplex containing Pex2p, Pex10p and Pex12p, and the docking complex comprising Pex13p, Pex14p and Pex17p (Fig. 2.2). Both subcomplexes are linked via Pex8p, which contains both targeting sequences for peroxisomal matrix protein import (PTS1 and PTS2) (Meinecke *et al*., 2010).
How the cargo or the cargo–receptor complex is translocated across the peroxisomal membrane is completely unknown. Pex8p triggers the association of the docking and the RING-finger complex and might contribute to cargo release. At the end of the pathway, Pex5p is recycled back to the cytosol in an ATP-dependent manner (Heiland and Erdmann, 2005).

2.1.2 Peroxisomal membrane protein import

The targeting and insertion of PMPs require other components than those involved in peroxisomal matrix protein import and is less well understood.
Only three of the 32 peroxins so far identified– Pex3p, Pex16p and Pex19p – are demonstrably involved in this process. It has been suggested that there are at least two distinct classes of peroxisomal membrane proteins. Class I PMPs are post-translationally inserted into the peroxisomal membrane in a Pex19p- and Pex3p-dependent manner, while class II PMPs, such as Pex3p and tail-anchored PMPs, are independent of Pex19p. Accumulating evidence suggests that class II PMPs might be targeted to the ER prior to their transport to peroxisomes (Heiland and Erdmann 2005; Schrader and Fahimi, 2008).

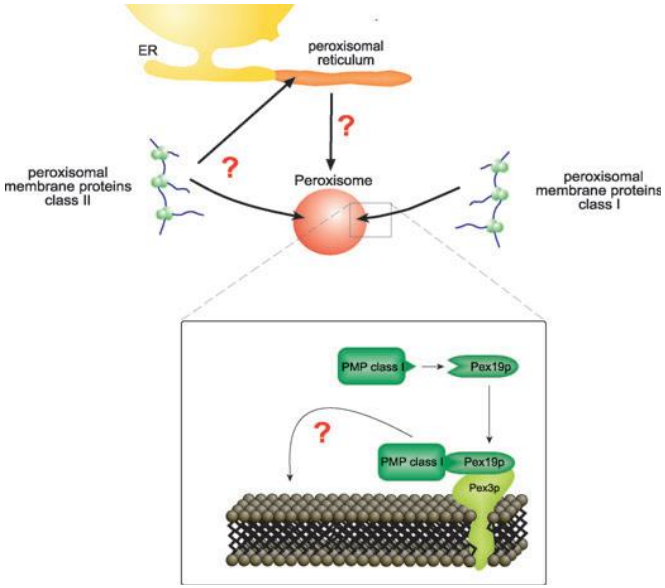

Fig. 2.3 Model of peroxisomal membrane biogenesis. Class I PMPs are recognized by Pex19p that directs them to the peroxisomal membrane. Membrane association of the Pex19p receptor–cargo complex is mediated by Pex3p. Topogenesis of class II PMPs is independent of Pex19p. These might be targeted to the ER prior to their transport to peroxisomes. How these proteins reach the ER and their final destination in the peroxisomal membrane is unknown *(Heiland and Erdmann, 2005).*

2.2 Metabolic functions of peroxisomes

Peroxisomes are involved in a wide range of anabolic and catabolic functions, including ROS metabolism (Schrader and Fahimi, 2006; Bonekamp *et al*., 2009), β-oxidation of very long chain fatty acids (VLCFAs) (Poirier *et al*., 2006; Wanders and Waterham, 2006), biosynthesis of polyunsaturated fatty acids (PUFAs) (Sprecher *et al*., 1995) and plasmalogens (Wanders 2004), cholesterol (Singh, 1997) and dolichol biosynthesis, and calcium homeostasis (Drago *et al*., 2008). The most relevant functions to the nervous tissue are described below.

2.2.1 ROS metabolism

Although mitochondria have been described as the major source of endogenous ROS generation (Rigoulet et al., 2011), peroxisomes have emerged as central organelles that play a key role in both production and scavenging of ROS (Schrader and Fahimi, 2006). This dual action derives from the fact that peroxisomes harbour both several H_2O_2-generating oxidases and antioxidant enzymes, including catalase (Fig. 2.3).

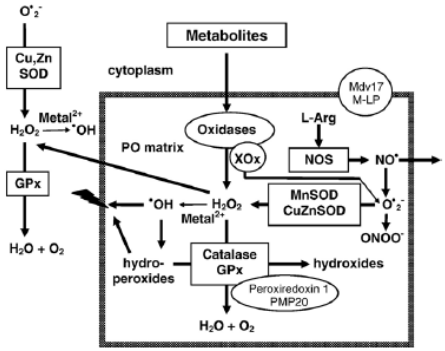

Fig. 2.3 Overview of peroxisomal ROS metabolism.
H_2O_2 is produced by several peroxisomal oxidases including XOx, and decomposed by catalase and GPx or converted to hydroxyl radicals (·OH). Hydroxyl radicals can damage the peroxisomal membrane by lipid peroxidation of unsaturated fatty acids. Peroxisomal oxidases also generate superoxide anions (O2·−) that are scavenged by MnSOD and CuZnSOD *(Schrader and Fahimi, 2006)*.

Peroxisomal oxidases include: (i) acyl-CoA oxidase (AOX, see below for pathway details); (ii) urate oxidase, involved in the final step of metabolic degradation of purines; (iii) xanthine oxidase (XOx) also involved in purine catabolism; (iv) D-amino acid oxidase; (v) D-aspartate oxidase; (vi) pipecolic acid oxidase; (vii) sarcosine oxidase; (viii) L-α-hydroxy acid oxidase; (ix) polyamine oxidase (Schrader and Fahimi, 2006).

Peroxisomal ROS-scavenging enzymes include: (i) catalase (CAT), which converts H_2O_2 into water through either the catalatic or the peroxidatic reaction; (ii) glutathione peroxidase (GPx), catalysing H_2O_2 removal with concomitant conversion of reduced glutathione (GSH) to glutathione disulfide (GSSG); (iii) copper zinc superoxide dismutase (CuZnSOD, SOD1) and manganese superoxide dismutase (MnSOD, SOD2), catalysing superoxide anion conversion into H_2O_2. While CAT is *bona fide* peroxisomal, all the other ROS-detoxifying enzymes are also present in other cell compartments. Oxidative balance within peroxisomes needs to be tightly regulated; shifting this equilibrium via endo- or exogenous

factors, aging or disease conditions leads to a deregulation of the system, causing oxidative stress (Bonekamp *et al.*, 2009).

2.2.2 Lipid metabolism

The main peroxisomal functions related to lipid metabolism have been recently reviewed by Wanders and coll. (2010). Fig. 2.4 summarizes the peroxisomal pathways of fatty acid α-oxidation (A), fatty acid β-oxidation (B, C, D), and plasmalogen biosynthesis (E).

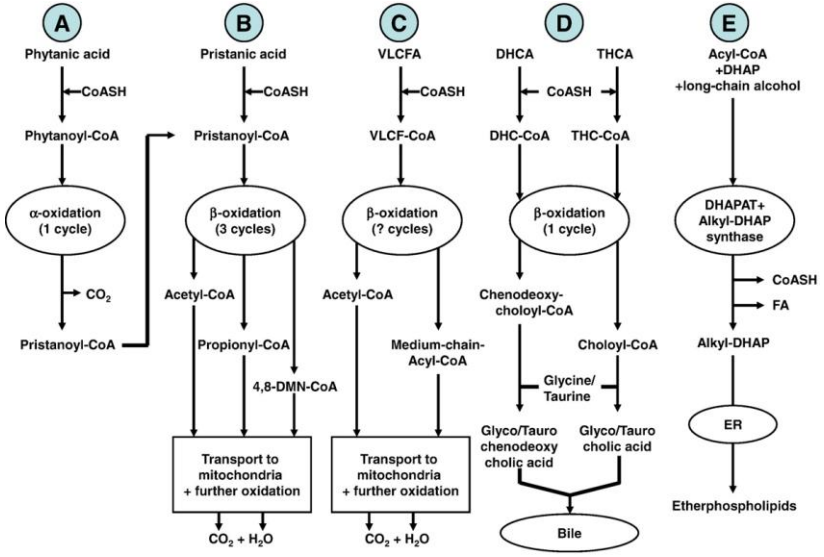

Fig. 2.4 A schematic representation of lipid metabolic pathways in peroxisomes.

(A) Peroxisomal α-oxidation pathway starts with activation of phytanic acid by hydroxylation to phytanoyl-CoA via phytanoyl-CoA hydroxylase. Then, phytanoyl-CoA is converted to pristanoyl-CoA and further oxidized as described in (B).

(B, C, D) Peroxisomal β-oxidation systems are involved in the oxidation of pristanic acid, very long chain fatty acids (VLCFA), and bile acid synthesis intermediates (dihydroxycholestanoic acid, DHCA, and trihydroxycholestanoic acid, THCA). In particular, pristanic acid undergoes three cycles of β-oxidation in peroxisomes to produce acetyl-CoA, propionyl-CoA, and 4,8-dimethylnonanoyl-CoA (4,8-DMN-CoA). Subsequently, these molecules are transported to the mitochondria for full oxidation to CO_2 and H_2O (B). For VLCFA β-oxidation, it has not been established yet how many cycles of β-oxidation take place in the peroxisomes (C). In liver, the bile acid intermediates DHCA and THCA undergo one cycle of β-oxidation in peroxisomes, with chenodeoxycholoyl-CoA and choloyl-CoA as end products, respectively. These two CoA-esters are then conjugated with either taurine or glycine within peroxisomes. Subsequently, the taurine- and glycine-esters are transported out of the peroxisome into the cytosolic space, to end up in bile (D).

(E) Etherphospholipid biosynthesis from acyl-CoA and dihydroxyacetone phosphate (DHAP) is catalyzed by dihydroxyacetone phosphate acyltransferase (DHAPAT) and alkyl-dihydroxyacetone phosphate synthase (alkyl-DHAP synthase), either localized in peroxisomes. Subsequently, the reduction of alkyl-DHAP to etherphospholipids can take place at the endoplasmic reticulum (ER) *(Wanders et al., 2010).*

Among these lipid-related functions, peroxisomal fatty acid β-oxidation, the details of which are illustrated in Fig. 2.5, is the most extensively characterized and attracts most attention, playing a central role in both catabolic and anabolic processes. In fact, it is not only essential to the degradation of several lipid species, but also participates in the biosynthetic pathway to polyunsaturated fatty acids (PUFAs).

The architecture of the peroxisomal β-oxidation system involves a set of four consecutive reactions: (1) dehydrogenation; (2) hydration (of the double bond); (3) dehydrogenation again; and (4) thiolytic cleavage. Through this 4-step pathway a 2-carbon unit is split from each fatty acid in the form of an acetyl-CoA unit, which can then be degraded in the citric acid (Krebs) cycle to produce CO_2 and H_2O (Fig. 2.5) (Wanders, 2004).

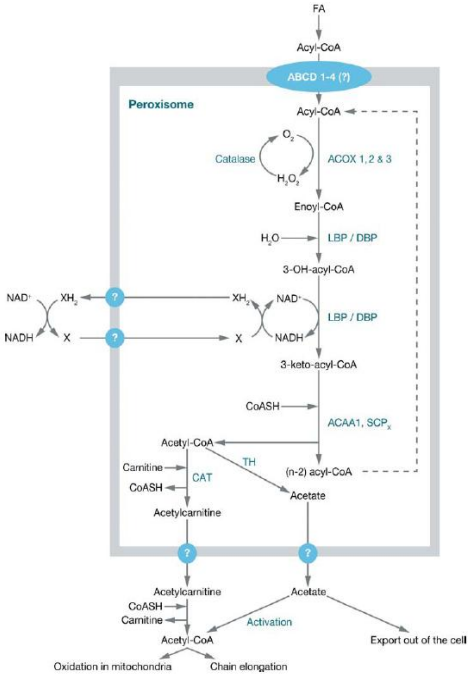

Fig. 2.5 Schematic representation of the peroxisomal β-oxidation pathway in humans. The first step is coupled to the reduction of molecular oxygen to H_2O_2 and catalyzed by acyl-CoA oxidase (ACOX), which is the first and rate-limiting enzyme of this pathway. In contrast with rat species, displaying three isoforms, human peroxisomes contain only two oxidases: the palmitoyl-CoA oxidase (ACOX1), that is specific for VLCFA, and the branched-chain acyl-CoA oxidase (ACOX2), involved in the pristanic acid β-oxidation and in the bile acid intermediates β-oxidation. The second and third steps are catalyzed by one of two so-called bifunctional proteins (LBP and DBP) harboring two separate enzymatic functions: enoyl-CoA hydratase and 3-hydroxy-acyl-CoA dehydrogenase activity. Finally, the last step of the pathway is carried out by two distinct enzymes, called 3-ketoacyl-CoA thiolase (ACAA1) and sterol carrier protein X (SCPx), capable of thiolytically cleaving 3-ketoacyl-CoA into a chain-shortened acyl-CoA and acetyl-CoA *(Wanders and Waterham, 2006).*

Interestingly, the transcriptional activation of genes involved in fatty acid oxidation in livers of rats and mice is regulated by α isotype of the peroxisome proliferator activated receptor (PPARα). Consistently, PPARα-null mice show deficiencies in peroxisomal fatty acyl-CoA oxidase, and in some of the other enzymes of the β-oxidation pathway, thus emphasizing the critical importance and prominent role of PPARα in lipid catabolism (Reddy and Hashimoto, 2001).

Chapter 3
Aims of the research project

The importance of peroxisomes for nervous system functioning is represented by their involvement in a wide variety of metabolic processes, including ROS and lipid metabolism. Concerning the maintenance of cellular redox status, peroxisomes participate in both ROS generation and removal. When this balance is disrupted towards ROS production, oxidative stress is generated.

The brain is prone to oxidative stress, and is inadequately equipped with antioxidant defence systems to prevent oxidative damage, leading to neurodegeneration. Notably, the nervous tissue is especially rich in PUFAs and plasmalogens, i.e., molecules especially susceptible to oxidative modifications (Lukiw and Bazan, 2008; Lessig and Fuchs, 2009). These lipids, whose biosynthesis partially occurs in peroxisomes, participate in several physiological processes in neural cells, ranging from regulation of membrane fluidity, to synaptic remodelling, to neuroprotection (Wanders and Waterham, 2006). Interestingly, decreases in plasmalogen content have been found in several neuropathological conditions, including Alzheimer's disease, dementia and ischemia and it has been proposed that plasmalogens may modulate the severity and progression of the disease (Goodenowe *et al*., 2007). Among PUFAs, docosahexaenoic acid (DHA; 22:6ω3) seems particularly relevant, since low dietary DHA is a factor increasing the risk of age-related cognitive decline and AD (Cunnane *et al*., 2009). However, the existing data favor a role of ω-3 PUFA supplementation in slowing cognitive decline in elderly individuals without dementia, but not for the prevention or treatment of dementia (including AD) (Fotuhi *et al*., 2009).

Normal peroxisomal metabolism is also required for several aspects of development of the nervous system. Indeed, peroxisomal dysfunctions in humans or mouse mutants are associated with white matter abnormalities, such as defects in myelination and axon degeneration (Faust *et al*., 2005; Hulshagen *et al*., 2008). Consistent with these findings, deficiency in PPARβ/δ, which is the most highly expressed PPAR isoform in oligodendrocytes, neurons, and astrocytes, results in brain developmental defects, including altered myelination and neuronal functioning in the CNS (Peters *et al*., 2000; Hall *et al*., 2008).

Moreover, peroxisomes play a key role in neuronal migration (Grabenbauer *et al*., 2001). For instance, peroxisome biogenesis disorders, among which Zellweger syndrome is the most severe, result in dramatically altered CNS neuronal migrations, causing heterotopias and defective cortical layering. Studies on PEX KO mice have shown that defects in neuronal differentiation, proliferation and survival may also contribute to CNS malformations (Baes and Van Veldhoven, 2006).

Consistent with their essential role in CNS development, peroxisomes are generally more abundant in differentiating neurons than in mature neurons and are

seen at sites such as axon terminals and dendrites, where they are rare in the mature nervous system (Arnold and Holtzman 1978; McKenna *et al*., 1976).
In the adult brain, peroxisomes are heterogeneously distributed along different subsets of neural cells. Immunocytochemical localization of catalase, which is a marker for peroxisomes, shows immunoreactivity in both neuronal and glial cells, albeit at different concentrations, correlating with cell size or type of neurotransmitter used in the nerve endings (Schad *et al*., 2003). Moreover, areas with lower amounts of peroxisomes have been correlated to a higher susceptibility to oxidative stress-related neurodegeneration, caused by acute events such as ischemia-reperfusion injury, or chronic neurodegenerative diseases, including AD. It is worth noting that many catalase-rich neurons, namely pyramidal cells of the hippocampal CA3 field and interneurons of the hippocampal formation, are spared in AD and highly resistant to ischemia-reperfusion injury. Conversely, catalase poor neurons in CA1 pyramidal layer and in the cerebral cortex, are prone to AD and extremely sensitive to ischemic damage (Moreno *et al*., 1995).
The involvement of peroxisomes in AD is strongly suggested by the direct link between peroxisomal proliferation and neuroprotection from Aβ-induced degenerative changes. Santos *et al*. (2005) demonstrated that exogenously administered Aβ peptide produces a decrease of peroxisomes in hippocampal neurons, concomitant to the appearance of neurodegeneration signs. Interestingly, in the same *in vitro* model, induction of peroxisomal proliferation attenuates Aβ-dependent toxicity.
These evidence prompted us to investigate the involvement of peroxisomes in AD, with special reference to their role in oxidative stress. We chose the transgenic strain Tg2576, which recapitulates human pathological phenotype and is especially suited to the study of early stages, for it is characterized by slow AD-like progression (Jacobsen *et al*., 2006). Our study was performed on early, advanced and late stages of the disease (3, 6, 9, 12, 18 months of age), focussing on the neocortex and hippocampus, i.e., the two areas where primary neuronal injury is known to occur. We chose to analyze female mice because epidemiological studies indicate that women have a higher risk of developing AD. Recent reports demonstrate that senile plaques are significantly more abundant in female Tg2576 mice than in males, suggesting that sex and/or endocrine factors strongly modulate cerebral β-amyloidogenesis in APP transgenic mice (Callahan *et al*., 2001; Hirata-Fukae *et al*., 2008).
As a preliminary step, we analyzed the distribution of neuronal and glial markers, in WT and Tg2576 ageing/diseased mice, in order to detect possible alterations in brain cytoarchitecture. Specifically, we used a neuronal marker (NeuN), an astrocyte marker (Glial Fibrillary Acidic Protein, GFAP), and a microglial marker (Ionized calcium-Binding Adaptor molecule 1, Iba1). Additionally, Congo Red staining was performed to study the appearance of amyloid plaques in the hippocampus and neocortex.
Next objective of my Ph.D. project was to characterize brain peroxisomes in 3-

month-old animals, which had so far been considered a pre-symptomatic stage (Jacobsen *et al*., 2006). Importantly, while our study was progressing, a paper from the group I collaborate with was published demonstrating that the onset of the disease can be established at the age of 3 months (D'Amelio *et al*., 2011). This finding strengthens the importance of the chosen age of this study, as 3 months may represent a good stage to recognize novel early AD markers, and the optimal temporal window for possible therapeutic intervention.

We comparatively studied the expression of several peroxisome-related markers in Tg2576 and WT neocortex and hippocampus, by biochemical and morphological techniques. Particularly, to determine the overall size of the peroxisomal population in the neocortex and hippocampus of 3-months-old Tg2576 mice, compared to WT mice, we investigated the immunolocalization of Peroxisomal Membrane Protein (PMP70), which according to Santos is a marker for peroxisomal population size (Santos *et al*., 1994). The protein expression of the peroxins Pex5p and Pex14p, were also investigated, to obtain some insight into possible alterations of peroxisomal biogenesis. Moreover, to investigate the presence of peroxisomes in neocortical and hippocampal neurons as well as in astroglial cells, we performed double immunofluorescence experiments of PMP70 in combination with NeuN and GFAP. I then analysed proteins belonging to the peroxisomal β-oxidation pathway, namely acyl-CoA-oxidase (AOX), which is the rate-limiting enzyme catalizing the first step of the cycle, and thiolase (THL), last enzyme of the pathway.

To deepen the study on the regulation of peroxisomal biogenesis in AD, I also investigated the distribution of peroxisome proliferator-activated receptors (PPARs), a family of ligand-activated transcription factors, belonging to the superfamily of nuclear receptors. Among these, PPARα seems especially relevant, for its direct involvement in peroxisomal induction, and for its recently proposed neuroprotective role in age-related inflammation (Chung *et al*., 2008). Specifically, I analyzed the PPARα intracellular distribution by immunoelectron microscopy to test its functional state, as a nuclear transcription factor.

Since peroxisomes play an important role in the protection against ROS, we assessed the protein levels of the H_2O_2-scavenging enzymes as catalase (CAT) and selenium-dependent glutathione peroxidase (GPX1), the former being selectively localized to peroxisomes and the latter being found inside these organelles, besides other cytoplasmic compartments. Based on light microscopic results, indicating extra-peroxisomal localization of catalase in 3-month-old Tg2576 hippocampus, we examined in further details its intracellular distribution, by ultrastructural analysis performed after catalase pre-embedding immunolocalization.

The study was then extended to advanced and late stages of Alzheimer's like disease, monitoring age- and genotype-dependent variations in the morphological distribution and protein levels of peroxisome-related proteins. The expression patterns of 3-, 6-, 9-, 12-, and 18-month-old Tg2576 mouse neocortex and hippocampus were compared with those of their WT counterparts, representing a

model for physiological aging. Notably, an involvement of peroxisomes in cell senescence has been demonstrated, particularly concerning the biogenesis of these organelles (Terlecky *et al*., 2006).

To further address the issue of the role of oxidative stress in AD progression, we assessed antioxidant response by analyzing other ROS-scavenging enzymes, namely Cu,Zn-superoxide dismutase (SOD1) and Mn-superoxide dismutase (SOD2), which were reported by some Authors to be present also inside peroxisomes (Schrader and Fahimi, 2006). Antioxidant enzyme expression in the neocortex and the hippocampus of Tg2576 mice was then correlated with markers of oxidative damage as acrolein, an indicator of free radical-induced lipid peroxidation, and 8-hydroxyguanosine (8-OHG) to detect nucleic acid oxidative damage.

Our results obtained, indicating significant variations in the peroxisomal population and peroxisomal proteins in ageing/diseased brain, could represent the basis of a next goal consisting in testing the possible neuroprotective role of peroxisomes against Aβ-mediated damage.

Section II

Results

Chapter 4
Age-related changes in the distribution of neuronal and glial cells in Tg2576 mouse cerebral cortex and hippocampal formation

To examine the brain cytoarchitecture in Tg2576 mice, as compared to WT, we performed immunohistochemical analyses, using NeuN as a neuronal marker, GFAP as an astrocytic marker, and Iba1 as a microglial marker. To investigate possible alterations in the distribution of neural cell populations during normal and pathological aging, we examined the brain from 3-, 6-, 9-, 12-, and 18-month-old mice, focusing on the cerebral cortex and hippocampal formation, as the primarily affected areas in AD.

NeuN immunoreactivity is selectively localized in neuronal nucleus and cytoplasm, as expected (Fig. 4.1). A regular neocortical and hippocampal cytoarchitecture in normal brain aging is observed. Even in Tg2576 mouse brain, NeuN expression pattern fails to show striking variations either in the number of NeuN-positive cells or in NeuN immunostaining levels. These observations suggest that massive neuronal death neither occur during normal aging nor in the progression of the disease, consistently with Jacobsen's report (Jacobsen *et al*., 2006). However, genotype-dependent differences in NeuN-positive cell arrangement and features can be detected at the late stages. Indeed, Tg2576 cerebral cortex, shows overall conserved layering until 12 months of age, as pyramidal neurons show normal arrangement and cellular features, including regular cell somata and apical dendrites. However, already at 12 months, a few neurons appear as displaced and abnormally oriented. In 18-month-old Tg2576 neocortex, the cytoarchitecture is profoundly altered, concomitant with the presence of large amyloid plaques (Fig. 4.1 A). While NeuN immunostaining is totally absent from these amorphous, extracellular structures, NeuN positive neurons, showing abnormally compressed cell bodies and distorted processes, are readily detected around plaques. Concerning the different regions of the hippocampal formation, regular features of CA1-CA3 pyramidal cells and interneurons, as well as granule cells of the dentate gyrus (DG), and mossy cells in the hilus, are observed throughout the considered ages (Fig. 4.1).

Senile plaques become apparent in the hippocampus of 18-month-old Tg2576 mice, particularly in the CA3 field (Fig. 4.1 B). At this advanced AD stage, while pyramidal cell somata remain apparently unchanged, neuronal processes are clearly altered, based on the intracellular distribution of NeuN. In fact, amyloid plaques, which are preferentially located in the stratum radiatum, are surrounded by dystrophic neurites, suggesting disturbed synaptic connectivity.

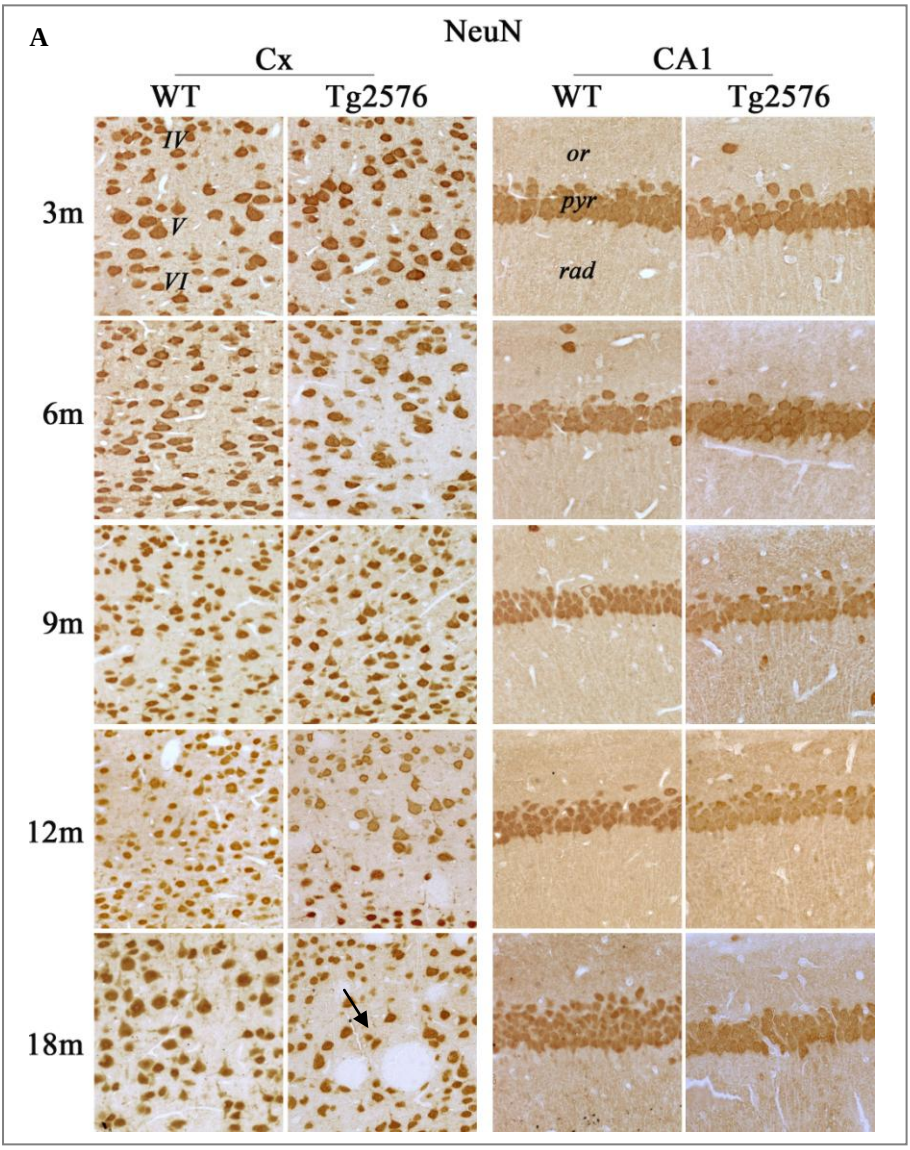

Fig. 4.1 NeuN immunohistochemical localization in 3-, 6-, 9-, 12-, and 18-month-old WT and Tg2576 brain. Panel A (this page), neocortex (Cx) and CA1 hippocampal field; Panel B (next page), CA3 and DG hippocampal regions. Arrows indicate amyloid plaques in 18-month-old Tg2576 brain regions. In the neocortex, these aggregates are surrounded by abnormally looking neurons, while in the CA3 hippocampal field they appear in close proximity to dystrophic neuritis. IV, V, VI, layers of the Cx; or, *stratum oriens*; pyr, *stratum pyramidale*; rad, *stratum radiatum*; gr, *stratum granulosum*.

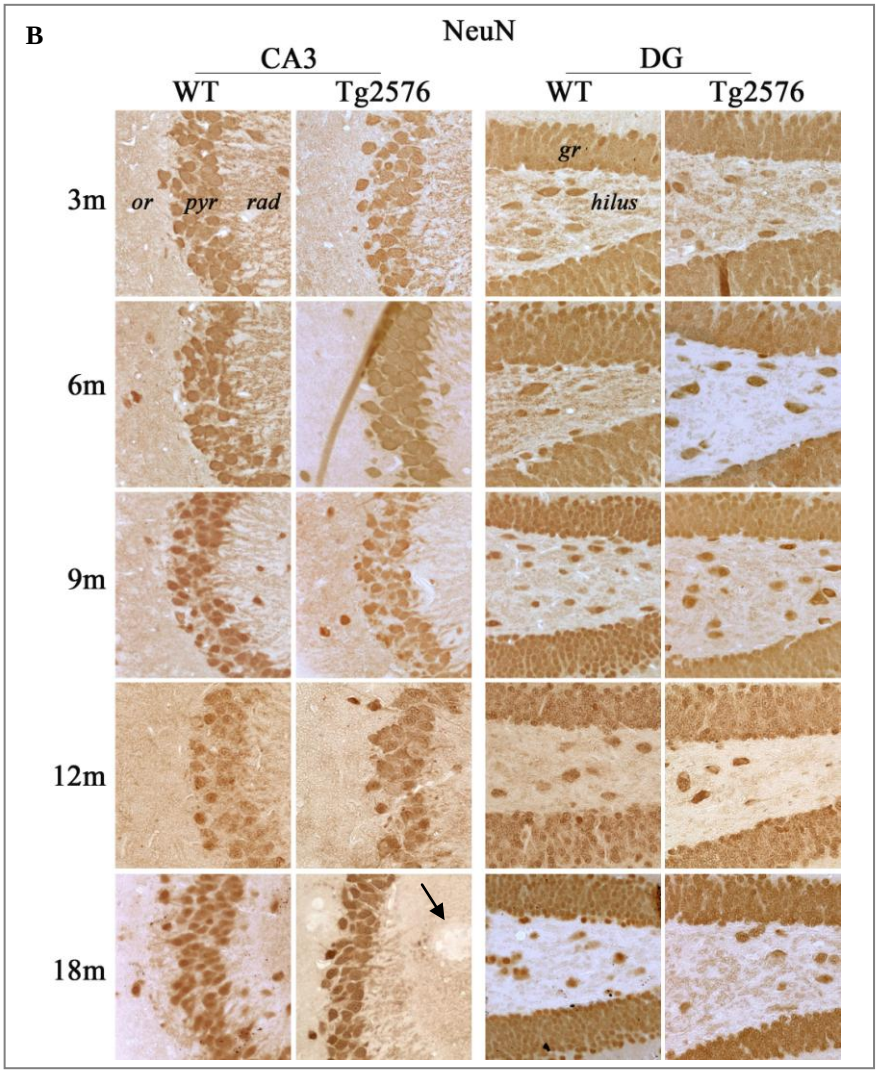

The immunohistochemical analysis performed using anti-GFAP, which is considered the astrocyte marker *par excellance*, shows strongly positive, star-shaped cells throughout the brain. Consistent with the literature, astrocytes appear especially abundant in the hippocampal formation, while being more sparse in the neocortex (Figs. 4.2 A, 4.3 A). We failed to detect any difference related to age or genotype in the distribution pattern of the GFAP-positive cells in the brain until 9 months of age. However, starting from this age, we could observe interesting changes, particularly in the Tg2576 neocortex (Fig. 4.2 A). Indeed, already at 9 months, GFAP immunostained astrocytes are more numerous in the Tg2576

neocortex, compared to earlier stages. Later on, a further increased frequency and altered morphology of neocortical astrocytes are observed in the pathological phenotype. The cellular features of these astrocytes, including increased cell size and highly ramified shape, are strongly suggestive of reactive astrogliosis, presumably in response to ongoing β-amyloid deposition. At the most advanced AD stage, remarkable astrogliosis is concomitant to the presence of large senile plaques. Interestingly, WT cerebral cortex shows no apparent changes in the distribution of GFAP-immunoreactivity occur during aging (Fig. 4.2 A).

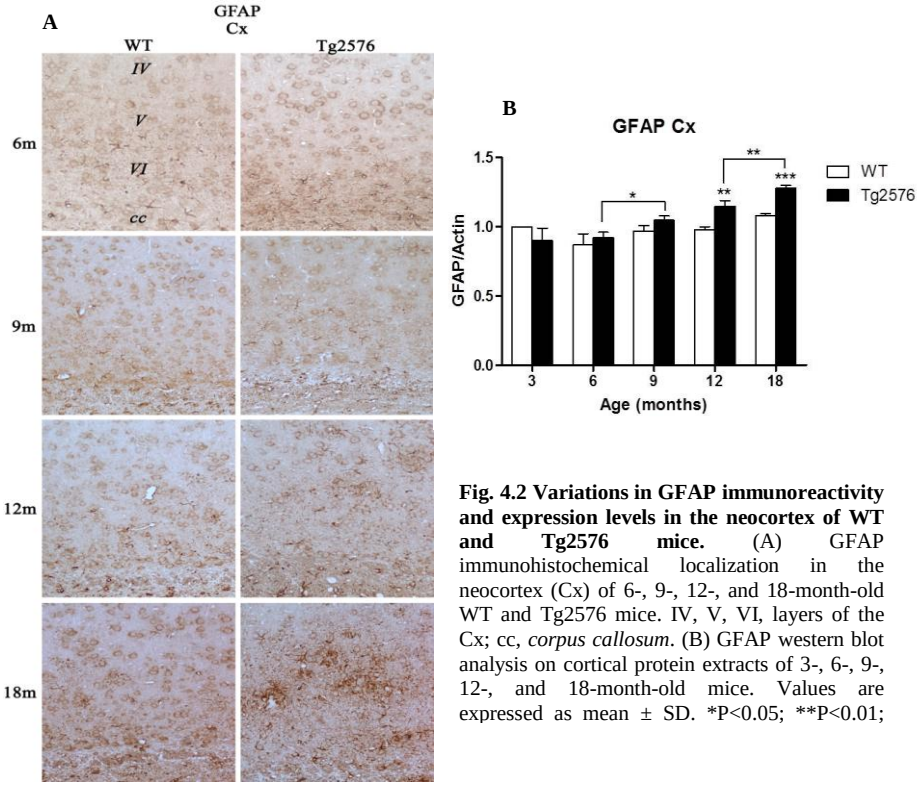

Fig. 4.2 Variations in GFAP immunoreactivity and expression levels in the neocortex of WT and Tg2576 mice. (A) GFAP immunohistochemical localization in the neocortex (Cx) of 6-, 9-, 12-, and 18-month-old WT and Tg2576 mice. IV, V, VI, layers of the Cx; cc, *corpus callosum*. (B) GFAP western blot analysis on cortical protein extracts of 3-, 6-, 9-, 12-, and 18-month-old mice. Values are expressed as mean ± SD. *P<0.05; **P<0.01;

These results are confirmed and quantified by western blot analysis performed on neocortical protein extracts of 3-, 6-, 9-, 12-, and 18-month-old WT and Tg2576 mice. A significant increase of the GFAP levels is already detected in 9-month-old Tg2576, compared to 6 months. This mild increase reflects an initial activation of astrocytes, concomitant with the early amyloid plaques deposition in the neocortex detectable already at 9 months with Congo Red staining (see below, Fig. 4.5). Genotype-dependent changes are observed at 12 and, even more, at 18 months, when GFAP content is strongly increased in Tg2576 neocortices, compared to their WT counterparts.

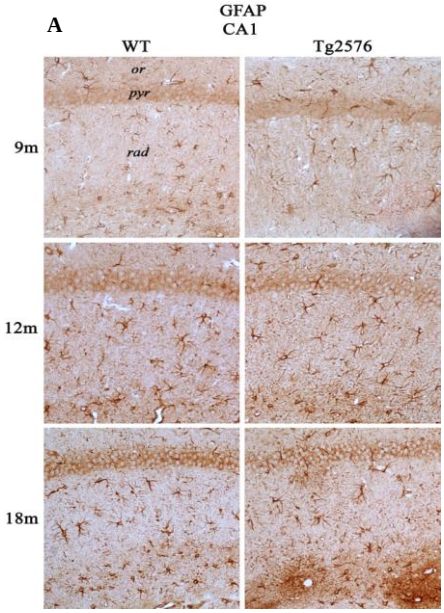

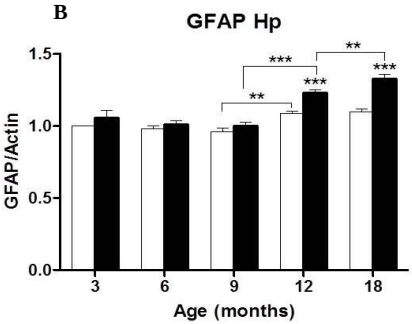

Fig. 4.3 Variations in GFAP protein levels and expression in the hippocampus of WT and Tg2576 mice. (A) GFAP immunohistochemical localization in CA1 hippocampal field of 9-, 12-, and 18-month-old WT and Tg2576 mice. or, *stratum oriens*; pyr, *stratum pyramidale*; rad, *stratum radiatum*; IV, V, VI, layers of the Cx; cc, *corpus callosum*. (B) GFAP western blot analysis on hippocampal protein extracts of 3-, 6-, 9-, 12-, and 18-month-old mice. Values are expressed as mean ± SD. **P<0.01; ***P<0.001.

In the hippocampus, astrocytes are generally abundant and large in size. Morphological and biochemical analyses show unchanged GFAP expression until 9 months of age (Fig. 4.3). At later stages, a significant increase in the intermediate filament levels is detected, especially in the pathological genotype, indicating onset of astrogliosis. Specifically, in the 18-month-old Tg2576 hippocampus, reactive astrocytes *foci* are apparent. While the overall immunohistochemical pattern shows relatively late increase in GFAP-positive cells, consistently with molecular results, this does not hold true for some districts of the hippocampal formation, namely the DG (Fig. 4.4). Indeed, in 3-month-old Tg2576 DG, GFAP-immunostaining is especially strong in cells located at the granule cell/hilus border, whereas at the same age the WT counterpart shows more dispersed and weaker immunoreactivity.

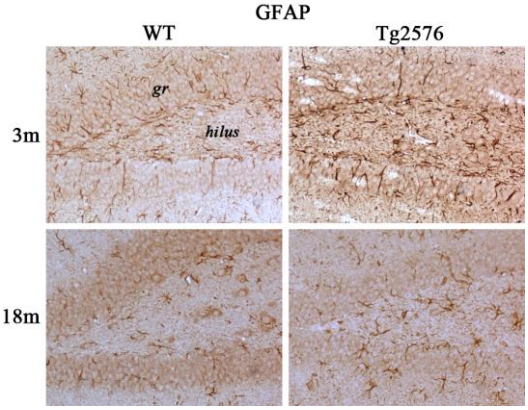

Fig. 4.4 GFAP immunohistochemical localization in the dentate gyrus of WT and Tg2576 mice at 3 and 18 months of age.

These intensely positive cells are reminiscent for location and morphological features, of neural stem cells/progenitors, suggesting activation of the neurogenesis process in early AD. Interestingly, remarkably fewer positive cells are seen in18-month-old DG, in a genotype-independent manner (Fig. 4.4).
To complete the analysis of the distribution of neural markers in aged/diseased brains, we performed Iba1 immunohistochemistry on neocortical and hippocampal sections of WT and Tg2576 brains. Iba1 immunolocalization results in cytoplasmic staining of activated microglial cells, which are poorly present in WT brain throughout the examined period, and in Tg2576 brain until 12 months of age (see Supplementary Fig. 1). Importantly, an increased microglial recruitment is observed in 18-month-old Tg2576 neocortex and hippocampus in correspondence with the amyloid plaques (for details, see below Fig. 4.5).
Immunohistochemical analyses, perfomed with NeuN, GFAP, and Iba1 primary antibodies on 18-month-old Tg2576 sections, has highlighted characteristic features of senile plaques (Fig. 4.5). In the neocortex these are widely present, both in the superficial and deep layers, thus causing a disruption of the neuronal arrangement, recognized in NeuN-immunoreacted sections. Differently, in the hippocampus large aggregates are mostly found in the *stratum radiatum*, far from the pyramidal cell bodies, so that the layering is apparently conserved. However, even in this area, alterations in the neuritic processes are observed, mainly consisting of dystrophic features. Strongly GFAP-reactive astrocytes, whose processes reach the core of the plaques themselves and activated microglial cells are found around and within the plaques.

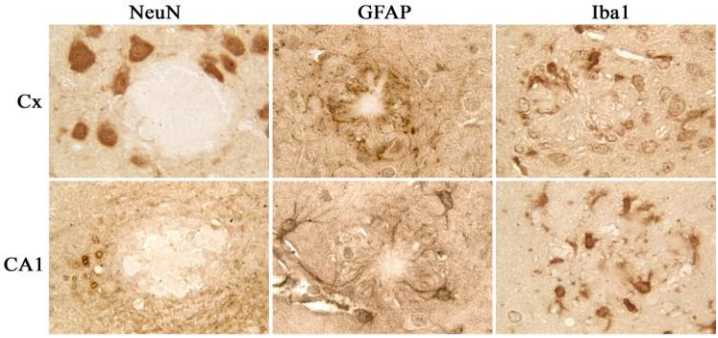

Fig. 4.5 Immunohistochemical localization of NeuN, GFAP, and Iba1 in the neocortex (Cx) and CA1 hippocampal field of 18-month-old Tg2576 brain.

To study the appearance of amyloid plaques we carried out Congo Red staining performed on neocortical and hippocampal paraffin-embedded sections of WT and Tg2576 brains at all ages considered. This protocol is used for the light microscopic detection of amyloid plaques, which show green birefringence using polarizing lenses. Congo Red analysis shows no Aβ deposits in WT brains at any

age, nor in Tg2576 brains until 6 months (data not shown). At 9 months of age, small amyloid plaques can be detected in the neocortex (Fig. 4.6). These become larger and more numerous in 12- and in 18-month-old diseased neocortex, while their first appearance in the hippocampal formation occurs at 18 months.

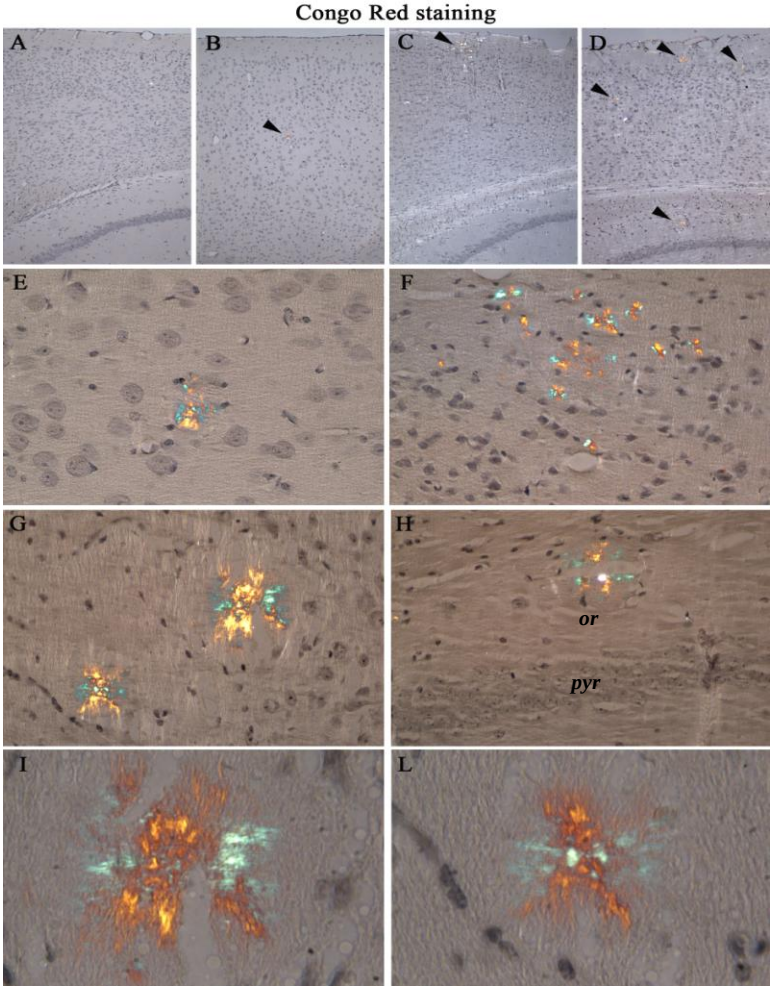

Fig. 4.6 Amyloid plaques detected by Congo Red staining performed on neocortical and hippocampal sections of 9-, 12-, and 18-month-old brains. (A) Plaques are absent from the neocortex of 9-month-old WT. (B) A small plaque is first observed in 9-month-old Tg2576 neocortex (arrowhead). (C) A group of amyloid plaques is detected in the superficial layer of 12-month-old Tg2576 neocortex (arrowheads). (D) Several large plaques are localized in the 18-month-old Tg2576 brain, both in the neocortex and in the hippocampal formation. (E-F) High magnification of amyloid plaques in the neocortex, shown in B and C, respectively. (G, H) High magnification of the amyloid plaques (shown in D), respectively localized in the neocortex and hippocampus. (I, L) Immersion-oil high power view of amyloid plaques shown respectively in G and H.

Chapter 5
Age-related variations in peroxisome-related proteins in the Tg2576 hippocampal formation

As the hippocampal formation is primarily affected by AD, we focused on this area to investigate the putative involvement of peroxisomes at the onset and during the disease progression. The expression and distribution of several peroxisome-related proteins in Tg2576 and WT brains of 3-, 6-, 9-, 12-, and 18-month-old mice was comparatively studied through a combined biochemical/morphological approach. Specifically, we investigated the expression of membrane (Pex5p, PMP70, Pex14p) and matrix (catalase, acyl-CoA oxidase, thiolase) peroxisomal proteins. Their relationship with markers of oxidative stress (8-hydroxyguanosine and acrolein) and antioxidant response (superoxide dismutases, glutathione peroxidase), was also analyzed. In particular, this section focuses on the hippocampal formation, while the neocortex will be examined in Chapter 6.

5.1 Peroxisomal biogenesis markers: Pex5p, PMP70, and Pex14p

Pex5p is a soluble receptor involved in the peroxisomal matrix protein import, harboring a type 1 signal sequence (PTS1). In keeping with the presence of two isoforms of Pex5p in mammalian cells (PEX5pS and PEX5pL) (Otera *et al*., 2000), two bands are seen in our western blot experiments performed on hippocampal protein extracts of 3-month-old WT and Tg2576 mice (Fig. 5.1). Densitometric analysis shows significantly higher protein levels in 3-month-old Tg2576 hippocampus, compared to WT littermates (Fig. 5.1 A). Accordingly, PEX5p immunolocalization in Tg2576 CA1 hippocampal field results in a stronger cytoplasmic staining of pyramidal neurons than in WT (Fig. 5.1 B), suggesting active biogenesis of peroxisomes at the onset of disease.

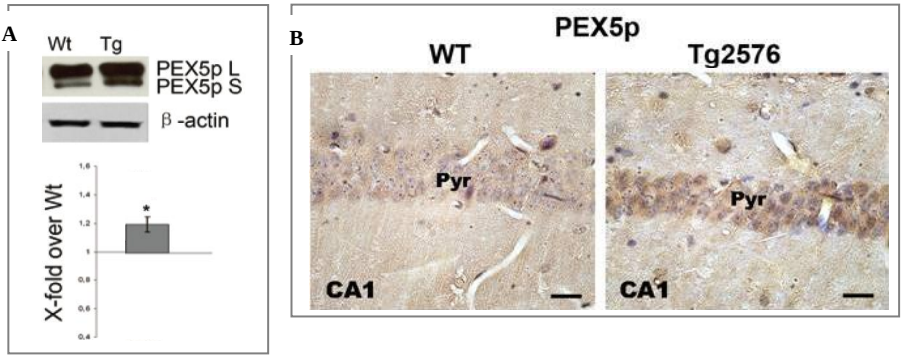

Fig. 5.1 PEX5p expression and distribution in the hippocampus of 3-month-old Tg2576 mice, as compared to their WT littermates. (A) Images of *β*-actin-normalized WB representative experiments for PEX5p. Two bands, corresponding to the two isoforms PEX5pL and PEX5pS, are seen. In the lower picture, the ratio between Tg2576 and WT densitometric values, obtained analysing the two bands together, is shown. Error bars, standard error of the mean. *P <0.05. (B) IHC distribution of PEX5p in CA1 hippocampal field of WT and Tg2576 brains. Pyr, pyramidal cell layer. Bars, 30 μm.

Differently from Pex5, acting as a shuttle protein, PMP70 is stably localized to peroxisomal membrane, thus being considered as a marker to evaluate the overall size of the peroxisomal population (Santos *et al*., 1994). We therefore analysed its expression in the hippocampus of Tg2576 mice, as compared to their WT littermates, at 3, 6, 9, 12, and 18 months, to highlight possible variations in the peroxisomal number during the disease progression. Our biochemical and morphological data on hippocampal protein extracts show an early and significant peroxisomal induction in 3-month-old diseased mice compared to controls, followed by a decrease at 6 months of age in WT and, even more pronounced, in Tg2576. At 9 and 12 months, PMP70 levels are relatively stable in both genotypes. A peak is then observed at 18 months, irrespective of the genotype (Fig. 5.2 A).

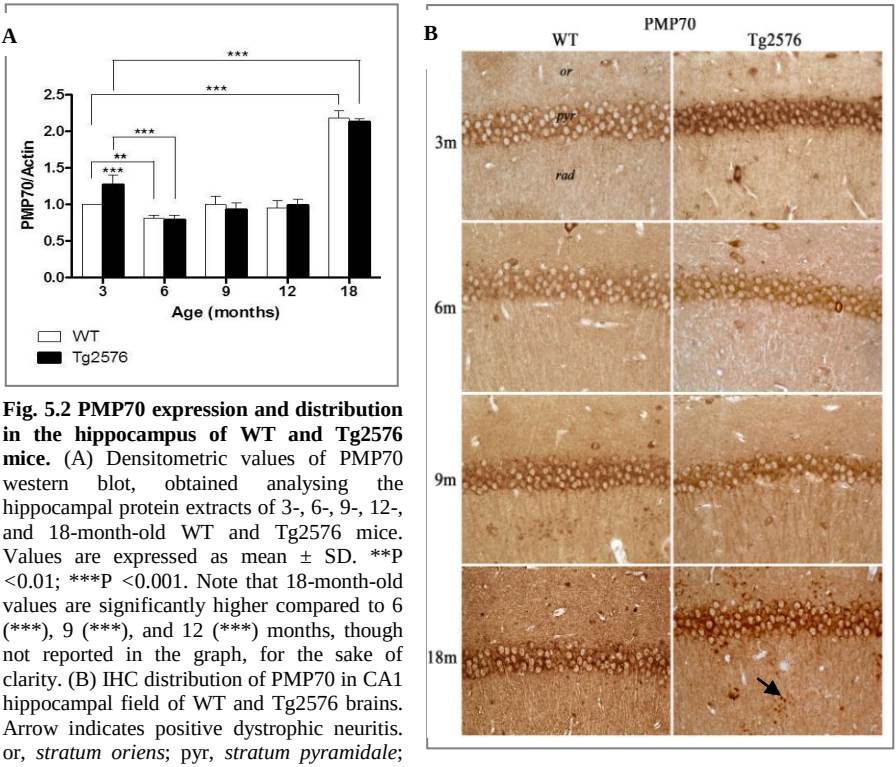

Fig. 5.2 PMP70 expression and distribution in the hippocampus of WT and Tg2576 mice. (A) Densitometric values of PMP70 western blot, obtained analysing the hippocampal protein extracts of 3-, 6-, 9-, 12-, and 18-month-old WT and Tg2576 mice. Values are expressed as mean ± SD. **P <0.01; ***P <0.001. Note that 18-month-old values are significantly higher compared to 6 (***), 9 (***), and 12 (***) months, though not reported in the graph, for the sake of clarity. (B) IHC distribution of PMP70 in CA1 hippocampal field of WT and Tg2576 brains. Arrow indicates positive dystrophic neuritis. or, *stratum oriens*; pyr, *stratum pyramidale*; rad. *stratum radiatum*.

These results are confirmed by PMP70 immunohistochemistry (Fig. 5.2 B). The hippocampus from 3-month-old Tg2576 mice appears strongly immunoreactive; in particular, neurons in the pyramidal layer of the CA1 subdivision are darkly stained in their somata, compared to WT, which instead are weakly positive (Fig. 5.2 B). At 6 months, hippocampal neurons show decreased PMP70 immunoreactivity, especially in the pathological genotype. Later on,

immunostaining levels remain stable in pyramidal cell bodies, even though a higher staining degree in neuronal dendrites extending in the *stratum radiatum* appear slightly more immunoreactive. PMP70 expression is sensibly increased in 18-month-old hippocampus of both genotypes, showing an interesting pattern of immunoreactivity. In the Tg2576, high levels of immunopositivity are observed in cell bodies, dendrites and in dystrophic neurites.

Based on our biochemical and morphological results indicating peroxisomal proliferation in 3-month-old Tg2576 hippocampus, we performed PMP70 pre-embedding immunoelectron microscopy (IEM) to verify the observed peroxisomal induction (Fig. 5.3). This approach allowed us to identify PMP70-positive peroxisomes in CA1 pyramidal neurons in both genotypes. The immunoreactions product appears confined to the membrane, as expected. Consistently with molecular and morphological data, ultrastructural analysis shows a higher number of peroxisomes in Tg2576 hippocampus.

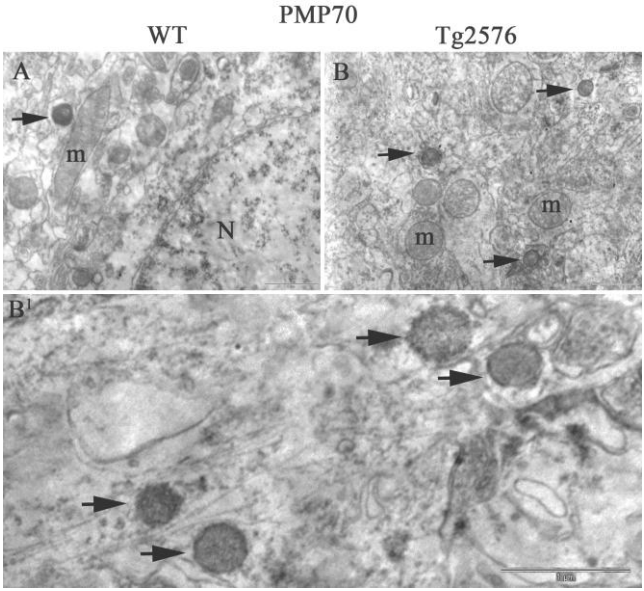

Fig. 5.3 PMP70 IEM in CA1 pyramidal neurons of the WT (A) and Tg2576 (B, B[1]) hippocampus at 3 months of age. Positive peroxisomes (arrows) are observed in CA1 pyramidal neurons in both genotypes but a higher number of peroxisomes is observed in the cytoplasm of Tg2576 neurons (B). (B[1]) Higher magnification of peroxisomes in 3-month-old Tg2576 pyramidal neurons. N, neuronal nucleus; m, mitochondria. Scale bar, 1 μm.

Moreover, to investigate the presence of peroxisomes in hippocampal neurons, as well as in astroglial cells, we performed double immunofluorescence experiments of PMP70 in combination with NeuN (Fig. 5.4 A) or GFAP (Fig. 5.4 B). They respectively demonstrate neuronal and astroglial peroxisomes, showing that both

populations are particularly abundant in the Tg2576 hippocampal formation, in agreement with biochemical and morphological results.

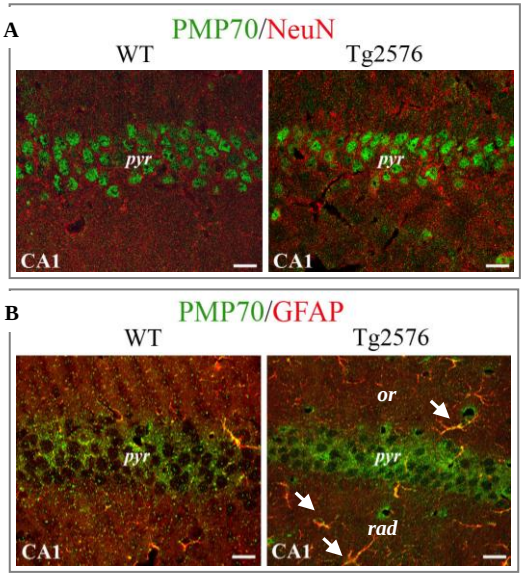

Fig. 5.4 Double IF of PMP70 (green) in combination with NeuN (red) or GFAP (red) in the CA1 hippocampal field of WT and Tg2576 3-month-old brain (A, B). (A) PMP70-signal is especially bright in the pyramidal cell somata (pyr). (B) PMP70-positive astrocytes are more numerous in Tg2576 (arrows) than in WT hippocampus, localizing both in the stratum oriens (or) and in the stratum radiatum (rad). Some atrocytic processes containing peroxisomes extend into the *stratum pyramidale* (pyr). Bars, 30 μm.

Since western blot analysis demonstrated a strong, though genotype-independent, PMP70 increase at 18 months, we further investigated this age-related induction, to ascertain whether it could be correlated with astrogliosis. To this aim, we performed double immunofluorescence experiments of PMP70 in combination with GFAP, on hippocampal sections from mice aged 18 months (Fig. 5.5).
In agreement with the above molecular and histochemical data, these immunofluorescence experiments revealed elevated PMP70 levels in both genotypes. Subtle differences can however be detected between the immunodistribution of the protein. Indeed, throughout Tg2576 hippocampal formation (CA1, CA3, DG fields), cells showing overlapping positivity to PMP70 and GFAP are more numerous, respect to WT. Nevertheless, in the same sections, peroxisomes are similarly expressed in WT and Tg2576 neurons, which of course appear as GFAP-negative. Taken together, these results suggest a relative contribution of glial peroxisomes to the overall peroxisomal population in the hippocampus, higher in Tg2576 animals, compared to their WT littermates.

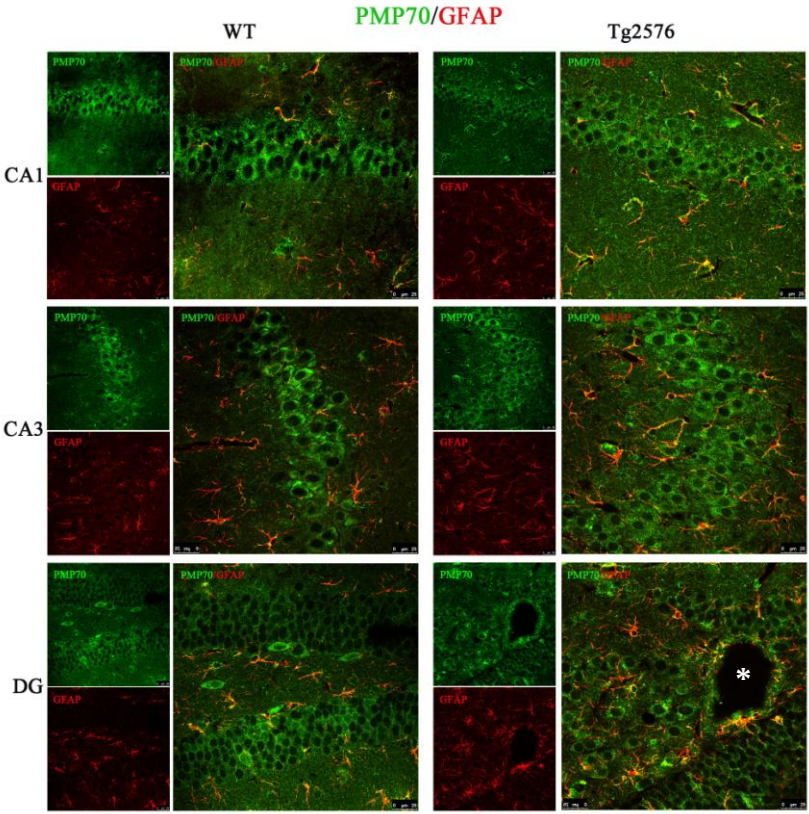

Fig. 5.5 Double IF of PMP70 (green) in combination with GFAP (red) in the hippocampal fields (CA1, CA3, DG) of 18-month-old WT and Tg2576 brain. Several PMP70+/GFAP+ cells (yellow) are observed in the different regions, being especially numerous in the pathological genotype. Note the numerous peroxisome-containing astrocytes surrounding an amyloid plaque (asterisk) in the Tg2576 DG.

The protein expression of the peroxin Pex14p, was also investigated at the onset and during the progression of disease, to gain some insight into possible alterations of peroxisomal biogenesis. Western blot analysis shows an age-related decrease of Pex14p levels, starting from 6 months of age, in normal hippocampus (Fig. 5.6), and from 9 months in the pathological genotype, suggesting impaired peroxisomal biogenesis. Remarkably, at 18 months Pex14p levels are significantly different in the two genotypes, showing a strong increase in Tg2576. These evidence are confirmed by morphological analysis of Pex14p immunohistochemistry, showing different degrees of staining in pyramidal neurons of CA1 hippocampal field (Fig. 5.6 B).

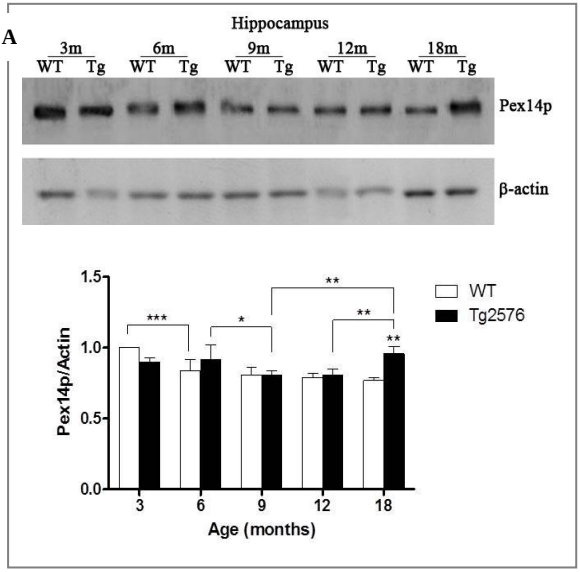

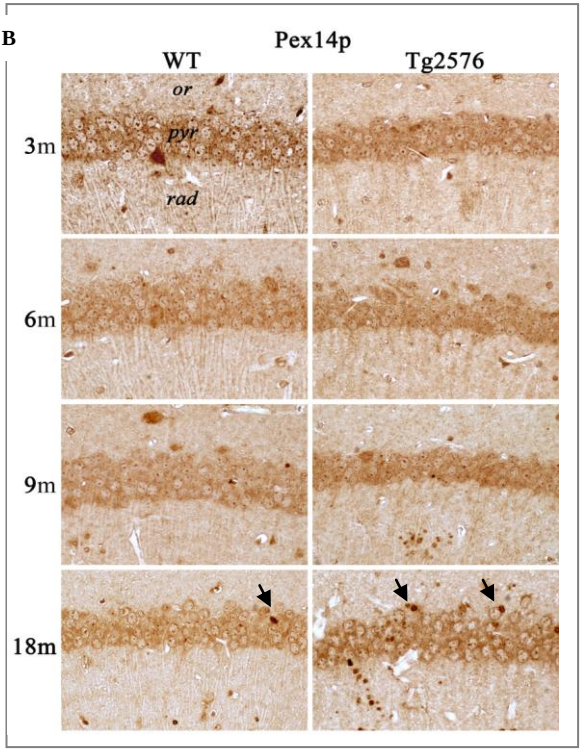

Fig. 5.6 Pex14p expression and distribution in the hippocampus of WT and Tg2576 mice. (A) Image of *β*-actin-normalized WB representative experiment for Pex14p, performed on hippocampal protein extracts of 3-, 6-, 9-, 12-, and 18-month-old WT and Tg2576 brains. In the lower picture, densitometric values of Pex14p western blot, are shown. Values are expressed as mean ± SD. *P <0.05; **P <0.01; ***P <0.001. Note that 3-month-old WT values are significantly higher compared to 9 (***), 12 (***), and 18 (***) months, though not reported in the graph, for the sake of clarity. (B) IHC distribution of PMP70 in CA1 hippocampal field of 3-, 6-, 9-, and 18-month-old WT and Tg2576 brains. Arrows indicate strongly immunoreactive glial cells in the pyramidal layer (pyr). or, *stratum oriens*; rad, *stratum radiatum*.

5.2 Peroxisomal β-oxidation enzymes

Since peroxisomes play an important role in brain lipid metabolism, we analyzed the expression of two peroxisomal β-oxidation enzymes, namely acyl-CoA-oxidase (AOX) and thiolase (THL) at the onset and during the progression of AD. AOX catalyzes the first and rate-limiting step of the cycle, while THL is the last enzyme of the pathway. Our results indicate that during normal aging AOX levels are fairly stable, except for the last considered time point (18 months), when a significant decrease is detected. By contrast, in 3-month-old Tg2576 hippocampus AOX is induced, and decreases soon afterwards (Fig. 5.7 A). This result is supported by AOX immunohistochemistry, showing intense immunoreactivity in CA1 pyramidal cell somata of 3-month-old Tg2576 hippocampus (Fig. 5.7 B), followed by a dramatic drop of immunostaining levels in the subsequent stages.

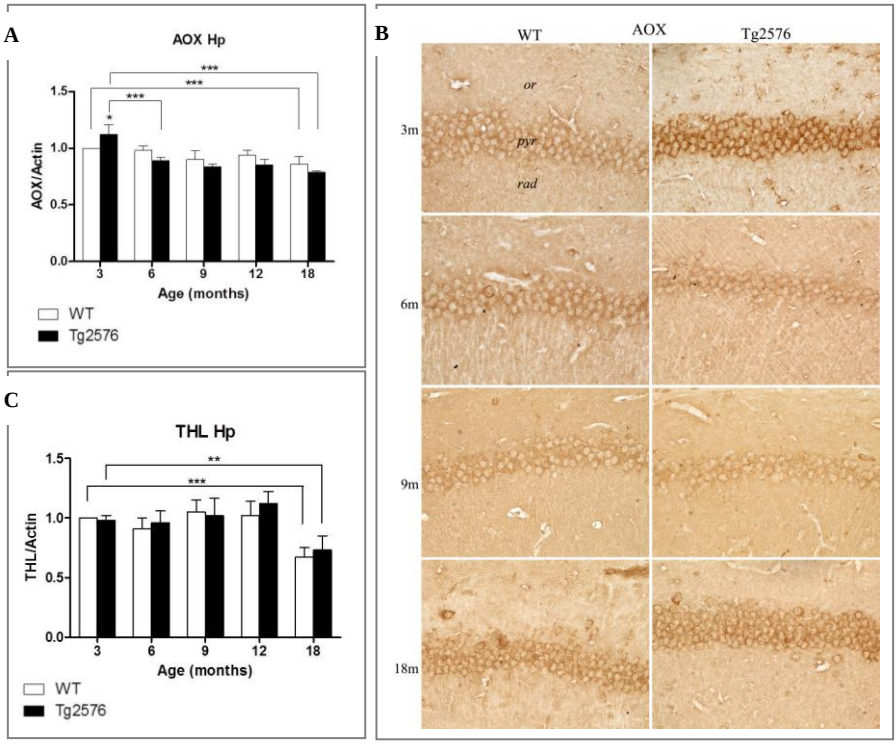

Fig. 5.7 Changes in the AOX and THL expression in the hippocampus of WT and Tg2576 mice. Densitometric values of AOX (A) and THL (C) western blot performed on hippocampal protein extracts of 3-, 6-, 9-, 12-, and 18-month-old WT and Tg2576 brains. Values are expressed as mean ± SD. Note that AOX 3-month-old Tg2576 values are significantly higher compared to 9 (***), and 12 (***) months, though not reported in the graph, for the sake of clarity. Note also that THL 18-month-old values are significantly lower compared to 6 (**), 9 (***), and 12 (***) months *P <0.05; **P <0.01; ***P <0.001. (B) AOX immunolocalization in CA1 hippocampal field of 3-, 6-, 9-, and 18-month-old WT and Tg2576 brains.

The expression pattern of THL is quite different from that shown by AOX, in that no genotype-variations occur during normal and pathological aging, until 12 months. However at 18 months of age, hippocampal THL levels are strongly decreased in both genotypes, compared to those of the earlier ages, suggesting an imbalance of peroxisomal β-oxidation pathway.

5.3 Expression of the peroxisome proliferator receptor alpha at the onset and at advanced stages of the disease

Since we observed variations of peroxisomal proteins, especially at the onset of the disease, we also addressed the putative involvement of the transcription factors family known as PPARs. We focussed on isotype α, for its direct role in regulating peroxisome biogenesis.

We found that PPARα immunohistochemical pattern is consistent with that of its target genes AOX and PMP70. Indeed, PPARα immunolocalization shows significantly higher levels in 3-month-old Tg2576 hippocampus, compared to its WT counterpart. At 18 months of age, PPARα expression levels are increased in the WT hippocampus, as compared to 3 months (Fig. 5.8).

Triple IF experiments of PPARα in combination with GFAP and NeuN, demonstrate PPARα expression in nuclei of neurons and glial cells (Fig. 5.9, IF).

Moreover, to ascertain PPARα nuclear localization – which is indispensible for its function as a transcription factor – we performed pre-embedding immunoelectron microscopy using anti-PPARα antibody, thus demonstrating the massive presence of the receptor within the nucleus of Tg2576 hippocampal pyramidal neurons, while in WT samples immuno-deposits are sparser (Fig. 5.9, IEM).

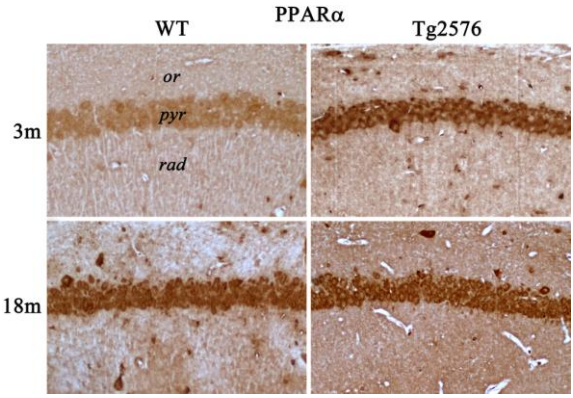

Fig. 5.8 PPARα expression in 3- and 18-month-old WT and Tg2576 CA1 hippocampal region. PPARα immunolocalization in pyramidal cell layer (pyr) shows a higher PPARα-immunoreactivity in Tg2576 hippocampus, than in its WT counterpart. At 18 months of age, high immunopositivity levels are detectable in both genotypes.
or, stratum oriens; *rad, stratum radiatum.*

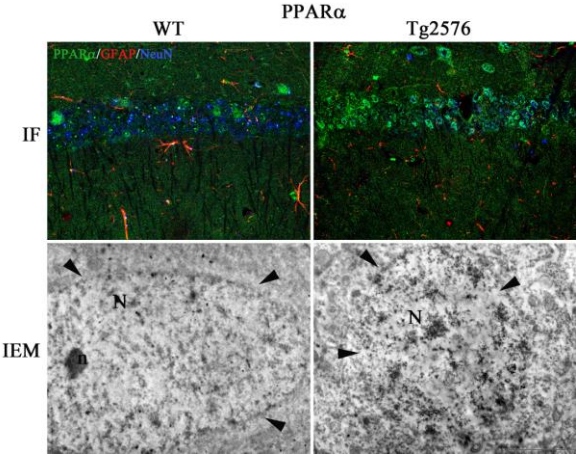

Fig. 5.9 PPARα expression in 3-month-old WT and Tg2576 CA1 hippocampal region. Triple IF for PPARα (green) in combination with GFAP (red) and NeuN (blue) demonstrates the presence of PPARα-positive neurons and astrocytes. Note the brightness of green signal in the Tg2576 section.
PPARα IEM in CA1 pyramidal neurons shows the nuclear localization of the immunoreaction product, especially concentrated in the Tg2576 neuron. Arrowheads indicate the nuclear envelope.

5.4 Oxidative stress markers at early and advanced AD stages

Activation of PPARα is likely due to the oxidative damage itself, since oxidized lipids have been proposed to activate this ligand-dependent transcription factor (Yeldandi *et al*., 2000). Such damage was investigated by IHC by antibodies to protein-bound acrolein, a marker of lipid peroxidation, and anti-8-hydroxyguanosine which allows to identify oxidative modifications to DNA and RNA, as it recognizes both 8-OHG and 8-OHdG.
The examined oxidative stress markers show a similar immunoreactivity pattern, strongly related to the genotype. Indeed, both acrolein and 8-OHG demonstrate that oxidative damage occurs early in pathological brains and is still detectable in the aged brain.

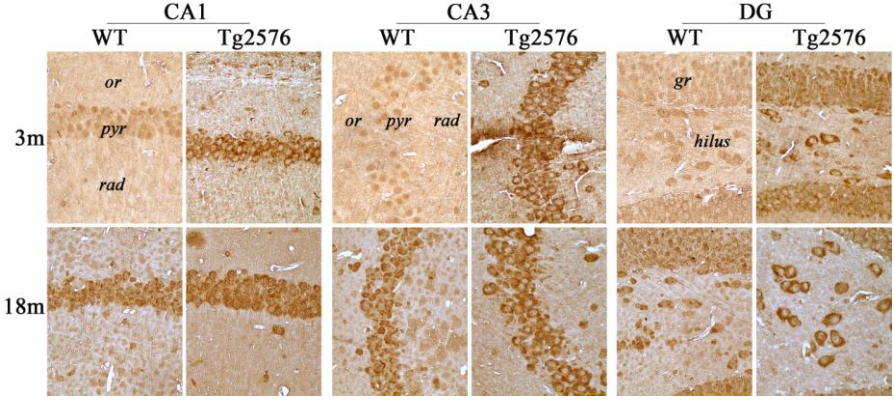

Fig. 5.10 Acrolein expression in CA1, CA3, and DG hippocampal fields of 3- and 18-month-old WT and Tg2576 mice. *pyr, stratum pyramidale; or, stratum oriens; rad, stratum radiatum.*

Acrolein immunopositivity is detected at 3 months in all Tg2576 hippocampal regions, being localized in the cytoplasm of pyramidal neurons of CA1 and CA3 fields, as well as in the mossy cells in the hilus of DG. At this age, WT sections show little – if any – immunopositivity. At the latest age considered (18 months), acrolein immunostaining is also detected in the WT, while the pattern shown by Tg2576 hippocampus is unchanged with respect to the onset of disease (Fig. 5.10).

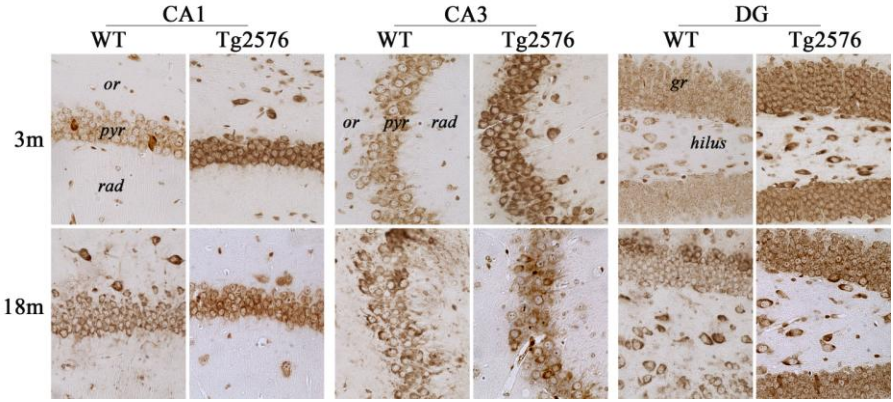

Fig. 5.11 8-OHG expression in CA1, CA3, and DG hippocampal fields of 3- and 18-month-old WT and Tg2576 mice. *pyr, stratum pyramidale; or, stratum oriens; rad, stratum radiatum.*

Immunolocalization of 8-OHG shows a substantially overlapping pattern with acrolein at 3 months of age, in that Tg2576 hippocampal formation demonstrates strong oxidative damage to nucleic acids. The staining predominantly appears cytoplasmic, most probably reflecting mRNA and/or mitochondrial DNA modifications (Fig. 5.11). At difference with its pathological counterpart, normal hippocampus displays faint immunoreactivity in the pyramidal cell layer of CA regions and in granule cells of the DG. Moreover, irrespective of the genotype, interneurons distributed in all the hippocampal subdivisions appear intensely immunoreactive. Later in the aging process (18 months), 8-OHG positivity increases in all WT hippocampal regions, while varying in a region-dependent manner in the Tg2576. In fact, pyramidal cells of CA1-CA3 fields show a decreased immunoreactivity, whereas staining in granule cell layer of DG is unchanged.

5.5 Age-related variations in ROS-scavenging enzymes expression in the Tg2576 hippocampal formation

Since peroxisomes play a pivotal role in the protection against ROS, we assessed the levels of the scavenging enzymes CAT, GPX1, SOD1 and SOD2. While CAT is *bona fide* a peroxisomal protein, all the other enzymes are localized in different cell compartments, but recently found also inside peroxisomes (Schrader and

Fahimi, 2006). High levels of CAT are detected in the pathological genotype at early stages, particularly at 6 months, when protein levels are significantly higher than the respective WT. An age-related decrease in CAT expression ensues, in both genotypes, suggesting impaired ability to remove H_2O_2 in the senescent hippocampus (Fig. 5.12).

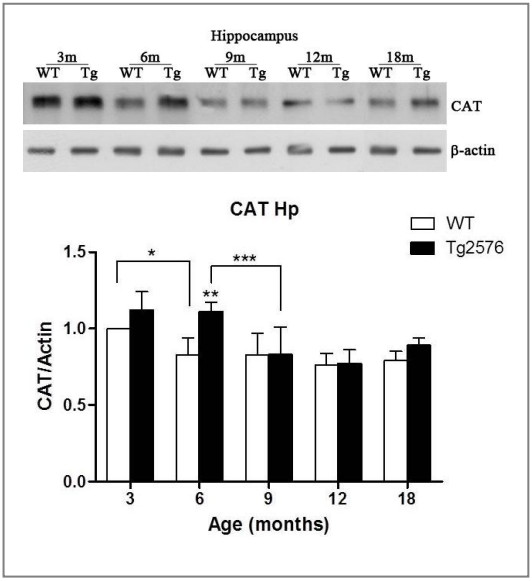

Fig. 5.12 Catalase expression in the hippocampus of WT and Tg2576 mice. Image of β-actin-normalized WB representative experiment for CAT, performed on hippocampal protein extracts of 3-, 6-, 9-, 12-, and 18-month-old WT and Tg2576 brains. In the lower picture, densitometric values of CAT western blot are shown. Values are expressed as mean ± SD. Note that CAT 3-month-old WT values are significantly higher compared to 12 (**) and 18 (**) months, though not reported in the graph, for the sake of clarity. Note also that CAT 6-month-old Tg2576 values are significantly higher compared to 12 (***) and 18 (*) months, though not reported in the graph, for the sake of clarity. *P <0.05; **P <0.01; ***P <0.001.

Our western blot experiments aimed to detect the cytosolic H_2O_2–scavenging enzyme GPX1, indicate no significant variations during normal aging, while differences in expression levels are seen in the pathological genotype during the disease progression. Differently from CAT results, lower GPX1 levels are detected in 3-month-old Tg2576 hippocampus as compared to WT. However, GPX1 expression in Tg2576 mice increases until 9 months, reaching higher levels than the respective WT. In the aged Tg2576 hippocampus a progressive decrease in GPX1 protein levels is observed (Fig. 5.13).

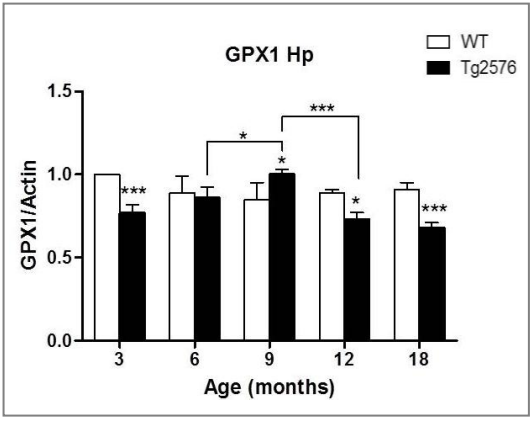

Fig. 5.13 GPX1 expression in the hippocampus of WT and Tg2576 mice. Densitometric values of GPX1 western blot performed on hippocampal protein extracts of 3-, 6-, 9-, 12-, and 18-month-old WT and Tg2576 brains. Values are expressed as mean ± SD.
*P <0.05; ***P <0.001.

The two enzymes responsible for the dismutation of superoxide anion to hydrogen peroxide, showing different intracellular distribution – SOD1 being mainly cytosolic and SOD2 mainly mitochondrial – share similar patterns of expression during normal aging. Indeed, both proteins show a progressive increase until 12 months of age, followed by a sharp decrease at 18 months. In the pathological genotype, relevant differences between the two SOD forms can be observed. SOD1 expression levels in Tg2576 follow a trend similar to the WT. However, the protein is significantly down-regulated at 3 months of age in Tg2576 hippocampus, compared to its WT counterpart. Moreover, at 12 months, even though the protein levels are relatively high compared to previous stages, they are lower in the pathological condition than in normal mice.
Differently from SOD1, mitochondrial SOD2 shows remarkably higher levels at 3 months in Tg2576 than in WT animals. Later on, the expression levels remain quite stable in the pathological genotype, failing to either increase at 12 months, or decrease at 18 months of age (Fig. 5.14).

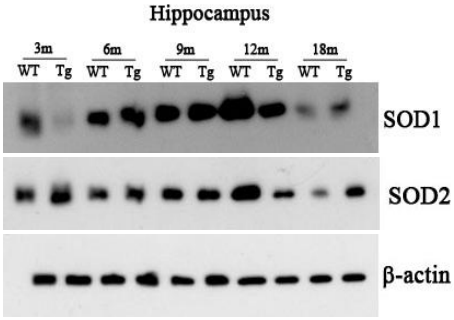

Fig. 5.14 Variations in the SOD1 and SOD2 expression in WT and Tg2576 hippocampus. Images of *β*-actin-normalized western blot representative experiments for SOD1 and SOD2, performed on hippocampal protein extracts of 3-, 6-, 9-, 12-, and 18-month-old WT and Tg2576 brains. In the lower pictures, densitometric values of SOD1 and SOD2 western blots, are shown. Values are expressed as mean ± SD.
Note that SOD2 12-month-old WT values are significantly higher compared to 3 (***) and 6 (***) months, though not reported in the graph, for the sake of clarity.
*P <0.05; **P <0.01; ***P <0.001.

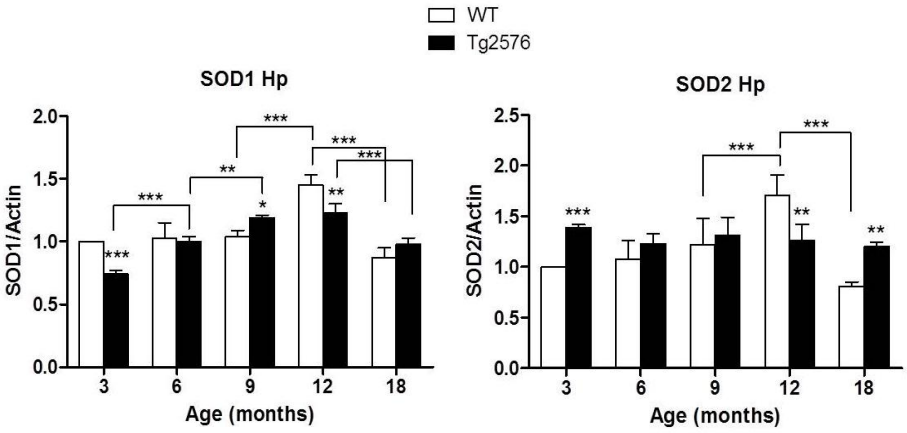

Chapter 6
Age-related variations in peroxisome-related proteins in the Tg2576 cerebral cortex

Since the neocortex is selectively affected by AD, even though at later stages of this progressive disease, we analyzed the expression and distribution of several peroxisome-related proteins also in this brain territory. Specifically, peroxisomal membrane proteins, namely PMP70 and Pex14p, as well as peroxisomal matrix enzymes, including CAT, AOX, and THL, were studied in the cerebral cortex of 3-, 6-, 9-, 12-, and 18-month-old Tg2576 mice, as compared to their WT littermates. Oxidative stress markers and antioxidant enzymes were also analyzed in the neocortex, in order to verify the overall redox status of this region.

6.1 Expression of peroxisomal biogenesis markers in the Tg2576 neocortex

Our PMP70 biochemical results on neocortical protein extracts show that the most interesting changes are observed at 6 months of age (Fig. 6.1 A). At this time point, protein levels are decreased, compared to 3 months, in both genotypes. This variation is especially dramatic in Tg2576 neocortex, which also shows significantly lower PMP70 levels, than its WT counterpart. Later on, PMP70 expression progressively increases, until 18 months of age, when levels are significantly higher than at 6 months in both genotypes.

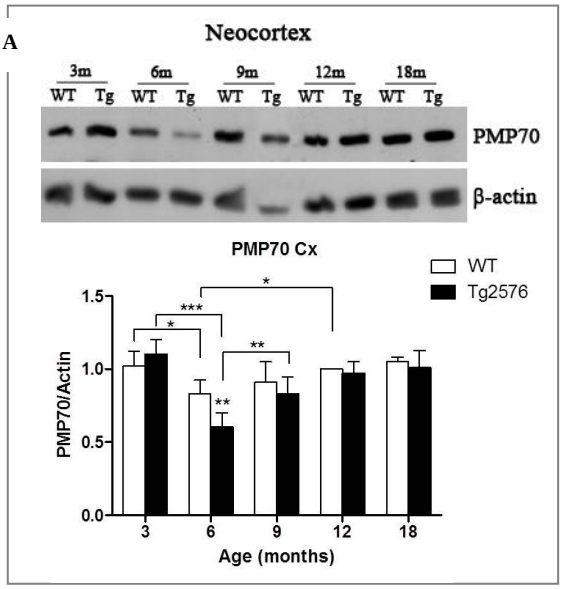

Fig. 6.1 Variations in the PMP70 expression and distribution in WT and Tg2576 cerebral cortex. (A) Image of β-actin-normalized WB representative experiment for PMP70, performed on neocortical protein extracts of 3-, 6-, 9-, 12-, and 18-month-old WT and Tg2576 brains. In the lower picture, densitometric values of PMP70 western blot, are shown. Values are expressed as mean ± SD. *P <0.05; **P <0.01; ***P <0.001. Note that PMP70 6-month-old Tg2576 values are significantly lower compared to 12 (***) and 18 (***) months, though not reported in the graph, for the sake of clarity. Note also that PMP70 6-month-old WT values are significantly lower compared to 18 (*) months. (B, next page) IHC distribution of PMP70 in 3-, 6-, 9-month-old WT and Tg2576 neocortex (IV-VI layers).

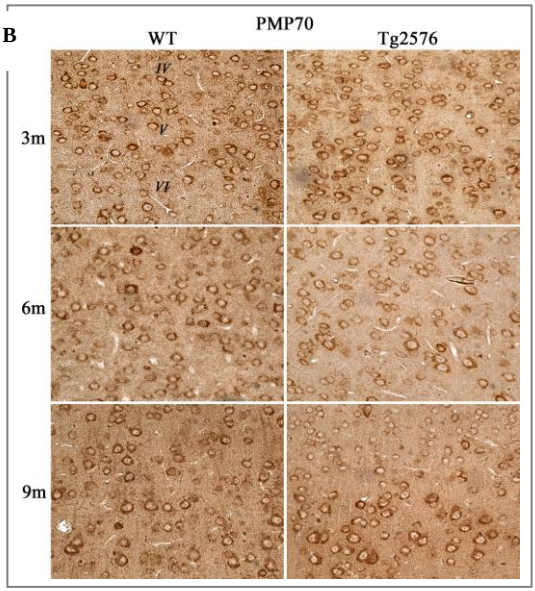

These results are confirmed by morphological data on neocortical sections (Fig. 6.1 B). PMP70 immunohistochemistry, showing specific cytoplasmic staining in pyramidal cells distributed in all the layers, reveals a decreased positivity between 3 and 6 months, especially prominent in the Tg2576. At 9 months, PMP70 immunoreactivity is again increased, even though no genotype-dependent variation is observed. At advanced ages, immunostaining levels remain stable in both 12- and 18-months-old mice (data not shown). As in the hippocampus, we performed double immunofluorescence experiments of PMP70 in combination with NeuN or GFAP in 3-month-old neocortex. Fig. 6.2 A shows the presence of peroxisomes in neocortical neurons particularly in the deep layers, while Fig. 6.2 B demonstrates peroxisomes in astroglial cells, particularly abundant in the superficial layers of the neocortex. Moreover, these experiments confirm molecular and light microscopic data, indicating that PMP70 levels are similar in both genotypes at an early AD stage (3 months).

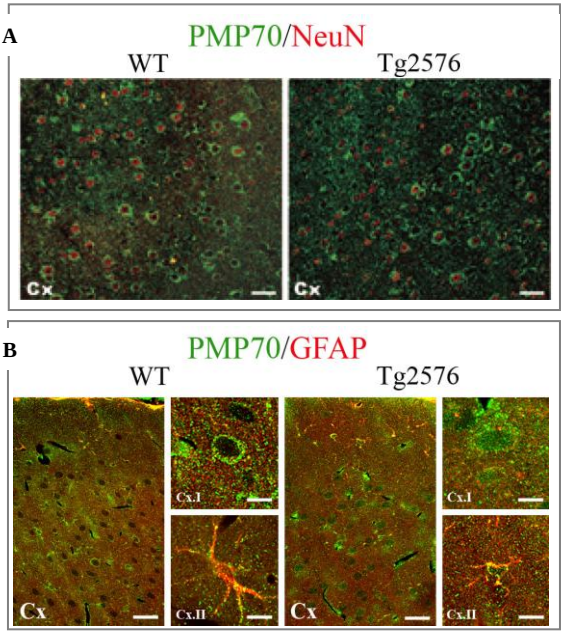

Fig. 6.2 Double IF of PMP70 (green) in combination with NeuN (red in A) or GFAP (red in B) in the cerebral cortex of WT and Tg2576 3-month-old brain. (A) PMP70-signal is similar in pyramidal neurons of neocortical deep layers. Bars, 30 μm. (B) PMP70-positive astrocytes are similarly present in superficial layers of the WT and Tg2576 parietal cortex. Cx.I, higher magnification of a cortical pyramidal neuron; Cx.II, higher magnification of an astrocyte. Bars 30 μm; bars in Cx.I and Cx.II, 10 μm.

Pex14p expression was also investigated in the neocortex at the onset and during the progression of disease, but our results fail to demonstrate either age- or genotype-related alterations of this peroxisomal biogenesis marker, as shown in Fig. 6.3. Consistently, IHC analysis shows no variation of Pex14p immunostaining levels (see Supplementary Fig. 2).

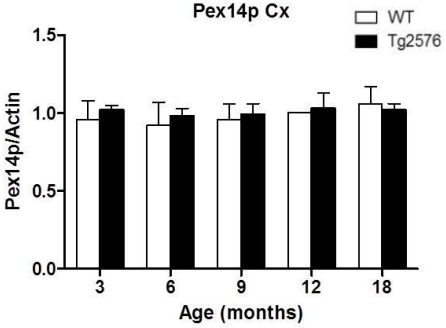

Fig. 6.3 Pex14p expression in WT and Tg2576 cerebral cortex of 3, 6, 9, 12, and 18 months of age. Densitometric values of Pex14p western blot performed on neocortical protein extracts, are shown. Values are expressed as mean ± SD.

6.2 Peroxisomal β-oxidation enzymes

Molecular data concerning AOX in the neocortex show no significant variation during aging or disease progression. The same pattern is observed for thiolase, showing stable levels of the protein in relation to normal and pathological stages considered. This suggests that no perturbation of the β-oxidation pathway occurs in the neocortex.

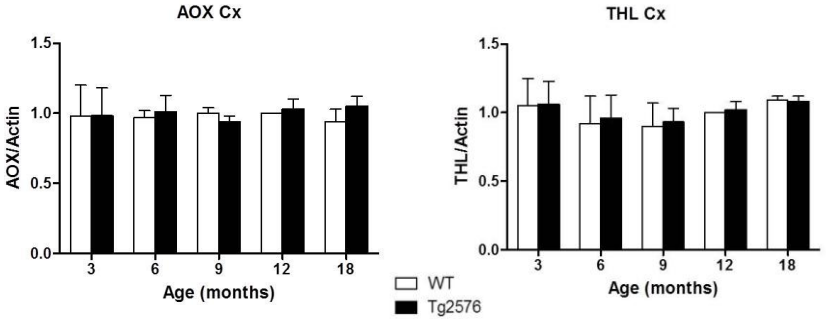

Fig. 6.4 Expression of peroxisomal β-oxidation enzymes in WT and Tg2576 cerebral cortex of 3, 6, 9, 12, and 18 months of age. Densitometric values of AOX and THL western blots performed on neocortical protein extracts, are shown. Values are expressed as mean ± SD.

6.3 Expression of PPARα in the first stages of the disease

PPARα immunohistochemistry, performed on cerebral cortex sections of 3-, 6-, and 9-month-old WT and Tg2576 mice, shows immunoreactive neurons in all cortical layers considered. In particular, high PPARα levels are detected at 3 months of age in both genotypes, followed by a decreased at 6 months especially prominent in the Tg2576 cerebral cortex. Later on, PPARα expression slightly increases even though its levels remain lower than those at 3 months of age. These morphological data are in agreement with biochemical results concerning PMP70 expression in the neocortex, suggesting a PPARα involvement in peroxisomal induction.

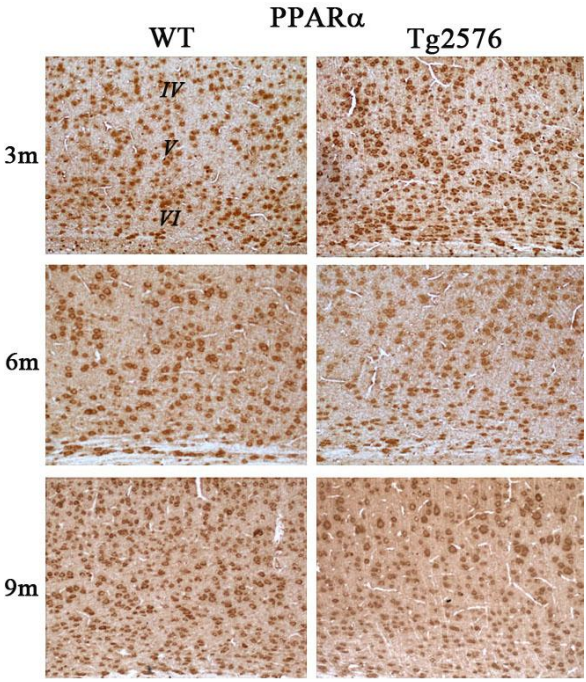

Fig. 6.5 Expression of PPARα in WT and Tg2576 cerebral cortex of 3, 6, and 9 months of age. PPARα immunolocalization in the neocortical layers (IV-VI) of WT and Tg2576 brains.

6.4 Expression of ROS-scavenging enzymes in the Tg2576 cerebral cortex

Concerning antioxidant defenses, we first analyzed the neocortical expression of catalase, a classical peroxisomal marker, responsible for H_2O_2 removal. CAT expression at 3 months is comparable in the two genotypes, similar to PMP70. In 6-month-old neocortex, protein levels significantly increase in the WT, thus

becoming higher than the respective Tg2576 (Fig. 6.6 A). Our results also demonstrate that CAT levels are unchanged during the disease progression. IHC experiments demonstrate similar catalase distribution and immonoreactivity levels during normal aging and AD progression, except for the 6-month-old Tg2576 neocortex where a lower staining is observed, as compared to their WT. (Fig. 6.6 B). Interestingly, CAT antibody occasionally reveals nuclear immunolocalization of the protein in neocortical neurons of 3-month-old Tg2576 brain, while in the WT the staining is exclusively found in the pericaryon (see insets in Fig 6.6 B).

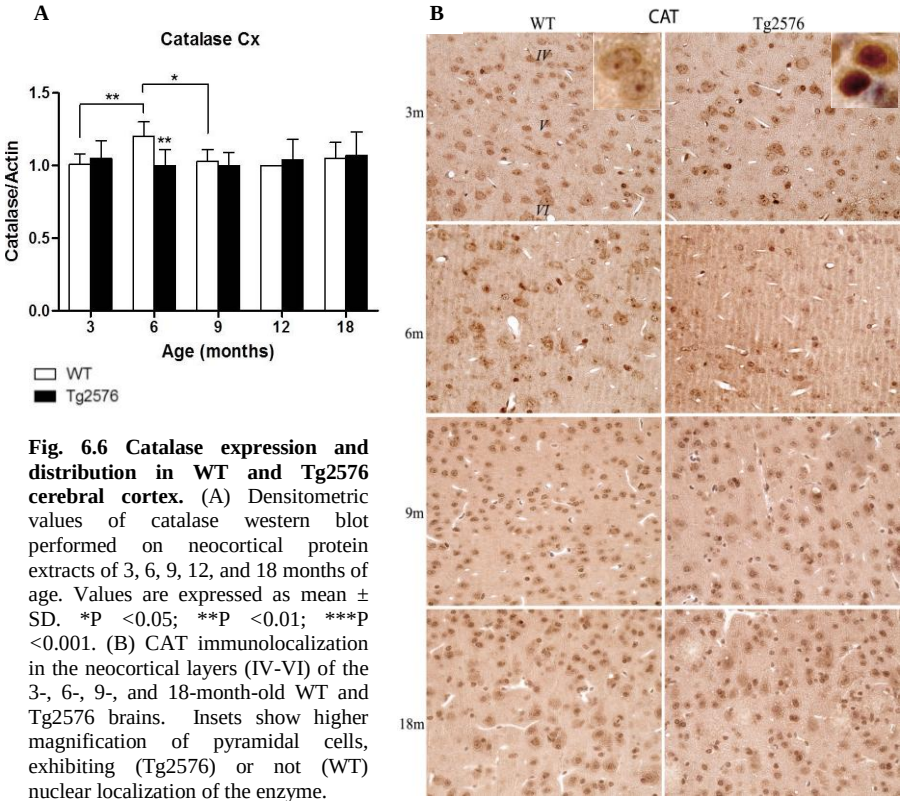

Fig. 6.6 Catalase expression and distribution in WT and Tg2576 cerebral cortex. (A) Densitometric values of catalase western blot performed on neocortical protein extracts of 3, 6, 9, 12, and 18 months of age. Values are expressed as mean ± SD. *P <0.05; **P <0.01; ***P <0.001. (B) CAT immunolocalization in the neocortical layers (IV-VI) of the 3-, 6-, 9-, and 18-month-old WT and Tg2576 brains. Insets show higher magnification of pyramidal cells, exhibiting (Tg2576) or not (WT) nuclear localization of the enzyme.

This finding prompted us to further investigate the ultrastructural distribution of CAT by pre-embedding IEM. Indeed, in WT cells CAT is exclusively localized to peroxisomes, while no DAB precipitates are seen in the rest of the cytoplasm or in the nucleus (Fig. 6.7, A, B). By contrast, in Tg2576 specimens, CAT intracellular distribution is not limited to peroxisomes, but extends to other compartments (Fig. 6.7, C-F). These include the nucleus, particularly the heterochromatin, the cytosol, especially in proximity to the outer mitochondrial membrane, and cell processes, where DAB deposits are associated with microtubules and post-synaptic densities.

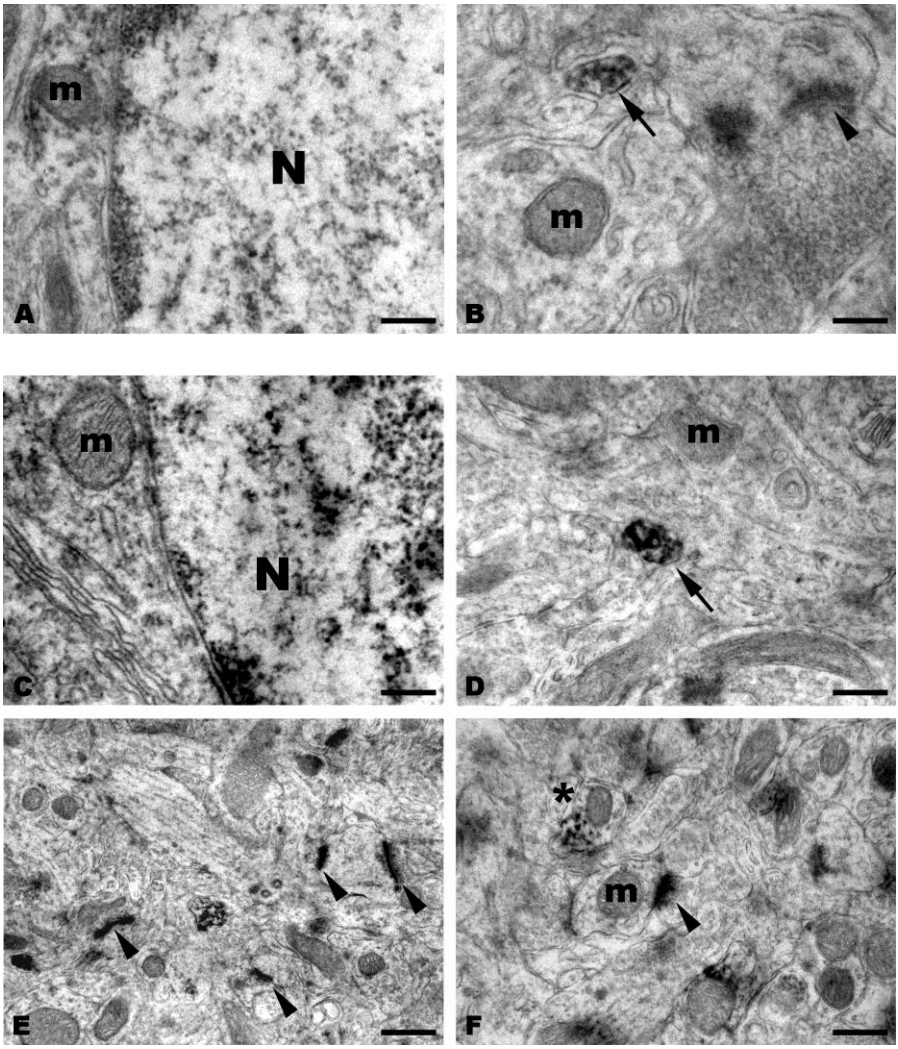

Fig. 6.7 CAT immunoelectron microscopic localization in cortical neurons of 3-month-old WT (A, B) and Tg2576 (C-F) animals. Positive peroxisomes (arrows) are observed in cells in both genotypes; by contrast, some neuronal nuclei (N) and post-synaptic densities (arrowheads) are exclusively labelled in Tg2576 specimens. Note association of DAB deposits with microtubules of some dendritic processes in Tg2576 sections (asterisk). m, mitochondria.

Differently from CAT expression, relatively stable at advanced aging stages (12-18 months), levels of cytosolic and mitochondrial superoxide dismutases (SOD1 and SOD2) are significantly altered at these ages (Fig. 6.8). In particular, our results demonstrate genotype-related variations starting from 12 months, when SOD1 and SOD2 expression is significantly higher in the diseased neocortex, compared to its

WT counterpart. At 18 months, Tg2576 neocortex shows a decrease in SOD1 and SOD2 levels while the respective WT displays increased protein expression.

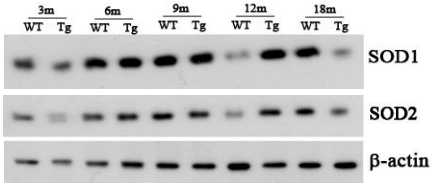

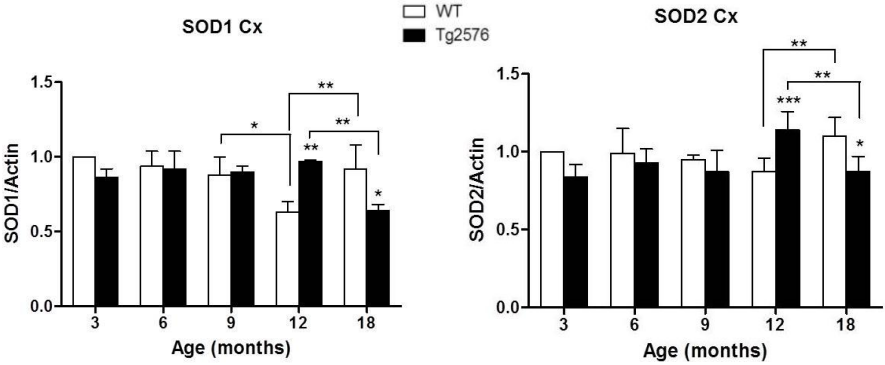

Fig. 6.8 Superoxide dismutases expression in WT and Tg2576 cerebral cortex of 3, 6, 9, 12, and 18 months of age. Image of *β*-actin-normalized WB representative experiment for SOD1 and SOD2, performed on neocortical protein extracts of 3-, 6-, 9-, 12-, and 18-month-old WT and Tg2576 brains. In the lower pictures, densitometric values of SOD1 and SOD2 western blots, are shown. Values are expressed as mean ± SD. *P <0.05; **P <0.01; ***P <0.001.

We also investigated the expression of the cytosolic protein GPX1, involved in the removal of H_2O_2 (Fig. 6.9). This enzyme shows an interesting pattern, as it initially is up-regulated and subsequently down-regulated in both genotypes. These age-related variations appear especially dramatic in the Tg2576 neocortex, which, at 9 and 18 months of age shows respectively higher and lower protein levels, compared to WT.

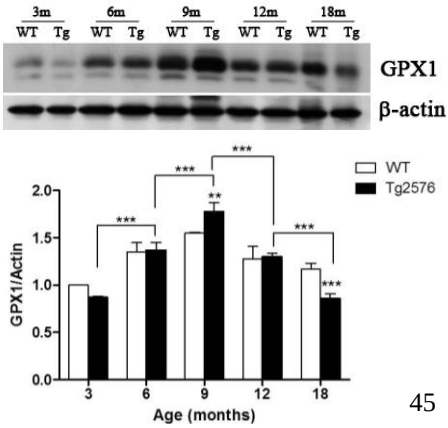

Fig. 6.9 GPX1 expression in WT and Tg2576 cerebral cortex. Image of *β*-actin-normalized WB representative experiment for GPX1, performed on neocortical protein extracts of 3-, 6-, 9-, 12-, and 18-month-old WT and Tg2576 brains. In the lower picture, densitometric values of GPX1 western blot, are shown. Values are expressed as mean ± SD. To sake clarity, only significant differences regarding the Tg2576 are shown. Concerning the WT the following significant variations are observed: 3 vs 6 months (***), 6 vs 9 months (**), and 9 vs 12 months (***). **P <0.01; ***P <0.001.

Section III

Discussion and Conclusions

Chapter 7
Discussion and Conclusions

In the present study, the first extensive characterization of brain peroxisomal population at the onset and during the progression of AD-type pathology in a transgenic mouse model (Tg2576, Hsiao *et al*., 1996) was accomplished. To relate possible variations in peroxisomal protein expression with age-related changes in tissue cytoarchitecture, we also examined the distribution and arrangement of neural cell types, focusing on the cerebral cortex and hippocampal formation, as the primarily affected areas in AD (Hyman *et al*., 1984; Reilly *et al*., 2003).

Our morphological and molecular data support the concept that the overall neuronal layering in the cerebral cortex and hippocampus is conserved until histopathological hallmarks are observed.
In the neocortex, cytoarchitectural changes are detected concomitant to senile plaques first appearance. Reports on the age of first detection of dense cored amyloid aggregates in the neocortex of Tg2576 animals are somewhat conflicting (Karawabayashi *et al*., 2001; Massaad *et al*., 2009), and our results obtained by Congo Red staining provide evidence that these deposits are indeed present as early as at 9 months of age. To this respect, it is worth mentioning that in the above studies the gender of the examined animals was not indicated, while in our study we selectively analyzed females, which reportedly show greater senile plaque load, compared to males (Callahan *et al*., 2001). In Tg2576 neocortex, we found that Aβ deposition determines displacement of neuronal cells and progressive hyperproliferation/hypertrophy of astrocytes and microglial cells, starting from 9 months. This glial induction may be related to initial inflammation processes, which have been classically considered as downstream events in AD pathology. According to some authors, the significance of microglia phagocytic activation would be an attempt to digest extracellularly deposited amyloid fibrils (Sasaki *et al*., 2002). Nevertheless, neuroinflammation has recently been proposed as an early event and prime mover in Alzheimer's disease, driving mitochondrial dysfunction and apoptotic induction. Interestingly, microglia with altered morphology appear early in rodent AD models, prior to development of frank amyloid plaques, thus representing a clearance mechanism impeding oligomeric Aβ deposition into larger aggregates (Town *et al*., 2011).
Differently from the cerebral cortex, in the Tg2576 hippocampus we could trace the first congophilic amyloid plaques as late as 18 months. While this observation is in overall agreement with previous studies (Jacobsen *et al*., 2006), it is worth noting that the first hippocampal dysfunctions, as assessed by different behavioral and molecular parameters, occur well before this stage, thus supporting the hypothesis that Aβ accumulation is not directly linked to the onset of pathology. Indeed, the classical amyloid cascade hypothesis has been recently challenged, in

favor of other mechanisms, possibly involving early oxidative stress as a causative factor in the generation of neuronal damage (Nunomura *et al*., 2010). Nevertheless, the role of amyloid β as a toxic molecule is still generally accepted, at least at more advanced AD pathogenetic stages. Indeed, our morphological analysis performed on 18-month-old hippocampal formation, highlighted disruption of neuropil areas, including the stratum radiatum and stratum oriens, where dystrophic neurites, associated with astrocyte and microglial recruitment, are detected around and within amyloid plaques.

One of the most intriguing results obtained from the analysis of hippocampal cytoarchitecture, is provided by GFAP immunostaining. Indeed, at the earliest age considered (3 months), we detected both a stronger intensity level for this intermediate filament and a higher number of positive cells in the DG of Tg2576 mice, with respect to its WT counterpart. While this marker is widely used to detect astroglial cells, it is relevant to mention that even neural stem/progenitor cells express GFAP in adult neurogenic regions of the brain, including the subgranular zone (SGZ) of the DG. Since the distribution and radial morphology of our GFAP-positive cells in this hippocampal subfield closely resembles those of neural stem cells, we can speculate that this population actually includes neural progenitors. This would imply that activation of neurogenesis occurs early in the disease, possibly triggered by neuronal damage. Later on (18 months), this pattern of GFAP immunoreactivity in the DG is no longer found, as dramatically decreased numbers of GFAP-positive cells at the granule cell/hilus border are detected, when compared to either younger Tg2576, or age-matching WT animals.

The issue of modulation of neurogenesis in the hippocampus during AD is still debated, as conflicting results are reported by different groups. Most Authors believe that neural stem cell proliferation, as assessed by BrdU labeling, is decreased in AD-like pathology (Dong *et al*., 2004), while two reports describe enhanced neuron generation in human AD and in a mouse model (Jin *et al*., 2004a; Jin *et al*., 2004b). Interestingly, investigation of the course of neurogenesis in the adult hippocampal SGZ, from primary progenitors to intermediate or amplifying progenitors has highlighted different features related to their mitotic rate. Primary progenitors, with astrocytic features, including GFAP and nestin expression and radial morphology, are thought to divide slowly, generating the subsequent intermediate progenitor. The next progenitor, which is GFAP-negative, while positive to neuronal markers, is considered to divide rapidly to produce immature neurons or neuron-committed progenitors (Namba *et al*., 2011). In this view, it will be relevant to further characterize the GFAP-positive cells observed in our Tg2576 specimens, in order to ascertain their astrocytic or primary progenitor nature, through the use of adequate markers, such as nestin.

Notably, our study on the distribution of the neuronal marker NeuN in the hippocampus and neocortex of Tg2576 mice aging 3 to 18 months, shows no change either in the number of positive cells or in the immunostaining levels, thus

suggesting that no appreciable cell death is present in Tg2576 model. This is in agreement with studies from other groups, which failed to describe neuronal cell loss in this mouse strain, even at late stages of the disease (Irizarry *et al.*, 1997). Therefore, we can conclude that more subtle alterations, affecting neuronal functionality, occur prior to histopathological manifestations. Indeed, several reports have demonstrated that behavioral and molecular changes in early AD result in impaired neurotransmission, rather than decreased survival (Jacobsen *et al*., 2006; Hermann *et al*., 2009; Smith *et al*., 2010; Havas *et al*., 2011). The recent paper by Cecconi's group (D'Amelio *et al*., 2011), focusing on 3-month-old Tg2576 mice, so far considered as pre-symptomatic, has indicated this age as the onset of disease, based on impaired memory performance, hippocampal electrophysiological deficits, decrease in dendritic spine density, and presence of activated caspase3 at the post-synaptic compartment. The proposed model involves free radical generation, resulting in dendritic spine loss and neuronal damage (D'Amelio *et al*., 2011). Accordingly, oxidative stress has been recently suggested as a primary culprit in AD pathogenesis, as nucleic acid oxidation is detected early in human AD brain (Nunomura *et al*., 2010). In this scenario, mitochondria certainly play a pivotal role, as both target and source of ROS (Rigoulet *et al*., 2011). Indeed Aβ-mediated synaptic dysfunction has been linked to mitochondrial alterations, including impaired functionality and compensatory induction of genes related to energy metabolism and apoptosis (Reddy *et al*., 2004; Manczak *et al*., 2006). Mitochondria, however, are not the sole organelles involved in ROS metabolism, since peroxisomes also play a central role in the removal and generation of these molecules (Schrader and Fahimi, 2006).

The importance of peroxisomes for nervous system functioning is represented by their involvement in a wide variety of metabolic processes, also including lipid metabolism. The nervous tissue is especially rich in PUFAs and plasmalogens, which are susceptible to oxidative modifications (Lukiw and Bazan, 2008; Lessig and Fuchs, 2009), and whose biosynthesis partially occurs in peroxisomes (Wanders and Waterman, 2006). Interestingly, decreases in plasmalogen and PUFA content have been found in AD patients (Goodenowe *et al*., 2007; Kou *et al*., 2011). Among PUFAs, DHA seems particularly relevant, since low dietary intake is a risk factor of age-related cognitive decline and AD (Cunnane *et al*., 2009). Conversely, DHA supplementation results in beneficial effects on cognitive decline and reduces Aβ production (Grimm *et al*., 2011; Hashimoto and Hossain, 2011). Participation of peroxisomes in lipid metabolism mainly involves the β-oxidation pathway of VLCFA. Remarkably, these have been found to accumulate in human AD brain, allowing to hypothesize a peroxisomal dysfunction (Kou *et al*., 2011).
To investigate the involvement of peroxisomes in AD pathology, we characterized the peroxisomal population from a molecular and morphological point of view, by

examining the expression of biogenesis markers, membrane proteins, and matrix enzymes, at the disease onset (3 months), and during its progression (6, 9, 12, 18 months).

Overall, our results on the hippocampal formation demonstrate an early and significant peroxisomal induction in 3-month-old Tg2576 mice compared to WT. Indeed, PMP70, considered a marker for evaluating the size of peroxisomal population (Santos *et al*., 1994) is upregulated, as assessed by WB and immunolocalization techniques. More specifically, IHC revealed especially intense immunostaining in the pyramidal layer of hippocampal CA1 subdivision of Tg2576 mice, while PMP70 immunoelectron microscopy showed a higher number of peroxisomes in Tg2576 neuronal cell somata, with respect to WT. This evidence is in agreement with a recent work from Berger's group, based on immunofluorescent localization of the same marker, indicating an increased peroxisomal volume density in neuronal cell bodies of human AD brain (Kou *et al*., 2011). According to these Authors, this higher concentration of somatic peroxisome density may be due to impaired peroxisome trafficking along the microtubules. To this respect, Pex14 has recently been involved in microtubule-based peroxisome motility in human cells (Bharti *et al*., 2011). Our data, showing unchanged levels of this membrane protein, suggest that newly formed peroxisomes may contain relatively low ratio Pex14/PMP70, possibly involving altered peroxisome trafficking.

Consistent with the results obtained for PMP70, several other peroxisome-related proteins, including Pex5, AOX, and PPARα, are upregulated in 3-month-old Tg2576 hippocampus, arguing for a peroxisomal proliferation occurring at the very beginning of AD pathology. This could represent a compensatory response to early neuronal insult; in particular, we believe that this response is activated to cope the impaired energy metabolism, occurring at this early stage (Reddy *et al*., 2004; Ferrer, 2009). Indeed, all the above molecules are involved in some step of the fatty acyl β-oxidation pathway. Namely, Pex5 is responsible for the import of PTS1-bearing matrix enzymes, including AOX (Meinecke *et al*., 2010); PMP70 is an ATP-binding cassette half-transporter residing in the peroxisomal membrane and participating in the translocation of VLCFA (Wanders *et al*., 2007); AOX is the rate limiting enzyme of the β-oxidation cycle (Wanders *et al*., 2010); and PPARα directly regulates PMP70 and AOX transcription (Fourcade *et al*., 2001; Kane *et al*., 2006). Strikingly, the other crucial enzyme for the pathway, i.e., THL, fails to undergo similar increase, indicating possible inefficiency of the β-oxidation pathway in the Tg2576. This would imply accumulation of VLCFA-derived intermediates in the brain, in line with the recent findings on the brain of AD patients (Kou *et al*., 2011).

Induction of AOX in 3-month-old Tg2576 hippocampus is also likely to result in enhanced hydrogen peroxide production, since AOX is an H_2O_2-producing oxidase. We therefore evaluated the levels of CAT, i.e., the major antioxidant

enzyme localized inside the peroxisomes. As we failed to detect any genotype-dependent variation in CAT levels at 3 months of age, we hypothesize an intraperoxisomal overproduction of H_2O_2, leading to leakage of this highly diffusible and relatively stable molecule to the cytosol. On the other hand, GPX1, another major H_2O_2–scavenging enzyme, is down-regulated in 3-month-old Tg2576 hippocampus, suggesting that an imbalance between generation and removal of hydrogen peroxide. Concerning the involvement of other ROS scavenging enzymes, SOD1 shows significantly lower levels in Tg2576 hippocampus, compared to its WT counterpart. Interestingly, this cytosolic protein is selectively damaged by H_2O_2, thus being itself a major target of oxidative damage (Fujiwara *et al*., 2007). Somewhat surprisingly, mitochondrial superoxide dismutase (SOD2), is significantly increased in the hippocampus of 3-month-old Tg2576 mice. This result, in agreement with the involvement of these organelles at early AD stages (Manczac *et al*., 2006), could be also interpreted in the light of reports demonstrating induction of mitochondrial genes in young Tg2576 mice, as a compensatory response to their impaired metabolism (Reddy *et al*., 2004). It should be here emphasized that the augmentation of SOD2, converting superoxide ion to H_2O_2, in the absence of parallel increase in any of the H_2O_2 scavengers, likely contributes itself to redox imbalance.

Therefore, our data prefigures an early oxidative stress condition occurring in the hippocampus, strongly supporting the idea that this is the primary culprit in AD pathogenesis (Nunomura *et al*., 2010). To gain further insight in this issue, we took advantage of markers for detecting oxidative modification to biomolecules, such as lipids and nucleic acids (Singh *et al*., 2010; Nunomura *et al*., 2010). Our results, which are the first to report lipoperoxidation and DNA/RNA oxidation in the hippocampus of 3-month-old Tg2576 mice, strongly support the hypothesis that oxidative stress is already present at this early stage of disease. This condition appears to specifically involve neuronal mitochondria, since anti-8-OHG/OHdG preferentially stains the cytoplasm of hippocampal cells, indicating that either RNA or, more plausibly, mitochondrial DNA is affected by redox imbalance. This damage is indeed likely to be specifically due to the genotoxic action of hydroxyl radical, in turn resulting from breakdown of H_2O_2. A very similar situation has been described in rodent liver after chronic treatment with a peroxisome proliferator (Kasai *et al*., 1989), a classical model in which the dramatic increase of H_2O_2-producing oxidases is not accompanied by catalase induction (Reddy *et al*., 1986). Remarkably, treatment with a PPARα agonist also produces decreased GPX activity (Ciriolo *et al*., 1982), thus reinforcing the idea that changes occurring in our model at 3 months of age are the result of PPARα activation.

Peroxisomal proliferation mediated by PPARα is also confirmed by ultrastructural analysis, showing nuclear immunolocalization of this receptor in 3-month-old Tg2576 hippocampal pyramidal neurons. It remains to be determined what is the molecular trigger activating this transcription factor. PPARα natural ligands,

though remaining partially elusive, include several lipids, ranging from VLCFA, to a variety of oxidized molecules (Yeldandi *et al*., 2000).
Overall, our data allow to envision a self-perpetuating oxidative damage in which peroxisomes are early involved, most probably playing a pro-oxidant, rather than an anti-oxidant role.
During the progression of AD pathology, peroxisomal population undergoes dramatic changes, in that several proteins, including PMP70, Pex14p, and AOX, are decreased in 6-month-old Tg2576 hippocampus. This may reflect an impaired peroxisomal biogenesis or autophagic removal of excess organelles. To this respect, work in progress by our group suggests that levels of pro-autophagic protein AMBRA1 are reduced at 6 months of age in Tg2576 hippocampus, thus allowing to hypothesize that the decrease in peroxisomal population is mainly due to organelle damage. In contrast with the general trend of the above peroxisomal markers, relatively high levels of CAT are detected in the Tg2576 hippocampus at the same age, suggesting a late response to peroxisomal induction, in agreement with what described in the liver following peroxisomal agonists administration (Reddy *et al*., 1986).
Other antioxidant enzymes show interesting changes at more advanced stages of the disease. Indeed, GPX1 and SOD1 increase from 6 to 9 months of age in the Tg2576 hippocampus, suggesting a late response, not involving the peroxisomes. However, at 12 months, when amyloid plaques start to form, GPX1, SOD1 and SOD2 show significantly lower levels in the Tg2576 mice, with respect to WT. Accordingly, decreased activities of SOD1 and GPX have been reported in patients with symptomatic AD by Casado *et al*. (2008). Importantly, the overexpression of SOD2 in Tg2576 results in diminished plaque deposition around 12 months, suggesting a role of the superoxide anion in promoting APP processing through the amyloidogenic pathway (Massaad *et al*., 2009).
A striking result regarding peroxisomes was obtained on 18-month-old mouse hippocampus. In fact, a peak of PMP70 expression is observed irrespective of the genotype, allowing to hypothesize a change in peroxisomal population related to the ageing process. Consistently, its main regulator, PPARα, shows intense immunoreactivity in the aged hippocampus, in both WT and Tg2576 animals. As glial cells are known to undergo numerical increase and hypertrophy during aging (Amenta *et al*., 1998), we examined the expression of PMP70 in relation to the astroglial marker GFAP, by double immunofluorescence. Confocal microscopy revealed elevated PMP70 levels in both genotypes. Moreover, subtle differences can be detected between the immunodistribution of the protein in the two genotypes. Indeed, cells showing overlapping positivity to PMP70 and GFAP are more numerous in Tg2576 hippocampal fields, than in their WT counterpart. This argues for a major contribution of glial peroxisomes to the overall peroxisomal population in 18-month-old Tg2576 hippocampus. Interestingly, at this age, Pex14 is selectively increased in Tg2576 hippocampus, and is showing especially strong

immunoreaction in glial cells, thus suggesting cell type-related heterogeneity in peroxisomal protein content. Differences in functional and morphological features of peroxisomes between astrocytes and neurons have been described by previous works (Arnold *et al*., 1979; Cimini *et al*., 1998). On the other hand, imbalanced enzymatic content of peroxisomes is suggested by the dramatic decrease in THL in 18-month-old hippocampus, also allowing to hypothesize that inefficient β-oxidation is associated with normal and pathological aging.
Antioxidant enzymes show protein-specific variations in the aged hippocampus. Overall, it is conceivable that a pro-oxidant environment is still present in the cytosol, rather than in peroxisomes, since decreased levels of GPX1 and SOD1 are observed in Tg2576 mice, while CAT is unchanged. Accordingly, oxidative damage markers reveal lipoperoxidation and nucleic acid oxidative modification in the pathological genotype and, to a lesser extent in physiologically aged mice. Interestingly enough, the degree of immunoreactivity for 8-OHG/8-OHdG is slightly reduced in 18-month-old Tg2576, compared to 3 months of age, in agreement with several authors (Cuajungco *et al*., 2000; Weidner *et al*., 2011).

The susceptibility to Aβ-mediated damage appears to strongly depend on the brain region considered. In fact, our results on the cerebral cortex show different behavior of the peroxisomal population, with respect to the hippocampus. Indeed, at 3 months of age, no variation in the expression levels of peroxisomal proteins was observed. Nevertheless, catalase showed a delocalization, as assessed by immunoelectron microscopy, being found at extraperoxisomal sites, including the nucleus, cytosol, and post-synaptic densities. While we cannot rule out the possibility that impaired translocation of this scavenging enzyme into the peroxisomes occurs in the neocortex, it is also conceivable that its transport to sensitive sites may contribute to enhancing protection against oxidative damage.
The most relevant quantitative change in the Tg2576 neocortex involves PMP70, the levels of which are dramatically reduced at 6 months, compared to both 3-month-old Tg2576 and 6-month-old WT. This finding is consistent with data on hippocampal tissue, and may reflect either the onset of neuronal damage or, most probably, down-regulation of this particular protein. In fact, Pex14, AOX, and THL are unchanged throughout the period considered.
Concerning the expression of antioxidant enzymes in the cerebral cortex, we found a peak in GPX1 levels in 9-month-old Tg2576 mice. This evidence is in agreement with Apelt *et al*. (2004), demonstrating increased GPX activity in cerebral cortex of Tg2576 mice at the same age. In view of the fact that 9 months is an especially critical stage of disease for the neocortex, based on the appearance of the first amyloid plaques, increased antioxidant defenses may represent a compensatory response to Aβ deposition. Accordingly, GPX overexpression has been observed to increase the resistance of neuronal cells to Aβ-mediated neurotoxicity (Barkats *et al*., 2000). We also found that cortical SOD1 and SOD2 levels were higher in

transgenic mice aging 12 months, concomitant with the progressive increase in plaque formation. This is consistent with immunocytochemical analysis of Tg2576 mouse brain in which marked increase in SOD1 was found around β-amyloid deposits (Papolla *et al*., 1998; Smith *et al*., 1998), as well as with enzymatic assays demonstrating higher SOD activity in Tg2576 cerebral cortex than in WT (Apelt *et al*., 2004). Similarly to GPX, increases in these scavenging enzymes appear to represent a response to ongoing oxidative stress. A specific role of the superoxide radical in mediating the neurotoxic action of β-amyloid has also been suggested, based on the protection against β-amyloid insult both *in vitro* (Keller *et al*., 1998) and *in vivo* (Celsi *et al*., 2004) by overexpression of SOD1 or SOD2.

In conclusion, the results obtained during my PhD project demonstrate early molecular changes in the hippocampal formation of Tg2576 mice, specifically involving peroxisomes. Three months of age is an especially promising time point for devising pharmacological strategies aimed at delaying or even preventing AD onset (Cimini *et al*., 2009; D'Amelio *et al*., 2011). In our view, potential therapies at this age should primarily target oxidative stress, possibly through treatment with antioxidant molecules. Several studies deal with the effects of PPAR agonists in different mouse models of AD (Mandrekar-Colucci and Landreth, 2011). These molecules are reported to counteract inflammatory processes and oxidative damage, via different signaling pathways. However, all of these studies have targeted isotypes other than α, namely PPARγ or PPARβ/δ. The use of PPARα ligands, so far unexplored, should be considered with some *caveat* regarding the window of treatments. In fact, it appears that induction of peroxisomal proliferation would be deleterious at 3 months in Tg2576 mice, since it would probably exacerbate peroxisomal H_2O_2-mediated neuronal damage. Based on our results, we instead suggest administration of PPARα agonists around 6 months of age, because this treatment may result in reversal of initial symptoms, including lipid metabolic dysfunctions.

REFERENCES

Alzheimer Disease Mutation Database. Alzheimer disease & Frontotemporal Dementia Mutation Database (online). (2010) http://www.molgen.ua.ac.be/admutations/

Amenta F, Bronzetti E, Sabbatini M, and Vega JA. (1998) Astrocyte changes in aging cerebral cortex and hippocampus: a quantitative immunohistochemical study. *Microsc Res Tech*., **43**:29-33.

Apelt J, Bigl M, Wunderlich P, and Schliebs R. (2004) Aging-related increase in oxidative stress correlates with developmental pattern of beta-secretase activity and beta-amyloid plaque formation in transgenic Tg2576 mice with Alzheimer-like pathology. *Int J Dev Neurosci*., **22**:475-484.

Arnold G, and Holtzman E. (1978) Microperoxisomes in the central nervous system of the postnatal rat. *Brain Res*., **155**:1-17.

Arnold G, Liscum L, and Holtzman E. (1979) Ultrastructural localization of D-amino acid oxidase in microperoxisomes of the rat nervous system. *J Histochem Cytochem*., **27**:735-745.

Ashe KH. (2001) Learning and memory in transgenic mice modeling Alzheimer's disease.*Learn Mem.*, **8**:301-308.

Baes M, and Van Veldhoven PP. (2006) Generalised and conditional inactivation of Pex genes in mice. *Biochim Biophys Acta*., **1763**:1785-1793.

Baes M. (2000) Mouse models for peroxisome biogenesis disorders. *Cell Biochem Biophys*., **32**:229-237.

Ballard C, Gauthier S, Corbett A, Brayne C, Aarsland D, and Jones E. (2011) Alzheimer's disease. *Lancet*, **377**:1019-1031.

Barkats M, Millecamps S, Abrioux P, Geoffroy MC, and Mallet J. (2000) Overexpression of glutathione peroxidase increases the resistance of neuronal cells to Abeta-mediated neurotoxicity. *J Neurochem*., **75**:1438-1446.

Behl C, Davis JB, Lesley R, and Schubert D. (1994) Hydrogen peroxide mediates amyloid beta protein toxicity. *Cell*, **77**:817-827.

Bekris LM, Yu CE, Bird TD, and Tsuang DW. (2010) Genetics of Alzheimer disease. *J. Geriatr. Psychiatry Neurol*., **23**:213-227.

Bharti P, Schliebs W, Schievelbusch T, Neuhaus A, David C, Kock K, Herrmann C, Meyer HE, Wiese S, Warscheid B, Theiss C, and Erdmann R. (2011) PEX14 is required for microtubule-based peroxisome motility in human cells. *J Cell Sci*., **124**:1759-1768.

Blennow K, de Leon MJ, and Zetterberg H. (2006) Alzheimer's disease. *Lancet*, **368**:387-403.

Bonda DJ, Wang X, Perry G, Nunomura A, Tabaton M, Zhu X, and Smith MA. (2010) Oxidative stress in Alzheimer disease: a possibility for prevention. *Neuropharmacology*, **59**:290-294.

Bonekamp NA, Völkl A, Fahimi HD, Schrader M. (2009) Reactive oxygen species and peroxisomes: struggling for balance. *Biofactors*, **35**:346-355.

Brites P, Mooyer PA, El Mrabet L, Waterham HR, and Wanders RJ. (2009) Plasmalogens participate in very-long-chain fatty acid-induced pathology. *Brain*, **132**:482-492.

Busciglio J, Pelsman A, Wong C, Pigino G, Yuan M, Mori H, and Yankner BA. (2002) Altered metabolism of the amyloid beta precursor protein is associated with mitochondrial dysfunction in Down's syndrome. *Neuron*, **33**:677-688.

Calhoun ME, Burgermeister P, Phinney AL, Stalder M, Tolnay M, Wiederhold KH, Abramowski D, Sturchler-Pierrat C, Sommer B, Staufenbiel M, and Jucker M. (1999) Neuronal overexpression of mutant amyloid precursor protein results in prominent deposition of cerebrovascular amyloid. *Proc Natl Acad Sci*., **96**:14088-14093.

Callahan MJ, Lipinski WJ, Bian F, Durham RA, Pack A, and Walker LC. (2001) Augmented senile plaque load in aged female beta-amyloid precursor protein-transgenic mice. *Am J Pathol*.,**158**:1173-1177.

Casado A, Encarnación López-Fernández M, Concepción Casado M, and de La Torre R. (2008) Lipid peroxidation and antioxidant enzyme activities in vascular and Alzheimer dementias. *Neurochem Res*., **33**:450-458.

Celsi F, Ferri A, Casciati A, D'Ambrosi N, Rotilio G, Costa A, Volonté C, and Carrì MT. (2004) Overexpression of superoxide dismutase 1 protects against beta-amyloid peptide toxicity: effect of estrogen and copper chelators. *Neurochem Int*., **44**:25-33.

Chishti MA, Yang DS, Janus C, Phinney AL, Horne P, Pearson J, Strome R, Zuker N, Loukides J, French J, Turner S, Lozza G, Grilli M, Kunicki S, Morissette C, Paquette J, Gervais F, Bergeron C, Fraser PE, Carlson GA, George-Hyslop PS, and Westaway D. (2001) Early-onset amyloid deposition and cognitive deficits in transgenic mice expressing a double mutant form of amyloid precursor protein 695. *J Biol Chem.*, **276**:21562-21570.

Chung JH, Seo AY, Chung SW, Kim MK, Leeuwenburgh C, Yu BP, and Chung HY. (2008) Molecular mechanism of PPAR in the regulation of age-related inflammation. *Ageing Res Rev.*,**7**:126-136.

Cimini A, Moreno S, D'Amelio M, Cristiano L, D'Angelo B, Falone S, Benedetti E, Carrara P, Fanelli F, Cecconi F, Amicarelli F, and Cerù MP. (2009) Early biochemical and morphological modifications in the brain of a transgenic mouse model of Alzheimer's disease: a role for peroxisomes. *J Alzheimers Dis*., **18**:935-952.

Cimini AM, Moreno S, Giorgi M, Serafini B, and Cerú MP. (1993) Purification of peroxisomal fraction from rat brain. *Neurochem Int*., **23**:249-260.

Cimini AM, Singh I, Farioli-Vecchioli S, Cristiano L, and Cerú MP. (1998) Presence of heterogeneous peroxisomal populations in the rat nervous tissue. *Biochim Biophys Acta*., **1425**:13-26.

Ciriolo MR, Mavelli I, Rotilio G, Borzatta V, Cristofari M, and Stanzani L. (1982) Decrease of superoxide dismutase and glutathione peroxidase in liver of rats treated with hypolipidemic drugs. *FEBS Lett.*, **144**:264-268.

Conquer JA, Tierney MC, Zecevic J, Bettger WJ, and Fisher RH. (2000) Fatty acid analysis of blood plasma of patients with Alzheimer's disease, other types of dementia, and cognitive impairment. *Lipid,*. **35**:1305-1312.

Cuajungco MP, Goldstein LE, Nunomura A, Smith MA, Lim JT, Atwood CS, Huang X, Farrag YW, Perry G, and Bush AI. (2000) Evidence that the beta-amyloid plaques of Alzheimer's disease represent the redox-silencing and entombment of abeta by zinc. *J Biol Chem*., **275**:19439-19442.

Cunnane SC, Plourde M, Pifferi F, Bégin M, Féart C, and Barberger-Gateau P. (2009) Fish, docosahexaenoic acid and Alzheimer's disease. *Prog Lipid Res*., **48**:239-256.

D'Amelio M, Cavallucci V, Middei S, Marchetti C, Pacioni S, Ferri A, Diamantini A, De Zio D, Carrara P, Battistini L, Moreno S, Bacci A, Ammassari-Teule M, Marie H, Cecconi F. (2011) Caspase-3 triggers early synaptic dysfunction in a mouse model of Alzheimer's disease. *Nat Neurosci.*, **14**:69-76.

De Duve C, and Baudhuin P. (1966) Peroxisomes (microbodies and related particles). *Physiol Rev*., **46**:323-357.

Depreter M, Espeel M, and Roels F. (2003) Human peroxisomal disorders. *Microsc Res Tech*., **61**:203-223.

Dong H, Goico B, Martin M, Csernansky CA, Bertchume A, and Csernansky JG. (2004) Modulation of hippocampal cell proliferation, memory, and amyloid plaque deposition in APPsw (Tg2576) mutant mice by isolation stress. *Neuroscience*, **127**:601-609.

Drago I, Giacomello M, Pizzo P, and Pozzan T. (2008) Calcium dynamics in the peroxisomal lumen of living cells. *J Biol Chem.*, **283**:14384-14390.

Dumont M, Wille E, Stack C, Calingasan NY, Beal MF, and Lin MT. (2009) Reduction of oxidative stress, amyloid deposition, and memory deficit by manganese superoxide dismutase overexpression in a transgenic mouse model of Alzheimer's disease. *FASEB J.*, **23**:2459-2466.

Elder GA, Gama Sosa MA, and De Gasperi R. (2010) Transgenic mouse models of Alzheimer's disease. *Mt Sinai J Med*., **77**:69-81.

Erdmann R, and Schliebs W. (2005) Opinion: peroxisomal matrix protein import - the transient pore model. *Nat Rev Mol Cell Biol*, **6**:738-742.

Farioli-Vecchioli S, Moreno S, and Cerù MP. (2001) Immunocytochemical localization of acyl-CoA oxidase in the rat central nervous system. *J Neurocytol*., **30**:21-33.

Farlow MR, He Y, Tekin S, Xu J, Lane R, and Charles HC. (2004) Impact of APOE in mild cognitive impairment. *Neurology*, **63**:1898-1901.

Faust PL, Banka D, Siriratsivawong R, Ng VG, and Wikander TM. (2005) Peroxisome biogenesis disorders: the role of peroxisomes and metabolic dysfunction in developing brain. *J Inherit Metab Dis*., **28**:369-383.

Ferrer I. (2009) Altered mitochondria, energy metabolism, voltage-dependent anion channel, and lipid rafts converge to exhaust neurons in Alzheimer's disease. *J Bioenerg Biomembr*., **41**:425-431.

Ferri CP, Prince M, Brayne C, Brodaty H, Fratiglioni L, Ganguli M, Hall K, Hasegawa K, Hendrie H, Huang Y, Jorm A, Mathers C, Menezes PR, Rimmer E, Scazufca M, and Alzheimer's Disease International. (2005) Global prevalence of dementia: a Delphi consensus study. *Lancet*, **366**:2112-2117.

Finder VH. (2010) Alzheimer's disease: a general introduction and pathomechanism. *J. Alzheimers Dis.*, **22**:5-19.

Forlenza OV, Diniz BS, and Gattaz WF. (2010) Diagnosis and biomarkers of predementia in Alzheimer's disease. *BMC Med*., **8**:89

Fotuhi M, Mohassel P, and Yaffe K. (2009) Fish consumption, long-chain omega-3 fatty acids and risk of cognitive decline or Alzheimer disease: a complex association. *Nature Reviews Neurology*, **5**:140-152.

Fourcade S, Savary S, Albet S, Gauthé D, Gondcaille C, Pineau T, Bellenger J, Bentejac M, Holzinger A, Berger J, and Bugaut M. (2001) Fibrate induction of the adrenoleukodystrophy-related gene (ABCD2): promoter analysis and role of the peroxisome proliferator-activated receptor PPARalpha. *Eur J Biochem*., **268**:3490-3500.

Fujiki Y. (2000) Peroxisome biogenesis and peroxisome biogenesis disorders. *FEBS Lett.*, **476**:42-46.

Fujiwara N, Nakano M, Kato S, Yoshihara D, Ookawara T, Eguchi H, Taniguchi N, and Suzuki K. (2007) Oxidative modification to cysteine sulfonic acid of Cys111 in human copper-zinc superoxide dismutase. *J Biol Chem*., **282**:35933-35944.

Gella A and Durany N. (2009) Oxidative stress in Alzheimer disease. *Cell. Adh. Migr.*, **3**:88-93.

Glenner GG and Wong CW. (1984) Alzheimer's disease and Down's syndrome: sharing of a unique cerebrovascular amyloid fibril protein. *Biochem. Biophys. Res. Commun.*, **122**:1131–1135.

Goodenowe DB, Cook LL, Liu J, Lu Y, Jayasinghe DA, Ahiahonu PW, Heath D, Yamazaki Y, Flax J, Krenitsky KF, Sparks DL, Lerner A, Friedland RP, Kudo T, Kamino K, Morihara T, Takeda M, and Wood PL. (2007) Peripheral ethanolamine plasmalogen deficiency: a logical causative factor in Alzheimer's disease and dementia. *J Lipid Res*., **48**:2485-2498.

Grabenbauer M, Fahimi HD, and Baumgart E. (2001) Detection of peroxisomal proteins and their mRNAs in serial sections of fetal and newborn mouse organs. *J Histochem Cytochem*., **49**:155-164.

Grimm MO, Kuchenbecker J, Grösgen S, Burg VK, Hundsdörfer B, Rothhaar TL, Friess P, de Wilde MC, Broersen LM, Penke B, Péter M, Vígh L, Grimm HS, Hartmann T. (2011) Docosahexaenoic acid reduces amyloid beta production via multiple pleiotropic mechanisms. *J Biol Chem*., **286**:14028-14039.

Haass C and Selkoe DJ. (2007) Soluble protein oligomers in neurodegeneration: lessons from the Alzheimer's amyloid beta-peptide. *Nat. Rev. Mol. Cell. Biol*., **8**:101-112.

Hall MG, Quignodon L, and Desvergne B. (2008) Peroxisome Proliferator-Activated Receptor beta/delta in the Brain: Facts and Hypothesis. *PPAR Res*., 2008:780452.

Hardy J and Selkoe DJ. (2002) The amyloid hypothesis of Alzheimer's disease: progress and problems on the road to therapeutics. *Science*, **297**:353-356.

Hardy JA and Higgins GA. (1992) Alzheimer's disease: the amyloid cascade hypothesis. *Science*, **256**:184-185.

Harvey RJ, Skelton-Robinson M, and Rossor MN. (2003) The prevalence and causes of dementia in people under the age of 65 years. *J. Neurol. Neurosurg. Psychiatry*, **74**:1206-1209.

Hashimoto M, and Hossain S. (2011) Neuroprotective and ameliorative actions of polyunsaturated fatty acids against neuronal diseases: beneficial effect of docosahexaenoic acid on cognitive decline in Alzheimer's disease. *J Pharmacol Sci*., **116**:150-162.

Havas D, Hutter-Paier B, Ubhi K, Rockenstein E, Crailsheim K, Masliah E, and Windisch M. (2011) A longitudinal study of behavioral deficits in an AβPP transgenic mouse model of Alzheimer's disease. *J Alzheimers Dis.*, **25**:231-243.

Heiland I, and Erdmann R. (2005) Biogenesis of peroxisomes. Topogenesis of the peroxisomal membrane and matrix proteins. *FEBS J.*, **272**:2362-2372.

Hermann D, Both M, Ebert U, Gross G, Schoemaker H, Draguhn A, Wicke K, and Nimmrich V. (2009) Synaptic transmission is impaired prior to plaque formation in amyloid precursor protein-overexpressing mice without altering behaviorally-correlated sharp wave-ripple complexes. *Neuroscience*, **162**:1081-1090.

Hirata-Fukae C, Li HF, Hoe HS, Gray AJ, Minami SS, Hamada K, Niikura T, Hua F, Tsukagoshi-Nagai H, Horikoshi-Sakuraba Y, Mughal M, Rebeck GW, LaFerla FM, Mattson MP, Iwata N, Saido TC, Klein WL, Duff KE, Aisen PS, and Matsuoka Y. (2008) Females exhibit more extensive amyloid, but not tau, pathology in an Alzheimer transgenic model. *Brain Res*., **1216**:92-103.

Hoepfner D, Schildknegt D, Braakman I, Philippsen P, and Tabak HF. (2005) Contribution of the endoplasmic reticulum to peroxisome formation. *Cell*, **122**:85-95.

Holtzman DM, Bales KR, Tenkova T, Fagan AM, Parsadanian M, Sartorius LJ, Mackey B, Olney J, McKeel D, Wozniak D, and Paul SM. (2000) Apolipoprotein E isoform-dependent amyloid deposition and neuritic degeneration in a mouse model of Alzheimer's disease. Proc. Natl. Acad. Sci., **7**:2892-2897.

Hruban Z, Vigil EL, Slesers A, and Hopkins E. (1972) Microbodies: constituent organelles of animal cells. *Lab Invest*., **27**:184–191.

Hsiao K, Chapman P, Nilsen S, Eckman C, Harigaya Y, Younkin S, Yang F and Cole G. (1996) Correlative memory deficits, Abeta elevation, and amyloid plaques in transgenic mice. *Science*, **274**:99-102.

Hulshagen L, Krysko O, Bottelbergs A, Huyghe S, Klein R, Van Veldhoven PP, De Deyn PP, D'Hooge R, Hartmann D, and Baes M. (2008) Absence of

functional peroxisomes from mouse CNS causes dysmyelination and axon degeneration. *J Neurosci.*, **28**:4015-4027.

Hyman BT, Van Hoesen GW, Damasio AR, and Barnes CL. (1984) Alzheimer's disease: cell-specific pathology isolates the hippocampal formation. *Science*, **225**:1168-1170.

Iqbal K, Alonso Adel C, Chen S, Chohan MO, El-Akkad E, Gong CX, Khatoon S, Li B, Liu F, Rahman A, Tanimukai H, and Grundke-Iqbal I. (2005) Tau pathology in Alzheimer disease and other tauopathies. *Biochim. Biophys. Acta.*, **1739**:198–210.

Irizarry MC, McNamara M, Fedorchak K, Hsiao K and Hyman BT. (1997) APPSw transgenic mice develop age-related A beta deposits and neuropil abnormalities, but no neuronal loss in CA1. *J Neuropathol Exp Neurol*, **56**:965-973.

Issemann I, and Green S. (1990) Activation of a member of the steroid hormone receptor superfamily by peroxisome proliferators. *Nature*, **347**:645–650.

Jacobsen JS, Wu CC, Redwine JM, Comery TA, Arias R, Bowlby M, Martone R, Morrison JH, Pangalos MN, Reinhart PH, and Bloom FE. (2006) Early-onset behavioral and synaptic deficits in a mouse model of Alzheimer's disease. *Proc Natl Acad Sci*, **103**:5161-5166.

Jin K, Galvan V, Xie L, Mao XO, Gorostiza OF, Bredesen DE, and Greenberg DA, (2004b) Enhanced neurogenesis in Alzheimer's disease transgenic (PDGF-APPSw,Ind) mice. *Proc Natl Acad Sci*., **101**: 13363–13367.

Jin K, Peel AL, Mao XO, Xie L, Cottrell BA, Henshall DC, and Greenberg DA, (2004a) Increased hippocampal neurogenesis in Alzheimer's disease. *Proc Natl Acad Sci*., **101**: 343–347.

Jomova K, Vondrakova D, Lawson M, and Valko M. (2010) Metals, oxidative stress and neurodegenerative disorders. *Mol Cell Biochem.*, **345**:91-104.

Kane CD, Francone OL, and Stevens KA. (2006) Differential regulation of the cynomolgus, human, and rat acyl-CoA oxidase promoters by PPARalpha. *Gene*., **380**:84-94.

Kasai H, Okada Y, Nishimura S, Rao MS, and Reddy JK. (1989) Formation of 8-hydroxydeoxyguanosine in liver DNA of rats following long-term exposure to a peroxisome proliferator. *Cancer Res*., **49**:2603-2605.

Kawarabayashi T, Younkin LH, Saido TC, Shoji M, Ashe KH and Younkin SG. (2001) Age-dependent changes in brain, CSF, and plasma amyloid β protein in the Tg2576 transgenic mouse model of Alzheimer's disease. *J Neurosc*., **21**:372-381.

Keller JN, Kindy MS, Holtsberg FW, St Clair DK, Yen HC, Germeyer A, Steiner SM, Bruce-Keller AJ, Hutchins JB, and Mattson MP. (1998) Mitochondrial manganese superoxide dismutase prevents neural apoptosis and reduces ischemic brain injury: suppression of peroxynitrite production, lipid peroxidation, and mitochondrial dysfunction. *J Neurosci*., **18**:687-697.

Kou J, Kovacs GG, Höftberger R, Kulik W, Brodde A, Forss-Petter S, Hönigschnabl S, Gleiss A, Brügger B, Wanders R, Just W, Budka H, Jungwirth

S, Fischer P, and Berger J. (2011) Peroxisomal alterations in Alzheimer's disease. *Acta Neuropathol*., **122**:271-283.

Lazarow PB, and Fujiki Y. (1985) Biogenesis of peroxisomes. *Annu Rev Cell Biol.*, **1**:489-530.

Lee VM, Goedert M, and Trojanowski JQ. (2001) Neurodegenerative tauopathies. *Annu. Rev. Neurosci*., **24**:1121-1159.

Leon S, Goodman JM, and Subramani S. (2006) Uniqueness of the mechanism of protein import into the peroxisome matrix: transport of folded, co-factor-bound and oligomeric proteins by shuttling receptors. *Biochim Biophys Acta*, **1763**:1552-1564.

Lessig J, and Fuchs B. (2009) Plasmalogens in biological systems: their role in oxidative processes in biological membranes, their contribution to pathological processes and aging and plasmalogen analysis. *Curr Med Chem*., **16**:2021-2041.

Lewis J, Dickson DW, Lin WL, Chisholm L, Corral A, Jones G, Yen SH, Sahara N, Skipper L, Yager D, Eckman C, Hardy J, Hutton M, and McGowan E. (2001) Enhanced neurofibrillary degeneration in transgenic mice expressing mutant tau and APP. *Science*, **293**:1487-1491.

Lovell MA, Ehmann WD, Butler SM, and Markesbery WR. (1995) Elevated thiobarbituric acid-reactive substances and antioxidant enzyme activity in the brain in Alzheimer's disease. *Neurology*, **45**:1594-1601.

Lukiw WJ, and Bazan NG. (2008) Docosahexaenoic acid and the aging brain. *J Nutr*., **138**:2510-2514.

Ma C, Agrawal G, and Subramani S. (2011) Peroxisome assembly: matrix and membrane protein biogenesis. *J Cell Biol*., **193**:7-16.

Manczak M, Anekonda TS, Henson E, Park BS, Quinn J, and Reddy PH. (2006) Mitochondria are a direct site of A beta accumulation in Alzheimer's disease neurons: implications for free radical generation and oxidative damage in disease progression. *Hum Mol Genet*., **15**:1437-1449.

Mandrekar-Colucci S, and Landreth GE. (2011) Nuclear receptors as therapeutic targets for Alzheimer's disease. *Expert Opin Ther Targets*., **15**:1085-1097.

Massaad CA, Washington TM, Pautler RG, and Klann E. (2009) Overexpression of SOD-2 reduces hippocampal superoxide and prevents memory deficits in a mouse model of Alzheimer's disease. *Proc Natl Acad Sci*., **106**:13576-13581.

Mayeux R. (2003) Epidemiology of neurodegeneration. *Annu. Rev. Neurosci.*, **26**:81-104.

McKenna O, Arnold G, and Holtzman E. (1976) Microperoxisome distribution in the central nervous system of the rat. *Brain Res*.,**117**:181-194.

Meinecke M, Cizmowski C, Schliebs W, Krüger V, Beck S, Wagner R, and Erdmann R. (2010) The peroxisomal importomer constitutes a large and highly dynamic pore. *Nat Cell Biol.*, **12**:273-277.

Moreno S, Mugnaini E, and Cerù MP. (1995) Immunocytochemical localization of catalase in the central nervous system of the rat. *J Histochem Cytochem*., **43**:1253-1267.

Moreno S, Nardacci R, Cimini A, and Cerù MP. (1999) Immunocytochemical localization of D-amino acid oxidase in rat brain. *J Neurocytol.*, **28**:169-185.

Namba T, Mochizuki H, Suzuki R, Onodera M, Yamaguchi M, Namiki H, Shioda S, and Seki T. (2011) Time-lapse imaging reveals symmetric neurogenic cell division of GFAP-expressing progenitors for expansion of postnatal dentate granule neurons. *PLoS One.*, **6**:e25303.

Nunomura A, Perry G, Aliev G, Hirai K, Takeda A, Balraj EK, Jones PK, Ghanbari H, Wataya T, Shimohama S, Chiba S, Atwood CS, Petersen RB, and Smith MA. (2001) Oxidative damage is the earliest event in Alzheimer disease. *J Neuropathol Exp Neurol.*, **60**:759-767.

Nunomura A, Tamaoki T, Tanaka K, Motohashi N, Nakamura M, Hayashi T, Yamaguchi H, Shimohama S, Lee HG, Zhu X, Smith MA, and Perry G. (2010) Intraneuronal amyloid beta accumulation and oxidative damage to nucleic acids in Alzheimer disease. *Neurobiol Dis.*, **37**:731-737.

Otera H, Harano T, Honsho M, Ghaedi K, Mukai S, Tanaka A, Kawai A, Shimizu N, and Fujiki Y. (2000) The mammalian peroxin Pex5pL, the longer isoform of the mobile peroxisome targeting signal (PTS) type 1 transporter, translocates the Pex7p.PTS2 protein complex into peroxisomes via its initial docking site, Pex14p. *J Biol Chem.*, **275**:21703-21714.

Pappolla MA, Chyan YJ, Omar RA, Hsiao K, Perry G, Smith MA, and Bozner P. (1998) Evidence of oxidative stress and in vivo neurotoxicity of beta-amyloid in a transgenic mouse model of Alzheimer's disease: a chronic oxidative paradigm for testing antioxidant therapies in vivo. *Am J Pathol.*, **152**:871-877.

Peters JM, Lee SS, Li W, Ward JM, Gavrilova O, Everett C, Reitman ML, Hudson LD, and Gonzalez FJ. (2000) Growth, adipose, brain, and skin alterations resulting from targeted disruption of the mouse peroxisome proliferator-activated receptor beta(delta). *Mol Cell Biol.*, **20**:5119-5128.

Petersen RC, Smith GE, Waring SC, Ivnik RJ, Tangalos EG, and Kokmen E. (1999) Mild cognitive impairment: clinical characterization and outcome. *Arch Neurol.*, **56**:303-308.

Platta HW, and Erdmann R. (2007) Peroxisomal dynamics. *Trends Cell Biol.*, **17**:474–484.

Poirier J, Davignon J, Bouthillier D, Kogan S, Bertrand P, and Gauthier S. (1993) Apolipoprotein E polymorphism and Alzheimer's disease. *Lancet*, **342**:697-699.

Poirier Y, Antonenkov VD, Glumoff T, Hiltunen JK. (2006) Peroxisomal beta-oxidation, a metabolic pathway with multiple functions. *Biochim Biophys Acta.*, **1763**:1413-1426.

Praticò D, MY Lee V, Trojanowski JQ, Rokach J, and Fitzgerald GA. (1998) Increased F2-isoprostanes in Alzheimer's disease: evidence for enhanced lipid peroxidation in vivo. *FASEB J.*, **12**:1777-1783.

Querfurth HW and LaFerla FM. (2010) Alzheimer's disease. *N Engl J Med.*, **362**:329-344.

Raber J, Huang Y, and Ashford JW. (2004) ApoE genotype accounts for the vast majority of AD risk and AD pathology. *Neurobiol. Aging*, **25**:641-650.

Rapoport M, Dawson HN, Binder LI, Vitek MP, and Ferreira A. (2002) Tau is essential to beta -amyloid-induced neurotoxicity. *Proc. Natl. Acad. Sci*., **99**:6364-6369.

Reddy JK and Hashimoto T. (2001) Peroxisomal b-oxidation and peroxisome peroliferator-activated receptor a: an adaptive metabolic system. *Annu. Rev. Nutr*., **21**:193–230.

Reddy JK and Rao MS. (1987) Xenobiotic-induced peroxisome proliferation: role of tissue specificity and species differences in response in the evaluation of the implications for human health. *Arch Toxicol Suppl*., **10**:43-53.

Reddy JK, Goel SK, Nemali MR, Carrino JJ, Laffler TG, Reddy MK, Sperbeck SJ, Osumi T, Hashimoto T, Lalwani ND. (1986) Transcription regulation of peroxisomal fatty acyl-CoA oxidase and enoyl-CoA hydratase/3-hydroxyacyl-CoA dehydrogenase in rat liver by peroxisome proliferators. *Proc Natl Acad Sci*., **83**:1747-1751.

Reddy PH, McWeeney S, Park BS, Manczak M, Gutala RV, Partovi D, Jung Y, Yau V, Searles R, Mori M, and Quinn J. (2004) Gene expression profiles of transcripts in amyloid precursor protein transgenic mice: up-regulation of mitochondrial metabolism and apoptotic genes is an early cellular change in Alzheimer's disease. *Hum Mol Genet*., **13**:1225-1240.

Reilly JF, Games D, Rydel RE, Freedman S, Schenk D, Young WG, Morrison JH, and Bloom FE. (2003) Amyloid deposition in the hippocampus and entorhinal cortex: quantitative analysis of a transgenic mouse model. *Proc Natl Acad Sci*., **100**:4837-4842.

Reitz C, Brayne C, and Mayeux R. (2011) Epidemiology of Alzheimer disease. *Nat. Rev. Neurol.*, **7**:137-152.

Rhodin J. (1954) Correlation of ultrastructural organization and function in normal experimentally changed convoluted tubule cells of the mouse kidney. Ph.D. thesis. Stockholm, Aktiebolaget Godvil.

Rigoulet M, Yoboue ED, and Devin A. (2011) Mitochondrial ROS generation and its regulation: mechanisms involved in H(2)O(2) signaling. *Antioxid Redox Signal*., **14**:459-468.

Roberson ED, Scearce-Levie K, Palop JJ, Yan F, Cheng IH, Wu T, Gerstein H, Yu GQ, and Mucke L. (2007) Reducing endogenous tau ameliorates amyloid beta-induced deficits in an Alzheimer's disease mouse model. *Science*, **316**:750-754.

Santos MJ, Kawada ME, Espeel M, Figueroa C, Alvarez A, Hidalgo U, and Metz C. (1994) Characterization of human peroxisomal membrane proteins. *J Biol Chem*., **269**:24890-24896.

Santos MJ, Quintanilla RA, Toro A, Grandy R, Dinamarca MC, Godoy JA, and Inestrosa NC. (2005) Peroxisomal proliferation protects from beta-amyloid neurodegeneration. *J Biol Chem*., **280**:41057-41068.

Sasaki A, Shoji M, Harigaya Y, Kawarabayashi T, Ikeda M, Naito M, Matsubara E, Abe K, and Nakazato Y. (2002) Amyloid cored plaques in Tg2576 transgenic mice are characterized by giant plaques, slightly activated microglia, and the lack of paired helical filament-typed, dystrophic neurites. *Virchows Arch.*, **441**:358-367.

Sayre LM, Perry G, and Smith MA. (2008) Oxidative stress and neurotoxicity. *Chem. Res. Toxicol.*, **21**:172-188.

Schad A, Fahimi HD, Völkl A, and Baumgart E. (2003) Expression of catalase mRNA and protein in adult rat brain: detection by nonradioactive in situ hybridization with signal amplification by catalyzed reporter deposition (ISH-CARD) and immunohistochemistry (IHC)/immunofluorescence (IF). *J Histochem Cytochem.*, **51**:751-760.

Schrader M, and Fahimi HD. (2006) Peroxisomes and oxidative stress. *Biochim Biophys Acta*., 1763:1755-1766.

Schrader M, and Fahimi HD. (2008) The peroxisome: still a mysterious organelle. *Histochem Cell Biol.*, **129**:421-440.

Shen C, Chen Y, Liu H, Zhang K, Zhang T, Lin A, and Jing N. (2008) Hydrogen peroxide promotes Abeta production through JNK-dependent activation of gamma-secretase. *J Biol Chem.*, **283**:17721-17730.

Shie F. S., LeBoeur R. C. and Jin L. W. (2003) Early intraneuronal Abeta deposition in the hippocampus of APP transgenic mice. *Neuroreport*, **14**:123–129.

Singh I. (1997) Biochemistry of peroxisomes in health and disease. *Mol Cell Biochem.*, **167**:1-29.

Singh M, Nam DT, Arseneault M, and Ramassamy C. (2010) Role of by-products of lipid oxidation in Alzheimer's disease brain: a focus on acrolein. *J Alzheimers Dis.*, **21**:741-756.

Smith MA, Hirai K, Hsiao K, Pappolla MA, Harris PL, Siedlak SL, Tabaton M, and Perry G. (1998) Amyloid-beta deposition in Alzheimer transgenic mice is associated with oxidative stress. *J Neurochem.*, **70**:2212-2215.

Smith MA, Zhu X, Tabaton M, Liu G, McKeel DW Jr, Cohen ML, Wang X, Siedlak SL, Dwyer BE, Hayashi T, Nakamura M, Nunomura A, and Perry G. (2010) Increased iron and free radical generation in preclinical Alzheimer disease and mild cognitive impairment. *J Alzheimers Dis.*, **19**:363-372.

Sprecher H, Luthria DL, Mohammed BS, and Baykousheva SP. (1995) Reevaluation of the pathways for the biosynthesis of polyunsaturated fatty acids. *J Lipid Res.*, **36**:2471-2477.

Stamer K, Vogel R, Thies E, and Mandelkow E. (2002) Tau blocks traffic of organelles, neurofilaments, and APP vesicles in neurons and enhances oxidative stress. *J. Cell. Biol.*, **156**:1051-1063.

Stefanini S, Serafini B, Nardacci R, Vecchioli SF, Moreno S, and Sartori C. (1995) Morphometric analysis of liver and kidney peroxisomes in lactating rats and their

pups after treatment with the peroxisomal proliferator di-(2-ethylhexyl)phthalate. *Biol Cell*., **85**:167-176.

Steinberg SJ, Dodt G, Raymond GV, Braverman NE, Moser AB, and Moser HW. (2006) Peroxisome biogenesis disorders. *Biochim Biophys Acta*., **1763**:1733-1748.

Sultana R and Butterfield DA. (2010) Role of oxidative stress in the progression of Alzheimer's disease. *J Alzheimers Dis*., **19**:341-353.

Tabner BJ, El-Agnaf OM, Turnbull S, German MJ, Paleologou KE, Hayashi Y, Cooper LJ, Fullwood NJ, and Allsop D. (2005) Hydrogen peroxide is generated during the very early stages of aggregation of the amyloid peptides implicated in Alzheimer disease and familial British dementia. *J Biol Chem*., **280**:35789-35792.

Takahashi RH, Almeida CG, Kearney PF, Yu F, Lin MT, Milner TA, Gouras GK. (2004) Oligomerization of Alzheimer's beta-amyloid within processes and synapses of cultured neurons and brain. *J Neurosci*., **24**:3592-3599.

Tehranian R, Hasanvan H, Iverfeldt K, Post C and Schultzberg M. (2001) Early induction of interleukin-6 mRNA in the hippocampus and cortex of APPsw transgenic mice Tg2576. *Neurosci Lett*., **30**:54-58.

Terlecky SR, Koepke JI, and Walton PA. (2006) Peroxisomes and aging. *Biochim Biophys Acta.*, **1763**:1749-1754.

Titorenko VI, and Mullen RT. (2006) Peroxisome biogenesis: the peroxisomal endomembrane system and the role of the ER. *J Cell Biol.*, **174**:11-17.

Town TC, Mori T, Cohen RM, Tan J, and Rezai-Zadeh K. (2011) Neuroinflammation as an early event and prime mover in Alzheimer's disease. Neuroscience Meeting Planner online.Program#422.01

Völkl A, Baumgart E, and Fahimi HD. (1988) Localization of urate oxidase in the crystalline cores of rat liver peroxisomes by immunocytochemistry and immunoblotting. *J Histochem Cytochem*., **36**:329-336.

Walsh DM and Selkoe DJ. (2007) A beta oligomers - a decade of discovery. *J Neurochem*, **101**:1172-1184.

Wanders RJ, and Waterham HR. (2006) Biochemistry of mammalian peroxisomes revisited. *Annu Rev Biochem*., **75**:295–332.

Wanders RJ, Ferdinandusse S, Brites P, and Kemp S. (2010) Peroxisomes, lipid metabolism and lipotoxicity. *Biochim Biophys Acta*., **1801**:272-280.

Wanders RJ, Visser WF, van Roermund CW, Kemp S, and Waterham HR. (2007) The peroxisomal ABC transporter family. *Pflugers Arch*., **453**:719-734.

Wanders RJ. (2004) Peroxisomes, lipid metabolism, and peroxisomal disorders. *Mol Genet Metab*., **83**:16-27.

Weidner AM, Bradley MA, Beckett TL, Niedowicz DM, Dowling AL, Matveev SV, LeVine H 3rd, Lovell MA, and Murphy MP. (2011) RNA oxidation adducts 8-OHG and 8-OHA change with Aβ42 levels in late-stage Alzheimer's disease. *PLoS One*., **6**:e24930.

Westerman MA, Cooper-Blacketer D, Mariash A, Kotilinek L, Kawarabayashi T, Younkin LH, Carlson GA, Younkin SG and Ashe KH. (2002) The relationship between Abeta and memory in the Tg2576 mouse model of Alzheimer's disease. *J Neurosci*., **22**:1858-1867.

Wirths O, Multhaup G, and Bayer TA. (2004) A modified beta-amyloid hypothesis: intraneuronal accumulation of the beta-amyloid peptide--the first step of a fatal cascade. *J Neurochem*., **91**:513-520.

Yeldandi AV, Rao MS, and Reddy JK. (2000) Hydrogen peroxide generation in peroxisome proliferator-induced oncogenesis. *Mutat Res*., **448**:159-177.